Ministry of higher education
and scientific research
University of Babylon
College of science
Department of Applied Geology

The Petroleum System of the Abu Ghirab Oilfield in the Zagros Fold Belt Basin, Southeastern Iraq

A Thesis
Submitted to the College of science University of Babylon in
Partial Fulfillment of the Requirements for the
Degree of Master of Science in Geology.

By
Abdullah Ahmed Hadi Jwad Almamouri
B.Sc. Applied Geology 2019

Supervised by

Prof.Dr. Amer Jassim Al-Khafaji
Dr. Ali Duair Al-Musawi

2022 A.C **1444 A.H**

بسم الله الرحمن الرحيم

﴿وَلَمَّا بَلَغَ أَشُدَّهُ وَاسْتَوَى آتَيْنَاهُ حُكْمًا وَعِلْمًا
وَكَذَلِكَ نَجْزِي الْمُحْسِنِينَ ﴾

صدق الله العظيم

القصص- الآية ١٤

الاهـــــداء

الى صاحب الفضل الاول والاخير الى الهادي سواء السبيل... **الله جل جلاله**

إلى من قاد قلوب البشرية وعقولهم إلى مرفأ الأمان، معلم البشرية الأول.... **محمد وآله الكرام**

إلى من شرفني بحمل اسمه، إلى من أفتقد حرارة تصفيقه فرحاً بإنجازي في هذه اللحظة.ولا أفتقد دعواته التي أجنى ثمارها.. **والدي رحمه الله**

إلى حلوة اللبن التي ما خالط لبنها يوماً سكّر المصالح صاحبة الحبل السري الذي لا زال أثره باقياً فيّ حتى الآن.. **امي**

إلى السند... **اخي**

الى استاذي ومرشدي..الدكتور عامر جاسم

إلى من ربطني بهم علاقة النسب . وعطر الصداقة . . وورد المحبة

إلى إخوة جمعني بهم ميدان العمل والدراسة ... **زملائي الكرام**

الى كل يدٍ وقلبٍ سار معي درب الانجاز لاكون....

الى كل هؤلاء اهدي هذه الدراسة راجياً من الله أن تكون نافذة علم وبطاقة معرفة . .. وأن ينفعنا وينفع بنا ،،

عبدالله العموري

Acknowledgements

"In the name of Allah the Most Merciful, the Most Compassionate".

First of all, I would like to thank Allah Almighty very much for his great blessing and success for me to complete this study.

My thanks, gratitude and appreciation go to my supervisors; Prof. Dr. Amer J. Al-Khafaji and Ali Duair Al-Musawi for their guidance and encouragement throughout this study.

I would like to thank Department of Geology at the University of Babylon. for providing opportunities and facilities for the completion of this research.

My thanks and appreciation go to all staff of the Reservoirs and Fields Development in the Ministry of Oil.

My thanks and appreciation to all staff of the Oil Exploration Company. Especially Mr. AbdSalam Muhammad for helping me with my project.

My thanks and appreciation go to all staff of the Petroleum Research and Development Center.

My thanks and appreciation extend to all staff of the Missan Oil Company.
My thanks, gratitude and appreciation go to all my friends and colleagues who supported and helped me.

My thanks, appreciation and respect go to that person who stood by my side throughout the days of study and work...

Abdullah Al-Mamouri

Summary

The Zagros Fold Basin and the Mesopotamian Basin extend from northern to southern Iraq. Most of the huge oil fields are located in these two basins, and they contain most of the oil and gas reserves in Iraq. This study included identifying the elements and processes of the total petroleum system for the Abu Ghraib oil field, which is located in the Missan Governorate in southeastern Iraq near the border with Iran. The Asmari Formation is the main reservoir of the oilfield, and the secondary reservoirs are represented by the Mishrif Formation, Nahr Omar, and Mauddud Formations. To achieve the goal of this study, many software such as Didger, IP, Petrel, and PetroMod were installed and used. A suite of well logs for five vertical wells in the Abu Ghirab oilfield, which are AG1, AG-3, AG-7, AG-13, and AG-17, are used to determine the petrophysical properties of the reservoir units. Three crude oil samples were taken at different depths from wells AG-1, AG-7, and AG-10 and then subjected to geochemical analysis such as gas chromatography, gas chromatograph-mass spectrometry, and carbon isotope analysis.

The petrophysical properties of the main Asmari reservoir units were investigated, based on the interpretations of the available well logging, using the Petrophysics Interactive program V3.5. The lithology of the reservoir was determined to be composed of limestone and dolomite. The Asmari Formation consists of three main reservoir units separated by two shale layers. These units are Jeribe-Euphrates, Upper Kirkuk, and Middle-Lower Kirkuk and are then divided into eight secondary reservoir units, according to the readings of GR and their content of shale and petrophysical properties. The secondary reservoir units are A1, A2, A3, B1, B2, B3, B4, and C. The units B2-B3 have excellent petro- physical properties and are considered one of the best units of the Asmari Formation due to the high percentages of hydrocarbon saturation. Unit C contains high percentages of water saturation, except for the AG-13 well which has high oil saturation.

Geochemical analyses were carried out for three samples of crude oil using gas chromatograph technology and gas chromatograph-mass spectrometry from the Jeribe Formation, the Middle Kirkuk, and the Upper Kirkuk. The results showed that non-biologically corrosive and non-waxy oils were generated from sediments of carbonate source rocks deposited in an unventilated marine environment with low thermal maturity.

1D basin and petroleum system modeling, was built. After the interpretation of the results of the source analysis, it was found that the source rocks of the region are represented by the Sargelu Formation, the Nagma Formation of the Jurassic age, and Upper Jurassic to Lower Cretaceous the formations of Yamama and Sulaiy. also determined the time of oil generation from the Late Cretaceous period and stopped at the Paleogene and the early Neogene. peak expulsion took place in the late Miocene and Pliocene when these depocenters had expanded along the Zagros foredeep trend, and generation ended in the Holocene when deposition in the foredeep ceased. These oils were collected in the Tertiary and Cretaceous reservoirs, and it was found that these oils are a mixture of Jurassic and Cretaceous source rocks.

Contents

List of Figures

List of Tables

Chapter one
Introduction

Chapter One

Introduction

1.1.Preface

Iraq is one of the Middle East's oil-richest countries and is regarded as the region's largest oil reserve since it is derived from several petroleum systems, including the Paleozoic (Tsp202301), Jurassic (Tsp202302), and Cretaceous-Tertiary (Tsp203001) eras (Verma *et al.*, 2004). as shown in the Figure (1-1).

The two primary basins in Iraq, which run from northern to southern Iraq, are the Mesopotamian Basin and the Zagros Fold Belt. They are huge oilfields in these two Iraqi basins house huge oil and gas reserves. (Sadowani and Aqrawi, 2000; Al-Sakini, 1992; Sadooni, 1993).

Although the Zagros Fold-thrust belt is one of the oldest researched and exploited petroleum provinces in the world, it has not yet reached its full potential, mostly due to political considerations. Currently, efforts are being undertaken to create play concepts that might cover the entire orogenic belt.

A period of rapid expansion began in 1908 with the discovery of petroleum in Iran and Iraq. Production first came from Cenozoic reservoirs, and Iranian and Iraqi companies frequently exchanged important knowledge during this early stage of exploration. The area produced some very perceptive works that can be regarded as "firsts" in their fields.

In the Abu Gharib oil field, the production is from the Asmari reservoir, and the naming of this reservoir by This name was given based on the final reports by the oil companies operating in the region and by the Ministry of Oil.

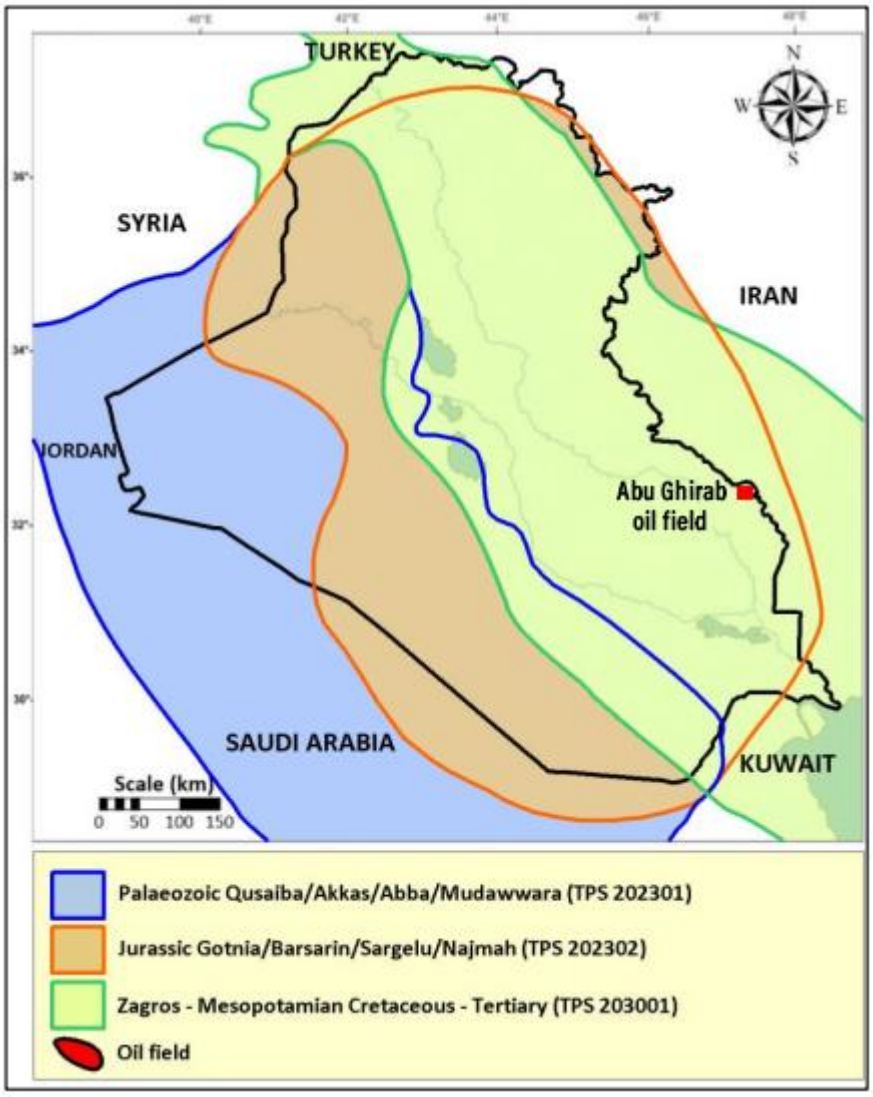

Figure(1-1): Map showing the extent of Total Petroleum Systems in Iraq. Modified from (Verma et al., 2004).

1.2. Aims of the study

1- Study the petroleum system of Abu Ghraib oil field of the Zagros, southeastern Iraq.

2- Study the petrophysics properties of the main reservoirs.

3- Study the geochemistry properties of the oils and probable source rocks.

4- Determine the reservoirs cap rocks.

5- Build 3D petrophysical model for Asmari Formation in Abu Ghirab oil field.

1.3. A brief Overview about the study Area

1.3.1.Geographic situation and study area

Missan province has the Missan oilfields, which are close to the Iraq–Iran border .It is about 350 km southeast of Baghdad and approximately 175 km north of Basra. Three main field, Abu Ghirab, Buzurgan, and Fauqi oilfields, are part of the Missan oilfields, which were discovered between 1969 and 1973 (CNOOC, 2011).

Abu Ghirab oil field is situated in the Missan Governorate in the southeast of Iraq (fig.1-2), close to the Iranian border. With coordinates of 3575000-360000 northing lines and 71000-73500 easting lines, it has an axial length of around 30 km and a breadth of about 5 km. Five vertical wells in Abu Ghirab oil field were investigated (AG-1, AG3, AG7, AG13, AG17).

Location coordinates for the wells examined in this investigation are shown in table (1-1)

Table (1-1): Location coordinates of the studied wells according to Missan Oil Company wells final reports.

Well No.	Top (m)	Bottom (m)	Geographic Coordinates (UTM)	
			Easting (X)	Northing (Y)
AG-1	2887 m	3100.12m	724204	3585424
AG-3	2927m	4003.5m	726700	3583233
AG-7	2936m	3237m	727068	3584151
AG-13	2965m	3265m	726005	3585000
AG-17	2984m	4180.5m	728230	3582123

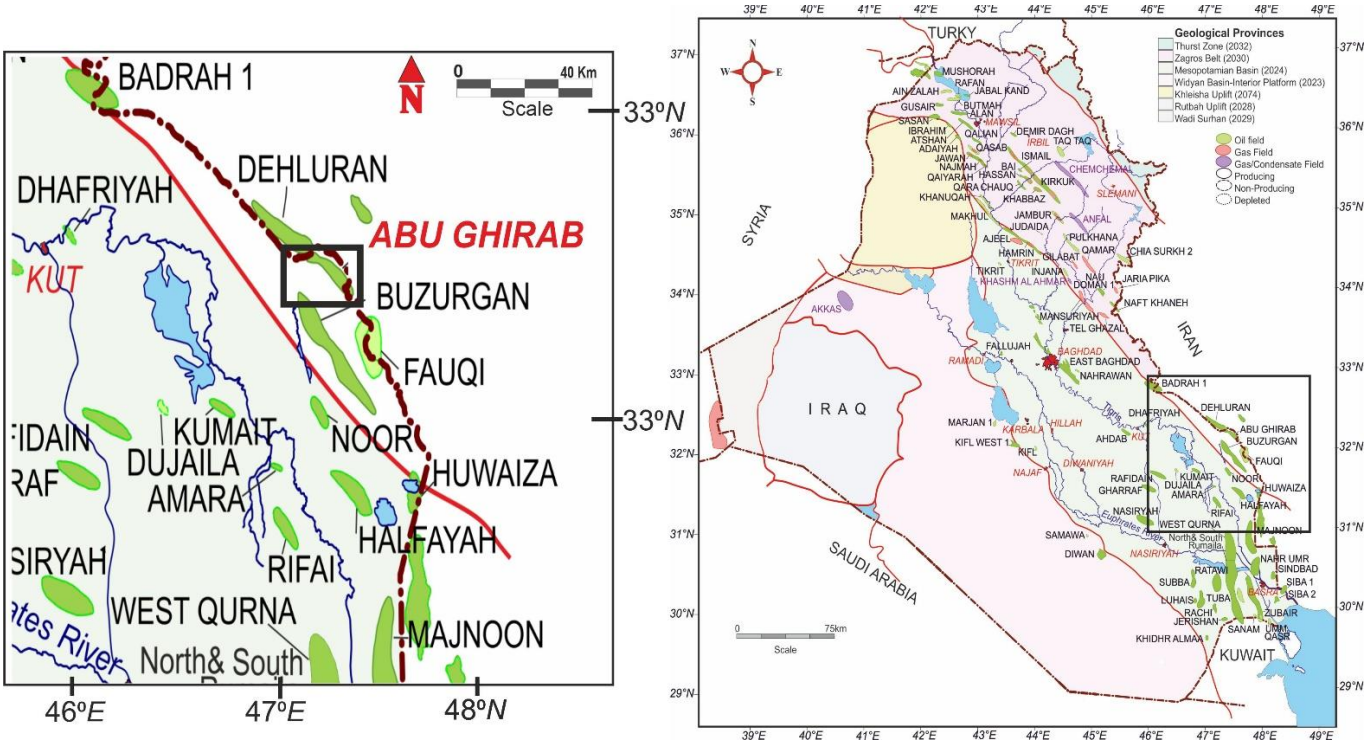

Figure (1-2): Location map of Abu Ghirab (AG) oil fields (Al-Khafaji et. al., 2014)

1.3.2.Geological setting

Abu Ghirab oil field consists of a saddle zone and two northern and southern domes (Alhuraishawy, Ali khayoon,2005). According to tectonics, Abu Ghirab oil field is part of the Makhul-Hemrin subzone, low folded zone, and unstable shelf (Kirkuk embayments).

Due to the collision of the Arabian and Iranian plates, this region is particularly active, and as a result, Abu Ghirab field has a complicated structure. Abu Ghirab field is made up of two asymmetric culminations that are separated by a saddle, according to seismic survey data. The structure's axis is from north to south. The northern climax is shared with Iran, and this section is probably a continuation of the Dehleran field in Iran. It is around 16.5 km in length and 5.5 km in breadth in the south.

The northern climax of Iraq is around 3 km long and 2 km wide. According to numerous geological studies on Abu Ghirab structure, this structure was subjected to two different types of forces as a result of the folding movement:

the first was tension forces concentrated on the upper part of the structure, while the second was compression forces on the lower parts of the structure, which caused longitudinal tangential deformation with low intensity on the axis of the anticline and high deformation on the limbs (Alssad, H.F.K. 2010) (fig.1-3).

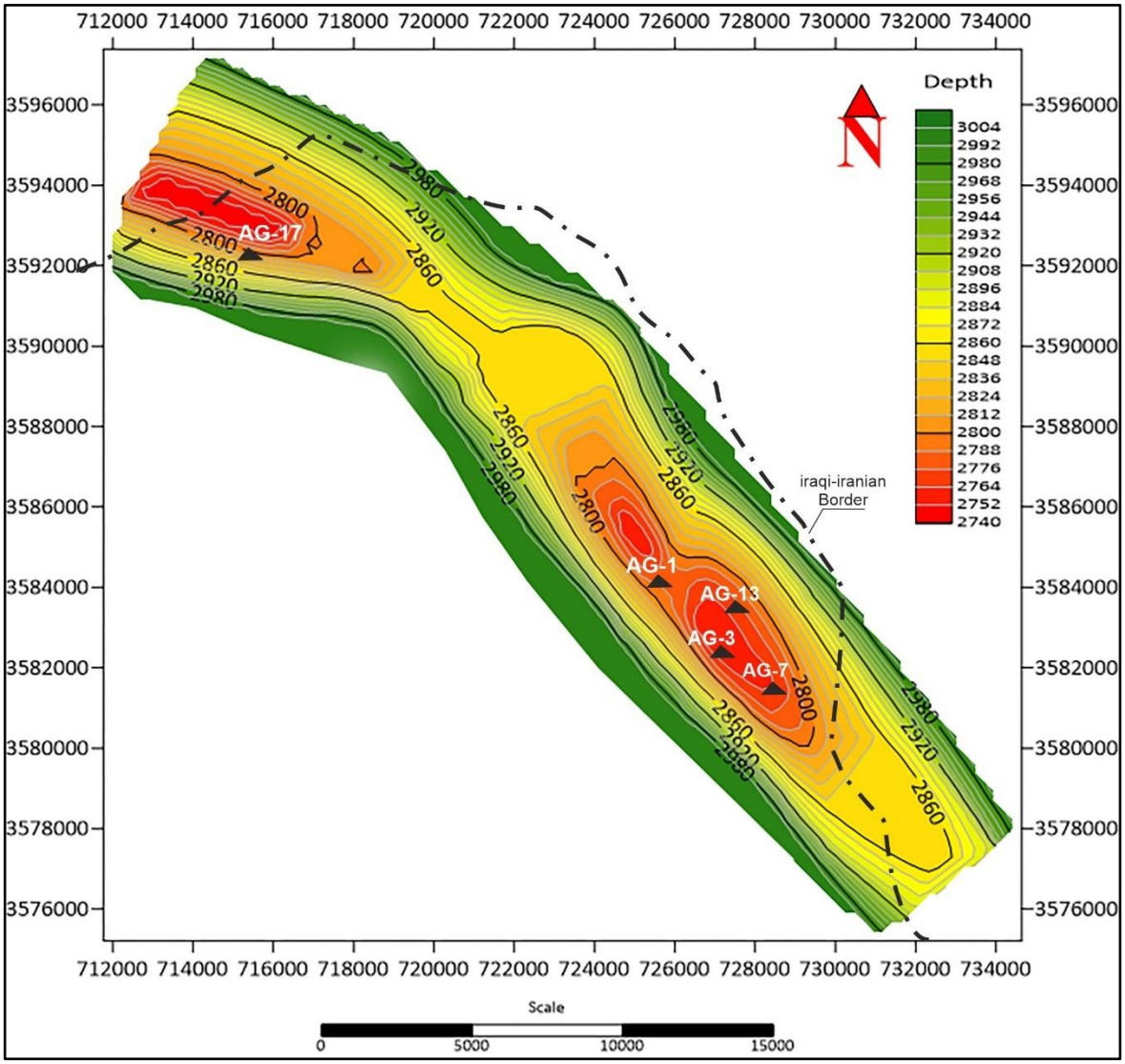

Figure(1-3): Structural map of the top of Jeribe-Euphrates Formation.

1.4.Structural and Tectonic Framework

1.4.1. Zagros Fold Belt

The Zagros Fold Belt runs the length of the triple junction boundary with Iran and Turkey, between the thrust zone (fig 1-4). In the early Paleozoic, Gondwana encompassed the region bordering the Paleo-Tethys Ocean to the

north, including the Zagros fold-and-thrust belt and the stable Arabian platform (e.g., Berberian and King 1981; Sepehr and Cosgrove 2004; Stocklin 1968).

The Neo-Tethys Ocean was created between the Iranian microplate and Arabia by Permo-Triassic rifting, which also closed the Paleo-Tethys in the north (for more information on this topic, see Misra and Mukherjee 2015). Neo-Tethyan passive margins emerged throughout the Jurassic and Cretaceous periods, and finally, in the Late Oligocene, the southern passive margin clashed with Eurasia (e.g., McQuarrie and van Hinsbergen 2013; Pirouz *et al*. 2017b).

According to (Masson *et al.*, 2005), the Zagros fold-and-thrust belt is currently shortening at a rate of approximately 11±2 mm/year, which accommodates about half of the 25±2 mm/year convergence between Arabia and Eurasia. Since the Early Pliocene, the region has experienced a minimum uplift of 1 mm/year (Hessami *et al.*,2006; Tatar *et al.*,2002).

The Urumieh-Dokhtar Cenozoic magmatic arc, the Sanandaj-Sirjan Mesozoic magmatic arc on the Eurasian plate, and the sedimentary Zagros basin over Arabia are the three major tectonic units that make up the present Zagros orogen (Hassanzadeh and Wernicke, 2016). According to Berberian (1995), the high Zagros or imbricated zone, the simply folded belt, the Dezful and Kirkuk embayments, and the Mesopotamia-Persian Gulf foredeep are the four primary structural divisions of the Zagros sedimentary basin (Fig. 1-4).

The high Zagros imbricated zone has high angle reversal faults, flipped structures, and tight folds. This zone is bounded to the north by the Main Zagros Reverse Fault (MZRF) or the Zagros suture, and to the south by the High Zagros fault (HZF). The neatly folded belt, as well as the Dezful and Kirkuk embayments, are located to the south of the HZF.

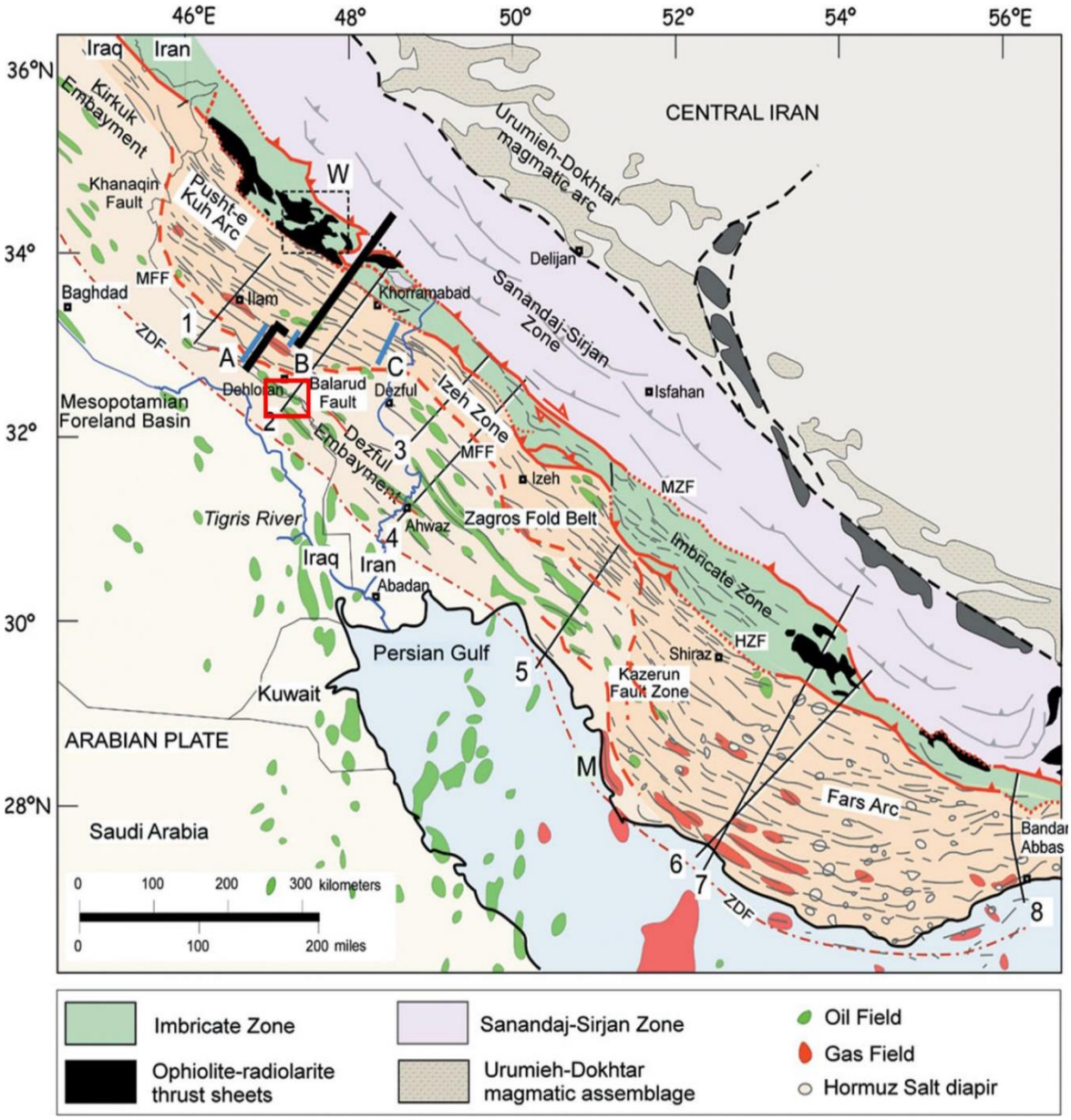

Figure(1-4): Structural sub-divisions of the Zagros fold-and-thrust belt foreland basin and showing the extent of major hydrocarbon fields (Vergés. *et al.*, 2011).

1.4.2.The Low Folded Zone

The biggest zone is the Low Folded Zone in the Western section of the Zagros belt. It is around 700 kilometers long and 100 kilometers broad. It covers around 56930 km2. This zone has a variety of folds of varying sizes and geometries (fig.1-5).

The folds followed an NW-SE tendency throughout most of the zone before shifting to an E-W trend northwestward into Turkish borders. Almost all of the anticlines in the eastern section have reversal faulting, which has

produced overriding on the NE and SW limbs, particularly in the Kirkuk Subzone (Al Naqib, K.1960).

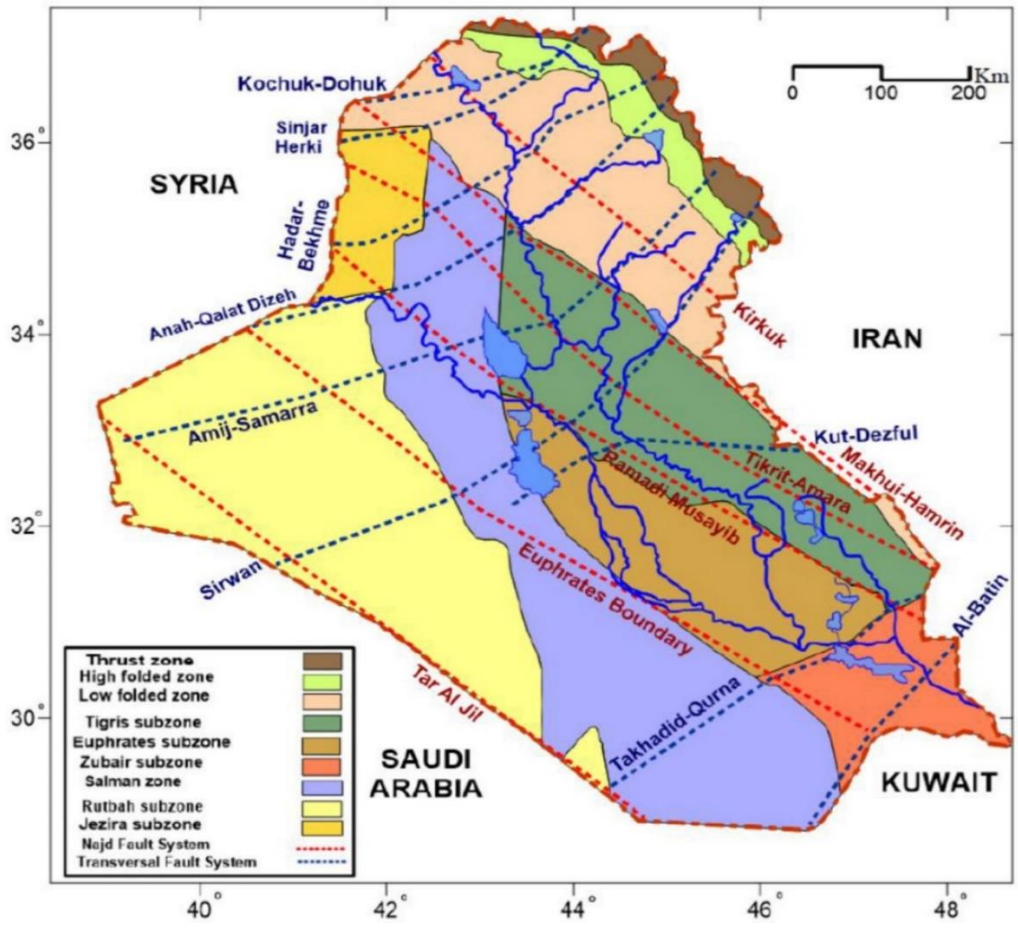

Figure(1-5): Tectonic map of Iraq (Jassim and Goff, 2006).

1.5. Stratigraphic Sequence

The study area is located in south east of the unstable shelf. The selected boreholes are distributed on the Low Folded Zone within the Makhul-Hemrin subzone (Jassim and Goff,2006) . Oligocene-Lower Miocene succession in the study area is represented mainly is divided to Kirkuk group and Jeribe – Euphrates.

The Oligocene cycle consists of nine formations, which are divided into three sequences: early (Palani, Sheikh Alas, Shurau), middle (Tarjil, Baba, Bajwan, Ibrahim), and late Oligocene age (Azkand and Anah). These Formations were combined into the Kirkuk group (Buday *et al*.,1980).

These Formations were combined into the Kirkuk group. It was discovered in a subterranean area in the north-eastern province of Kirkuk. The

environments of these sequences vary from the basin to the reef and back reef facies. The Bellen division was reduced from three cycles to two cycles, with a lower cycle made up of the formations Palani, Sheikh Alas, Shurau, and Tarjil, and an upper cycle made up of the formations Bajawan, Ibrahim and Anah, Azkand, and Baba (Buday *et al*.,1980).

In Iran, the deposits of the Oligocene age appear represented by the formation of Al-Asmari, so it is possible to equivalent the Asmari reservoir with its aggregates (Juraibi / Euphrates, Upper Kirkuk, member of Bazarkan, middle and lower Kirkuk), as it was found to be comparable to the formation of Al-Asmari age (Oligocene - Early Miocene), (Jassim & Goff, 2006).

The reservoir limits from below the formation of a Jaddala in a consistent manner, As for the top opening, the layer of anhydrite belonging to the fifth member, to form the opening in a compatible manner as well. As for the top, it is delimited by the anhydrite layer belonging to the fifth member, with the Fatha Formation in a compatible manner as well. The age of the reservoir was given (Oligocene - Early Miocene) depending on the stratification between the Jaddala Formation due to the late Eocene and the Fatha Formation due to the age of the middle Miocene (the final reports of the study wells).

The Tertiary period sediments in the unstable pavement area were divided into six sedimentary cycles, and the reservoir rocks belong to the (Oligocene, lower-middle Miocene). The deposits of the Oligocene period in Iraq were characterized by their limitations and lack of spread, as well as a reduction in their thickness as well. There are some problems with regard to the stratigraphy and delineation of the boundaries of this cycle (Buday, 1980). Sections of the Oligocene age in southeastern Iraq / Maysan Governorate differ from those mentioned in the north by changing the lithic facies of the sediments represented by clastic sediments (sandy, shale and clay).

The Oligocene period was characterized by the occurrence of tectonic complications that affected the progress and retreat of the sea, which led to a rapid environmental overlap and the diversity of facies horizontally and

vertically, which formed the current stratigraphic situation. As a result of the marine recession that occurred during the Oligocene, the sediments of that period in southern Iraq and Saudi Arabia are missing, as the Miocene sediments are located directly above the Eocene sediments (Al-Rubaie, 1992).

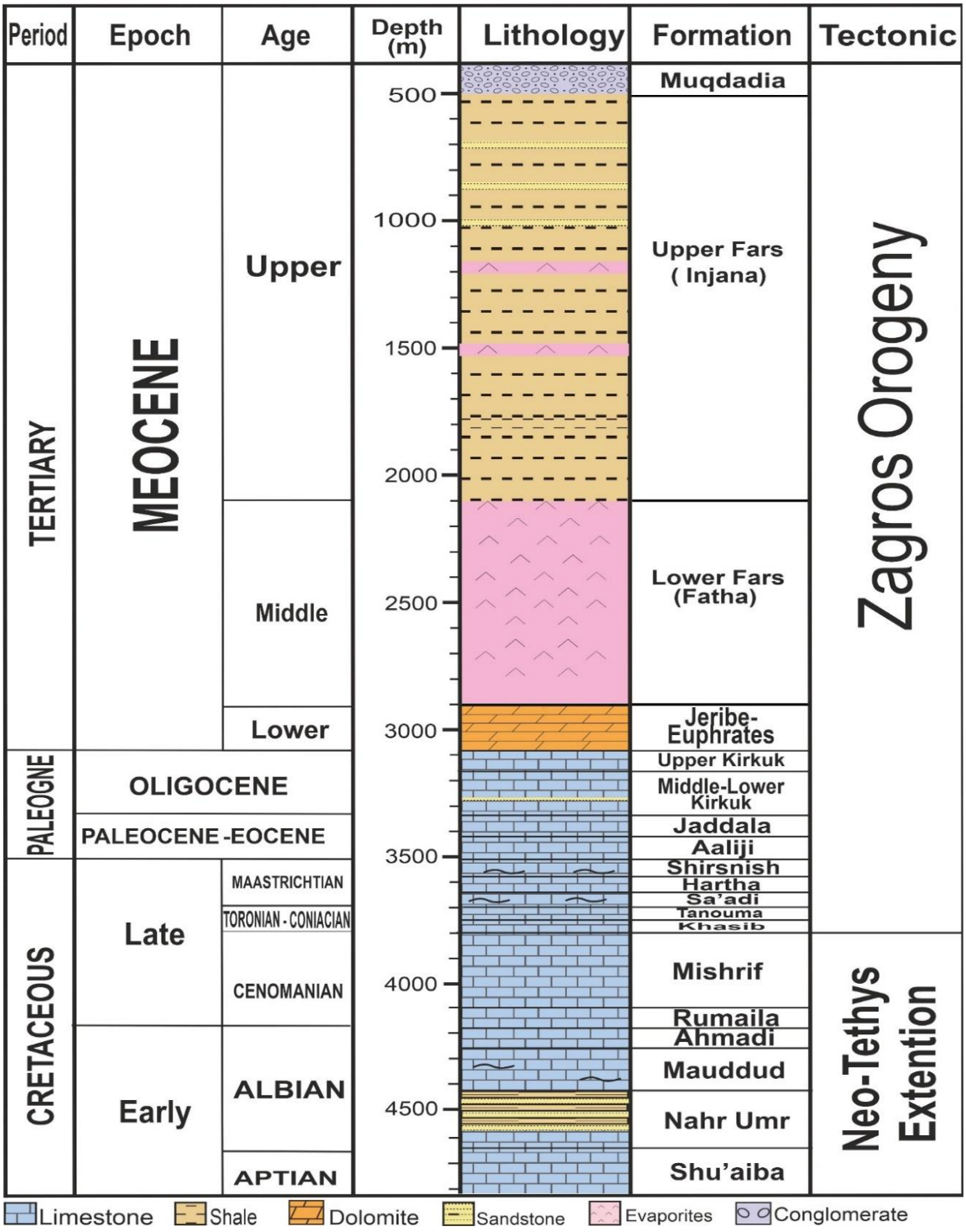

Figure(1-6) : Stratigraphic column of th Abu Ghirab (AG-17)according to the well final geological report

1.6. Materials and Methods

To provide reliable findings, several techniques and software tools are employed, including the following:

1.6.1. Data collection

The initial and most crucial stage of every research effort is data collection. The information needed for this research was gathered from the relevant Ministry of oil officials as well as from earlier investigations, final reports, maps, and petrophysical and geochemical studies of the Abu Ghirab oil field.

These data included an image of the Abu Ghirab oil field's structural contour map, images of the required well logs (Caliper, GR, SP, Sonic, Neutron, Density, and Resistivity logs) for the studied wells (AG-1, AG-3, AG-7, AG-13 -AG-17), a seismic section passing through the Abu Ghirab oil field, and end-of-well reports for the studied wells.

1.6.2. Analysis

1.6.2.1.Gas Chromatography

The gas chromatography (GC) method is used to isolate and identify hydrocarbon components in a crude oil rock extract or hydrocarbon fraction. A mobile phase (inert carrier gas) passes through a silica capillary column that contains a stationary phase in a narrow-diameter metal or glass tube, and specific ratios are computed, which are then used to analyze kerogen type, depositional environment, thermal maturity, and alteration effect (high molecular-weight liquid) . I was provided with three samples of crude oil that the Maysan Oil Company had prepared for study.

1.6.2.2. Gas Chromatography–Mass Spectrometry (GC-MS)

It combines the capabilities of gas-liquid chromatography and mass spectrometry to detect various compounds within a test sample. Gas chromatography is used to separate organic molecules, and the mass spectrometer acts as a detector for detailed chemical identification and structural information.

1.6.3. Software program

1.6.3.1. Didger software v5

Didger is an extremely precise digitizing application. Didger converts points, lines, and regions from charts, aerial photographs, paper maps, imported vector files, scanned raster images, and GeoTIFF photos into a flexible digital format usable by other programs.

1.6.3.2. Interactive petrophysics software v3.5 (IP)

IP is a smart and quick software platform for geoscientists who want to maximize the value of their subsurface findings. This activity may be completed with an interactive IP interface, increasing geoscientists' efficiency and productivity. IP is a collection of modules that may be used to analyze formations.

IP is a robust and versatile tool for transferring and analyzing well logs and a range of other critical data types, such as porosity and pore pressure, as well as reservoir production. The IP Basic package includes advanced data management, calculation, and deterministic workflow features.

1.6.3.3. Petrel software

Schlumberger invented and developed Petrel, a software tool used in petroleum exploration and production. It enables users to perform well correlation, analyze seismic data, construct models for investigated reservoirs, build maps, plan development strategies to increase reservoir production, and view the results of reservoir simulations.

It also allows users to make estimates. Throughout the reservoir's lifecycle, risk and uncertainty may be estimated.

1.6.3.4. PetroMod software

In this work, hydrocarbon generation, transport, and accumulation were modeled using the PetroMod software. PetroMod integrates multidimensional compaction, thermal, petroleum migration histories, geological, seismic, and stratigraphic interpretations with fluid movement in sedimentary basins.

1.7. Previos studies

1. **Beydoun (1992)** study Petroleum in the Zagros Basin The Zagros orogene is a conspicuous element of the Middle East hydrocarbon province. The Iranian and Iraqi oil fields in the Zagros foreland basin contain around one quarter of the vast oil reserves of the northeastern Arabian shelf.
2. **Al- Sharhan (1997)** researched Iraq's sedimentary basin and petroleum geology.
3. **Sepehr and Cosgrove (2004)** a research Describe of the Zagros Fold-Thrust Belt's structural foundation. The Zagros basin is divided by these fault zones into regions with various stratigraphic successions and rheological characteristics. Due to this, many structural designs evolved along the belt during the collision. In the Jurassic-Cretaceous, the Kazerun and Izeh Fault Zones served as a depositional system transition zone between the Lurestan and Fars areas and partially regulated the spread of the Kazhdumi Formation (one of the major source rocks).
4. **Pitman and Steinshouer *et al*.,(2004)** demonstrate how a basin-modeling approach may be used to predict petroleum formation and migration in the Mesopotamian Basin and Zagros Fold Belt.
5. **Alhuraishawy and Khayoon (2005)** Well logging and well-testing methodologies for the discovery of natural cracks in the Abughirab field and Asmari reservoir.
6. **Cooper (2007)** studied Fold and thrust belt structural type and hydrocarbon prospectivity: a worldwide study.

7. **Al-Khafaji (2010)** used carbon isotopes and biomarkers in a limited area of southern Iraq to study the relationship between crude oil and its source rock.
8. **Fouad (2012)** carried out a research project. The Western Zagros Fold-Thrust Belt, which is located on Iraqi soil, includes the Low Folded Zone as a crucial component. In this structural area, it is determined that the

mechanical characteristics of the folded sedimentary pile and the existence or absence of early created structural lines of weakness have had a first-order influence on the nature of the folding and faulting processes and their future evolution.

9. **Al-Ameri and Aqrawi (2013)** investigated the sedimentological characteristics of the mid-Cretaceous Mishrif reservoir in southern Mesopotamian.
10. **Hakimi and Najaf (2016)** they studied Origin of crude oils from oilfields in the Zagros Fold Belt, southern Iraq and Relation to organic matter input and paleoenvironmental conditions.
11. **Liu and Wen *et al*.,(2018)** studied Regional tectonic and sedimentary development, basin structural division, patterns of petroleum distribution, and key determinants of petroleum accumulation all point to it. It has gone through four key phases: the Mesozoic passive continental margin basin, the Cenozoic foreland basin, and the early Paleozoic intra-Cratonic pull-apart basin and platform margin basin. The basin was separated from southwest to northeast by the Zagros Mountain Front Fault and High Zagros Fault into the foredeep zone, simply folded zone, and Zagros thrust fault zone.
12. **Luo and Tan *et al.*,(2019)** Explanation of the study of the Asmar formation in the Zagros basin in northeastern Iraq, which contains a thick sequence of Oligocene-Lower Miocene carbonates and constitutes one of the best-known carbonate reservoirs in the world. It also contains dolostones, limestones, sandstones, and mudstones, and there is a general upward increase in the abundance of evaporates.
13. **Garzic and Vergés *et al.*, (2019)** used balanced and restored crustal-scale sections and forward modeling to study the Evolution of the NW Zagros Fold-and-Thrust Belt in the Kurdistan Region of Iraq.
14. **Al-Baldaw (2020)** studied, two wells of the Asmari Formation in the Abu Ghirab oil field, these wells were examined lithologically and their petrophysical characteristics were assessed.

Chapter Two
Reservoir properties

Chapter Two

Reservoir Properties

2.1. Introduction

The presence of a reservoir is one of the seven fundamental factors for commercial hydrocarbon accumulation. Theoretically, any rock may operate as an oil or gas reservoir. The majority of known deposits are located in sandstones and carbonates, although fields have also been discovered in shales and a range of igneous and metamorphic rocks. (Selley, 1998).

For a rock to function as a reservoir, it must possess the following two characteristics: To hold the hydrocarbons (oil or gas) within it, it must have pores (porosity). Furthermore, the holes must be linked to enable fluid circulation; in other words, the rock must be permeable (Selley, 1998).

In the Abu Ghirab oil field, the major field reservoirs which involve the largest amounts of oil accumulations are the Asmari Formation. Asmari Formation (Oligocene-Lower Miocene) divided into three sub-formation Jeribe-Euphrate and Kirkuk Group.Kirkuk group divided into three sub zones (upper Kirkuk, Middle-Lower Kirkuk) (Alsinbili, M.B. *et al*.,2013).

This work focused on studying the main reservoirs, Asmari, due to the availability of data needed to study them. We studied the petrophysical properties of reservoir below, based on the well logs data available to them, and to do so, we had to address the fundamental principles of well logs and petrophysical properties of reservoirs and how computing their works.

To do so, we need to understand the fundamental concepts of well logs and reservoir petrophysical parameters, as well as how to compute them.

2.2.Reservoir Evaluation:

However, the ultimate goal of well log interpretation is to assess the potential production of porous and permeable strata found during drilling. Along with the core analysis, a successful logging program can provide data for determining physical properties, defining lithology, identifying productive zones and accurately describing their depth and thickness, distinguishing

between oil and gas, and allowing a valid qualitative and qualitative interpretation of reservoir characteristics.

2.3. Basic principles of well logs

Well drilling gives a lot of geological and engineering information, especially when taking a core, but the process of taking a core is expensive in addition to the difficulty of obtaining it Therefore, the well log wire line probes were used to obtain additional information for the breached formations. The basic goal of well log interpretation is to use drilling to assess the potential production of porous and permeable formations.

Logging tools are one of the most advanced methods in terms of precision and complexity, and they are now playing a larger part in the geological decision-making process. Today, interpreting petrophysical logs is one of the most important and valuable tools accessible to a petroleum geologist.

2.3.1. Borehole Environmental Correction environment

The rock and fluids (rock-fluid system) in the area around a borehole are modified when a hole is bored into a formation. The drilling fluid contaminates the well's borehole and the surrounding rock, making logging measurements difficult (Gibson, 1982). The majority of the original formation water and hydrocarbons, if present, may be flushed away by filtration next to the borehole; this zone is known as the flushed zone (of resistivity R_{xo}). The displacement of formation fluids becomes less complete as you get further away from the borehole, resulting in a transition zone between mud filtrate and original formation fluid saturation, which is known as the transition or invaded zone (of resistivity R_{xo}).

The pores are then saturated with formation fluids (water, oil, and/or gas) in the area of the formation where they are not polluted by mud filtrate. This zone is referred to as the uninvaded zone (of resistivity Rt), as seen in (fig.2-1). The diameter of invasion refers to the size of the flushed zone (Di)

(Halliburton, 2001). The diameter of invasion, which is measured in inches depends on many factors (Gibson, 1982):

1- The nature of drilling mud.

2- The formation porosity and permeability.

3- The pressure differential between the mud column and the formation.

4- The time since the formation was first drilled.

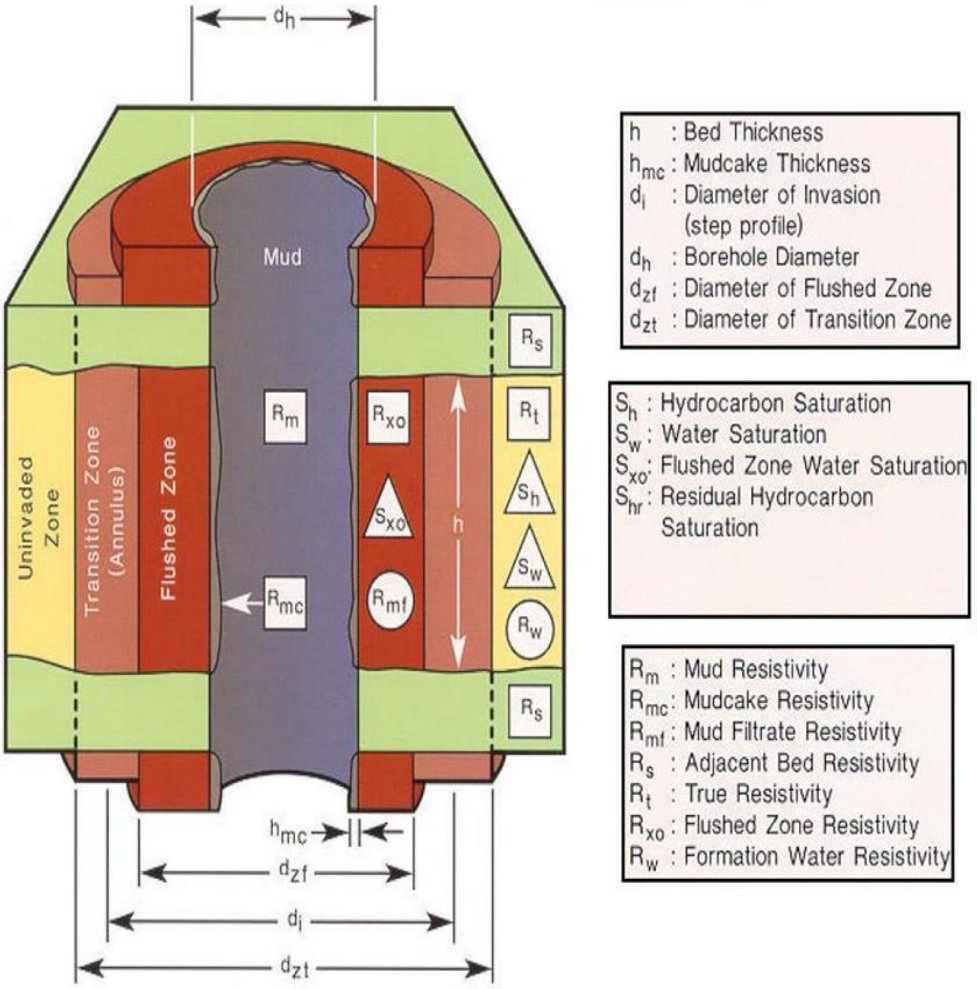

Figure (2-1): Showing the borehole environment (Halliburton, 2001).

2.3.2. Environmental Correction

The drilling activities, including the depth at which drilling fluid is invaded and the temperature difference between the surface and the depth of the formation, have an impact on the log readings. So, before calculating the reservoir's attributes, eliminate this influence. The environmental changes

made to well AG-7 using the Ip program are shown in (fig.2-2), together with those made to the other wells listed in Appendix A. The original and adjusted log readings of resistivity, density, neutron, and gamma-ray are found to match and deviate very slightly. The original reading is therefore used as input data for descriptions of petrophysical parameters.

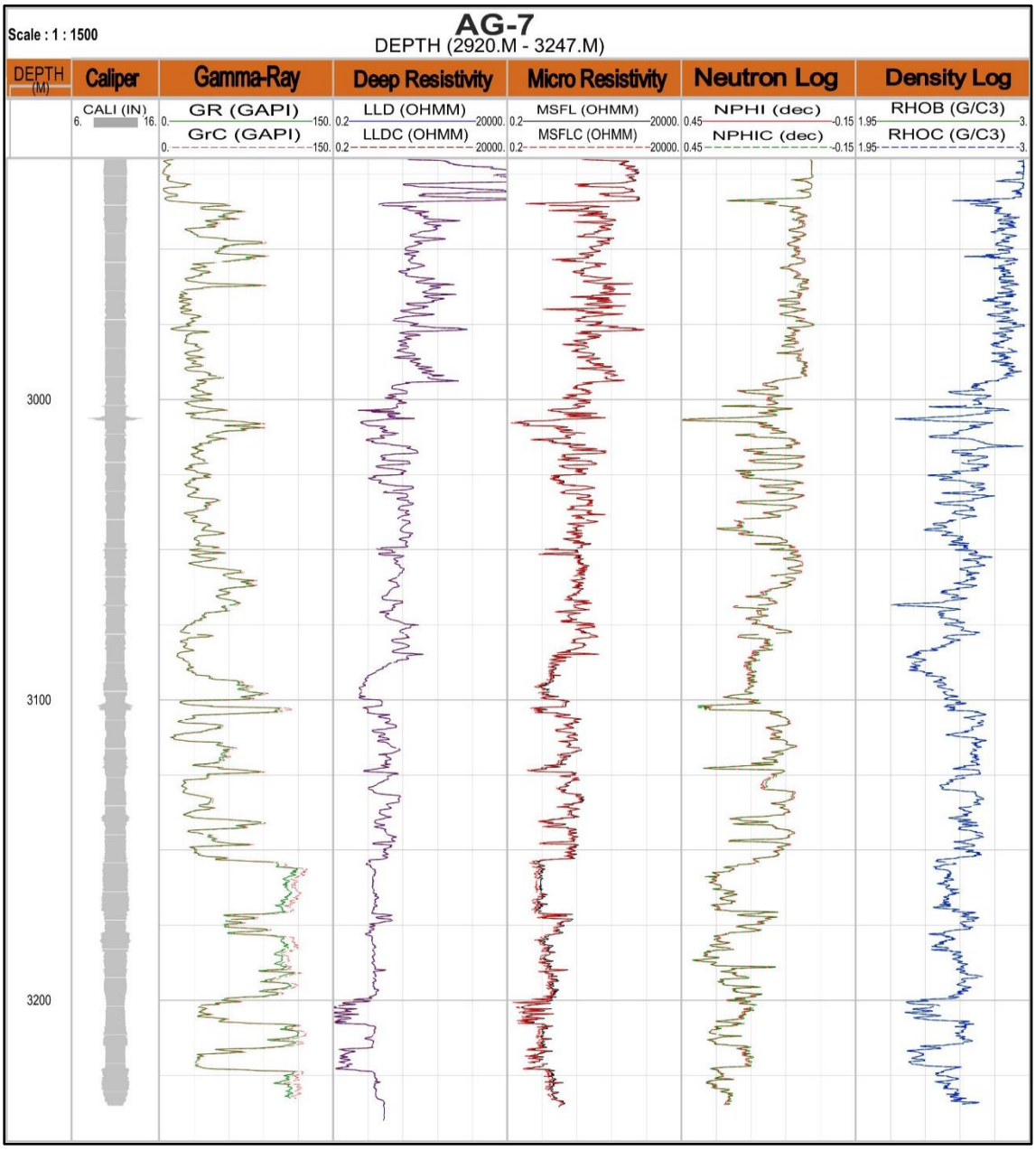

Figure (2-2): Environment correction for well logs measurement inAG-7.

2.3.3. Spontaneous Potential (SP)

The Spontaneous Potential (SP) log was one of the earliest electric logs utilized in the petroleum industry, and it has since played a key role in well log interpretation. The great majority of wells nowadays employ this type of log in their log suit. The Spontaneous Potential log is often used to

tell the difference between impermeable zones like shale and permeable zones like sand. It's measured in millivolts (Gibson, 1982).

The SP log is a record of direct current (DC) voltage (or potential) that naturally (or spontaneously) arises between a movable electrode in the bore hole and a fixed electrode at the surface (Asquith & Krygowski, 2004). The behavior of the SP log is mostly determined by the salinity differential between the drilling mud and the formation water shown in (fig.2-3) (Selley,1998).

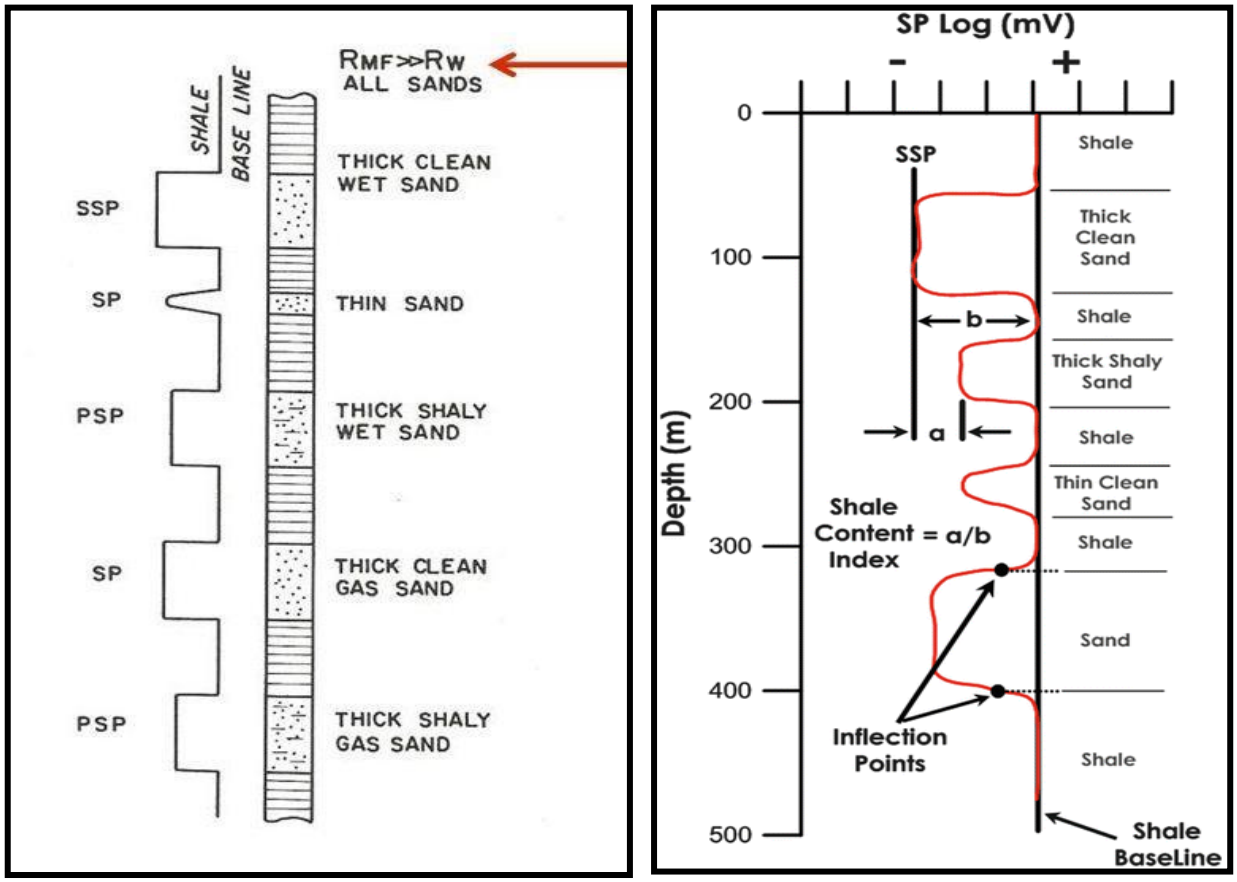

Figure (2-3): Explain Response log sp in front of rocks clastic (Selley,1998).

2.3.4. Gamma Ray log and Caliper:

Gamma-ray (GR) logs are used to determine lithologies and correlation zones by measuring natural radioactivity in formations. Shale-free sandstones and carbonates have low radioactive material concentrations and provide low gamma-ray measurements. Because of the abundance of radioactive elements in shale, the gamma-ray log response increases as shale content increases (Asquith and Krygowski, 2004).

Because the gamma measurement is impacted by hole diameter, it is usually used in conjunction with a caliper log, a mechanical instrument that records the borehole's diameter. (Selley,1998).

2.3.5.Resistivity logs

The oldest geophysical logging methods are electric logs, or resistivity logs, which were originally employed in oil and gas exploration by the Schlumberger brothers (Williams *et al.*, 2009). The capacity of a substance to hinder the flow of electric current through it is measured by its resistivity (Schlumberger, 1972).

Resistivity is the degree to which a substance " resists" or " hinders" the flow of electricity. The physical quality of a substance remains unaffected by its size or arrangement. In well logging, both resistivity and conductivity are commonly utilized, with one being the polar opposite of the other (Peters, 2006. The three main methods for determining the electrical resistivity of strata pierced by boreholes are the standard log, later blog, and Microspherically Focused Log approaches (Selley, 1998).

2.3.5.1.Normal log

With this log, electrical potential and current flow are established between an electrode on the sonde and an electrode on the surface (Selley, 1989).

2.3.5.2. Laterolog (LLD)

This log is based on very low-frequency current flows via a borehole from the tool to the formation. Electrode arrays on either side of the source electrode push the measuring current into a horizontal disk-shaped pattern around the borehole. Formation resistivity is determined by measuring the amount of current flowing from the tool. The tool must be able to make electrical contact with the formation. Laterolog's interpretation aims to measure true resistivity from the formation (Rt), which is then utilized to determine water and oil saturation in the uninvaded zone (Sw, Sh) (Asquith and Krygowski, 2004).

2.3.5.3.Micro spherically Focused Log (MSFL)

Micro spherically Focused Logs (MSFL) are shallow depth investigations that measure the invaded zone's (Rxo) resistivity. The electrodes are put on a pad that is pressed up against the borehole wall (Asquith and Gibson, 1982).

2.3.6 .Porosity Log

Porosity may be determined in three different ways: directly from cores, indirectly through geophysical well logs, and indirectly from seismic data (Selley, 1998).

In this study, porosity was determined using three different types of logs: density, neutron, and sonic logs.

2.3.6.1. Density log

The density log works by releasing gamma radiation from the tool and measuring the quantity of gamma radiation returned from the formation. As a result, the gamma-gamma tool is a common moniker for the equipment (Selley,1998), The Greek letter (ρ) denotes density, which is expressed in grams per cubic centimeter, or g/cm3.

The bulk density (ρb or RHOB) and the matrix density formation (solid and fluid portions) as determined by the logging instrument are employed by the density log. The rock's solid structure has a density called matrix density (Asquith and Krygowski, 2004).

The fluid collected in the pores around the borehole of a well is known as mud filtrate. Because the equipment only has a limited depth of research and effectively only analyzes the region of the formation invaded by filtrate from the drilling mud, this value for porosity is read. As a result, the fluid density can range from 1.0 g/cm3 for freshwater mud to 1.1 g/cm3 for saline mud. The accuracy of the density-derived porosity of reservoirs is also influenced by shale. The formation density log can be used to track porosity.

When the matrix density (*ρma*) and the density of the saturating fluids (*ρf*) are known, porosity may be calculated from the bulk density of clean liquid-filled formations (Asquith & Krygowski, 2004):

$$\Phi D = \frac{(p_{ma} - p_b)}{(p_{ma} - p_f)} \quad \ldots\ldots\ldots (2\text{-}1)$$

Where:

- $\boldsymbol{Ø_D}$: Porosity by density log.
- $\boldsymbol{\rho ma}$: Density of the dry rock (gm/cm^3), see table (2-2).
- $\boldsymbol{\rho f}$: Density of fluid (gm/cm^3) = 1 gm/cm^3 for freshwater or 1.1 gm/cm^3 for salt mud.
- $\boldsymbol{p_b}$: is the formation bulk density, gm/cc.

Table (2-1): Matrix densities values of common lithologies.Modified after (Asquith & Krygowski, 2004)

Lithology / Fluid	ρma or ρf gm/cm3 (kg/m3)
Sandstone	2.644 (2644)
Limestone	2.710 (2710)
Dolomit	2.877 (2877)
Anhydrite	2.960 (2960)
Salt	2.040 (2040)
Freshwater	1.0 (1000)
Saltwater	1.15 (1150)

2.3.6.2. Neutron log

Neutron logs, also known as porosity logs, are used to quantify the quantity of hydrogen in a deposit. In clean formations (no shale), the neutron log (NPHI) calculates liquid fluid porosity where the porosity is filled with oil or water (Asquith & Krygowski, 2004). Neutron logs are primarily used to demarcate porous formations and determine their porosity.

They are mostly affected by the amount of hydrogen in the formation (Schlumberger, 1972). In API units, the neutron log was kept. Because shale

always includes some bound water, the neutron log in unclean reservoirs will always produce a greater apparent porosity measurement than there is. Oil and water both have nearly the same amount of hydrogen, while hydrocarbon gas has less. In gas reservoirs, the neutron log may therefore provide a porosity reading (Selley, 1998).

We can make the corrections of Neutron, Density, and Sonic derived porosities by using the following relationships.

For Neutron porosity (Desbrandes, 1985)

$$\Phi N_{corr} = \Phi N - (V_{sh} * \Phi N_{sh}) \quad \ldots\ldots (2\text{-}2)$$

ΦN: neutron porosity

ϕNsh: is the neutron porosity in shale formation

Vsh = volume of shale

2.3.6.3. Acoustic or Sonic logs

The sonic instrument measures the interval transit time (t), which is the time in microseconds it takes for an acoustic wave to go through 1 foot (or 1 m) of a formation along a route parallel to the borehole. Both lithology and porosity influence the interval transit time (t). Interval transit times of clicks emitted from one end of the sonde traveling to one or more receivers at the other end are recorded using this approach. Sound waves travel quicker through a formation than through muck in a borehole (Selley, 1998). The Wyllie time-average equation (Wyllie *et al.*, 1958) can be used to calculate porosity:

$$\Phi s = \frac{(\Delta t_{log} - \Delta t_{ma})}{(\Delta t_f - \Delta t_{ma})} \quad \ldots\ldots (2\text{-}3)$$

When the volume shale>10%

$$\Phi s = \frac{(\Delta t_{log} - \Delta t_{ma})}{(\Delta t_f - \Delta t_{ma})} - \frac{\Delta t_{sh} - \Delta t_{ma}}{\Delta t_f - \Delta t_{ma}} \ldots\ldots (2\text{-}4)$$

Where:

Φ_s= sonic-derived porosity.

Δt_{log}= interval transit time in the formation(recorder by log).

Δt_f= interval transit time of the formation fluid (saltwater mud= 185 μsec/ft, fresh water mud 189 μsec/ft).

Δt_{ma}= interval transit time of matrix by using the table (2-3) (Schlumberger, 1972).

The interval transit time (Δt) of a formation is increased due to the presence of hydrocarbons (i.e.,hydrocarbon effect). If the effect of hydrocarbons is not corrected, the sonic-derived porosity is too high(Selley,1998). Hilchie (1978) suggests the following empirical corrections for hydrocarbon and gas effects that are used in current study:

$$\Phi s_{corr} = \Phi_s * 0.7 \text{ ----- gas } \ldots\ldots(2\text{-}5)$$

$$\Phi scorr = \Phi s * 0.9 \text{ ----- oil } \ldots..(2\text{-}6)$$

Φs_{corr} = corrected sonic porosity

Φs = sonic-derived porosity

Table (2-2): Interval transit times and sonic velocities for various matrixes (Schlumberger, 1972)

Lithology/Fluid	Matrix Velocity ft/sec	Δt_{matrix} or Δt_{fluid}(Wyllie) μsec/ft [μsec/m]	Δt_{matrix}(RHG) μsec/ft[μsec/m]
Sandstone	18,000 to 19,500	55.5 to 51.0 [182 to 186]	56[184]
Limestone	21,000 to 23,000	47.6[156]	49[161]
Dolomite	23,000 to 26,000	43.5[143]	44[144]
Anhydrite	20,000	50.0[164]	
salt	15,000	66.7[219]	
Casing(iron)	17,500	57.0[187]	
Freshwater mud filtrate	5,280	189[620]	
Saltwater mud filtrate	5,980	185[607]	

2.4 . Interpretation of well log data and Its Applications

2.4.1. Determination of Lithology and Mineralogy

2.4.1.1. Neutron-density lithology cross plot

One of the first quantitative interpretation techniques is the neutron-density cross plot. It is significant and commonly used because it offers strong lithological resolution for quartz, calcite, and dolomite as well as adequate resolution of porosity (Ellis and Singer, 2008).

The combination of these logs is used to determine lithology and porosity. The neutron log is represented on the horizontal axis, while the density log is represented on the vertical axis (Jia, 2010).

From figures (2-4, 5, 6,7, and 8) the Jeribe – Euphrates most point full on the dolomite line mainly in the study area and upper Kirkuk on the Limestone line, and Middle lower Kirkuk on the Limestone line and few points fall on the sandstone and limestone line which indicated on the lithology of Asmari is Formation.

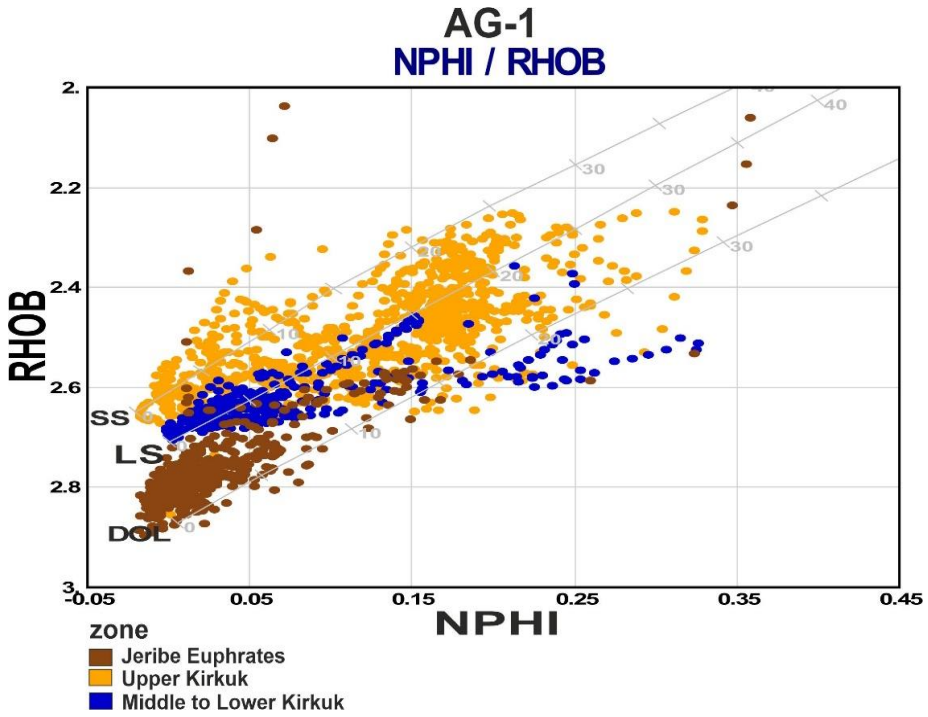

Figure (2-4): Neutron – Density cross plots of reservoir AG-1

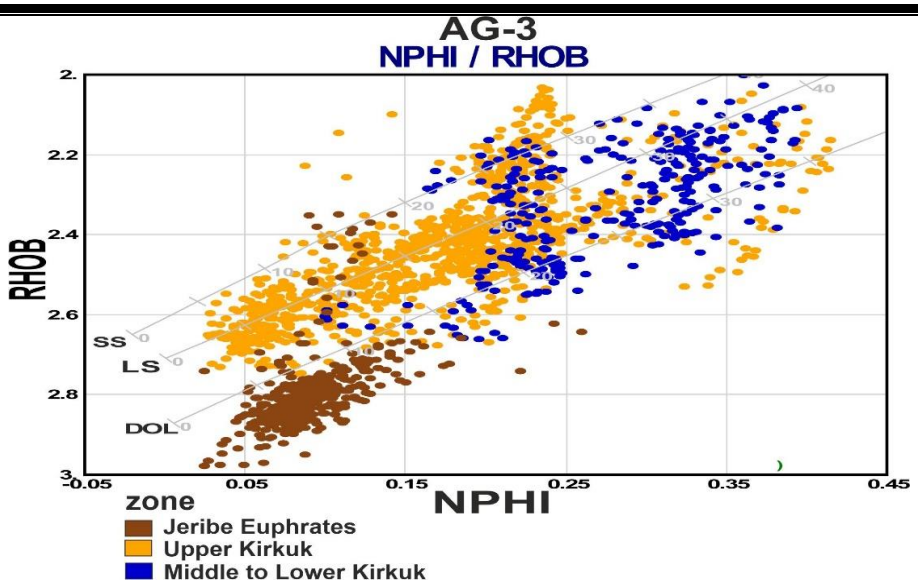

Figure (2-5): Neutron – Density cross plots of reservoir AG-3

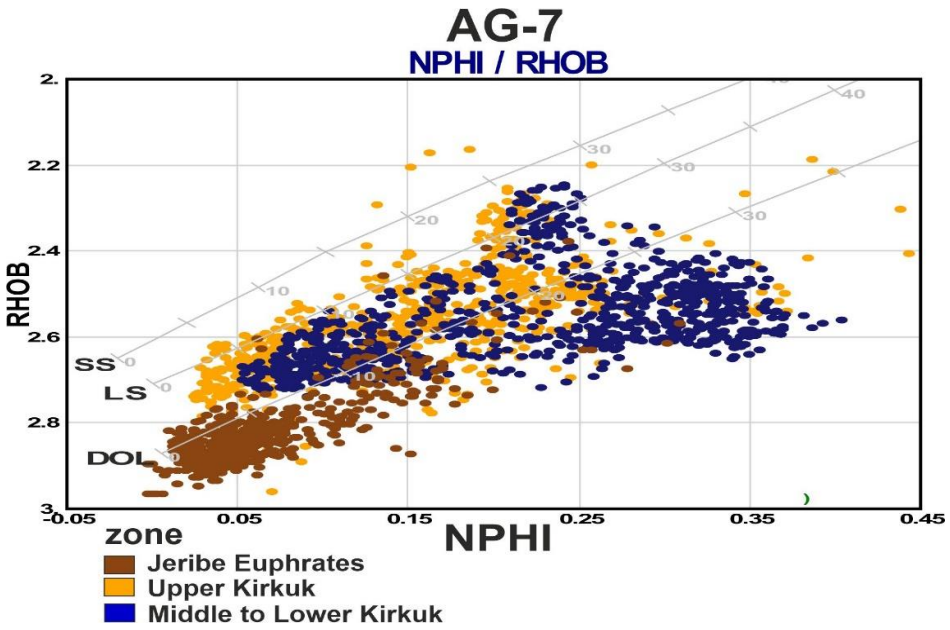

Figure (2-6): Neutron – Density cross plots of reservoir AG-7

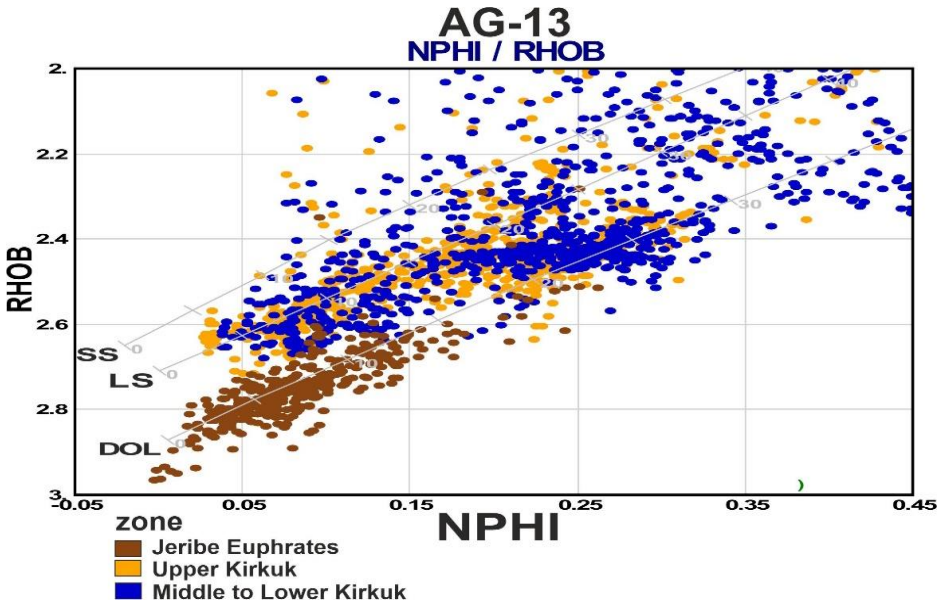

Figure (2-7): Neutron – Density cross plots of reservoir for AG-13

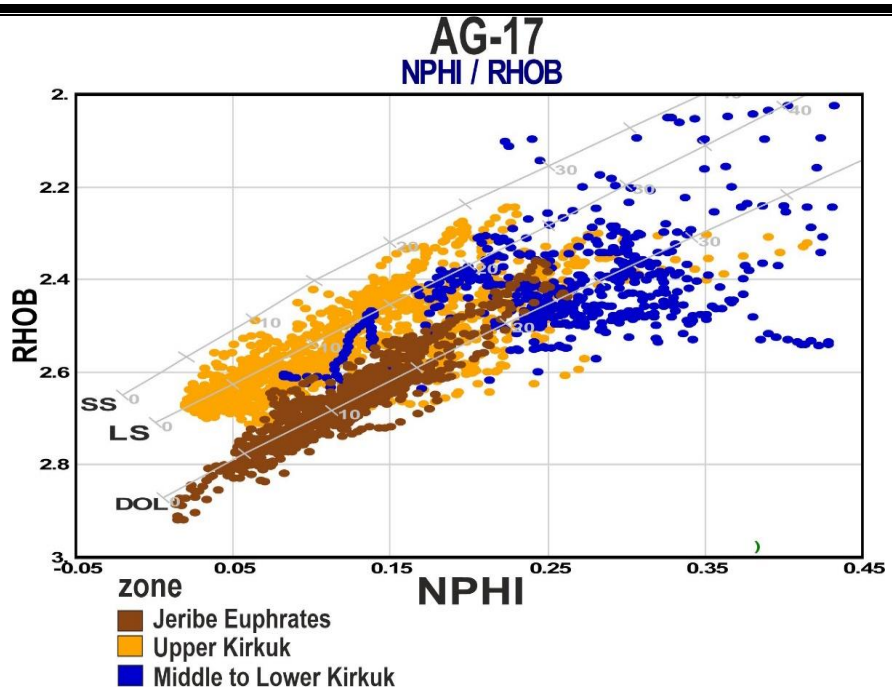

Figure (2-8): Neutron – Density cross plots of reservoir AG-17

2.4.1.2. M-N Lithology cross plot

The major purpose of this cross plot is to examine the data from all three porosity logs to discover the M and N values that are lithology-dependent. The M and N variables indicate the slopes of certain lithology lines on the Sonic-Neutron and Sonic-Density cross-plot charts, respectively. As a result, these variables (M and N) are largely independent of porosity, and mineralogy may be determined from a cross plot of these two variables. Gibson (Gibson, 1982). The letters M and N are defined as (Schlumberger, 2005).

$$M = \frac{\Delta tf - \Delta t \log}{\rho b - \rho f} * 0.01 \quad \text{…..(2-7)}$$

$$N = \frac{\emptyset NF - \emptyset N}{\rho b - \rho f} \text{…..(2-8)}$$

Where:

- ***Δtf*:** interval transit time in fluid (189 m/s for fresh water and 185 m/s for salt mud).
- ***Δt*:** interval transit time (the log reading).
- ***ρb*:** formation bulk density (the log reading).
- ***ρf*:** fluid density (1 gm/cm3 for freshwater or 1.1 gm/cm3 for salt mud).

- ***ØNF* :** neutron porosity for fluid = 1.
- ***ØN*:** neutron porosity.

figures (2-9, 10, 11,12, and 13) show that calcite and dolomite are the main mineral in the Asmari Formaion in the Abu Ghirab field with some Anhydrite, especially in well AG-17.

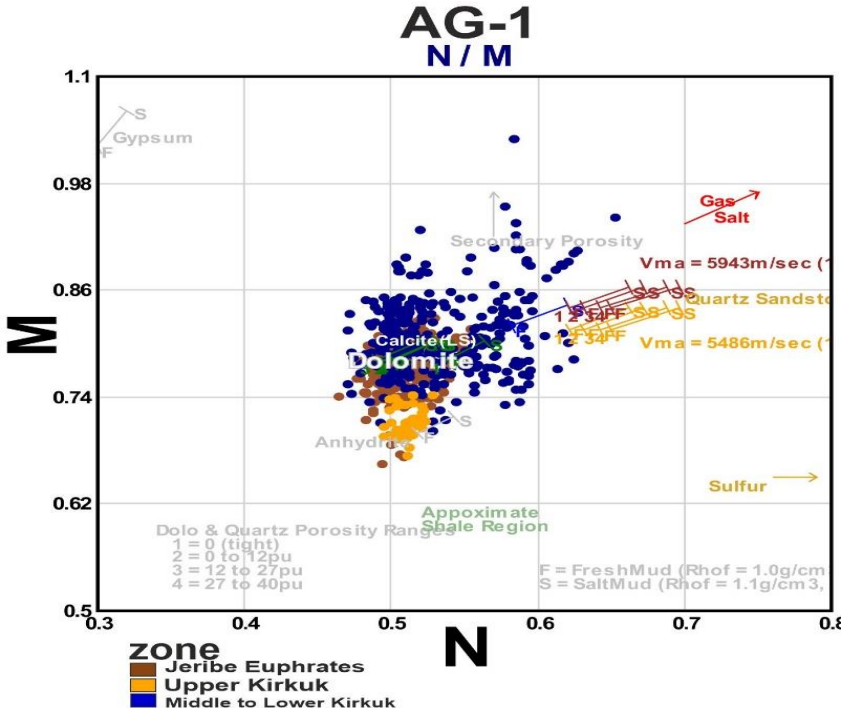

Figure (2-9): M – N cross plots of the reservoir for AG-1

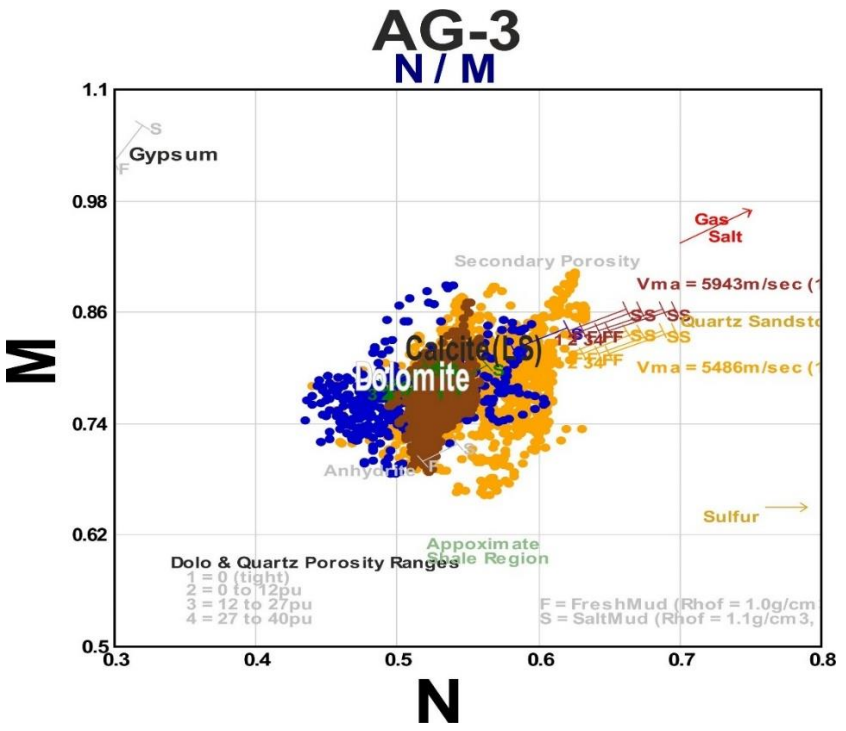

Figure (2-10): M – N cross plots of the reservoir for AG-3

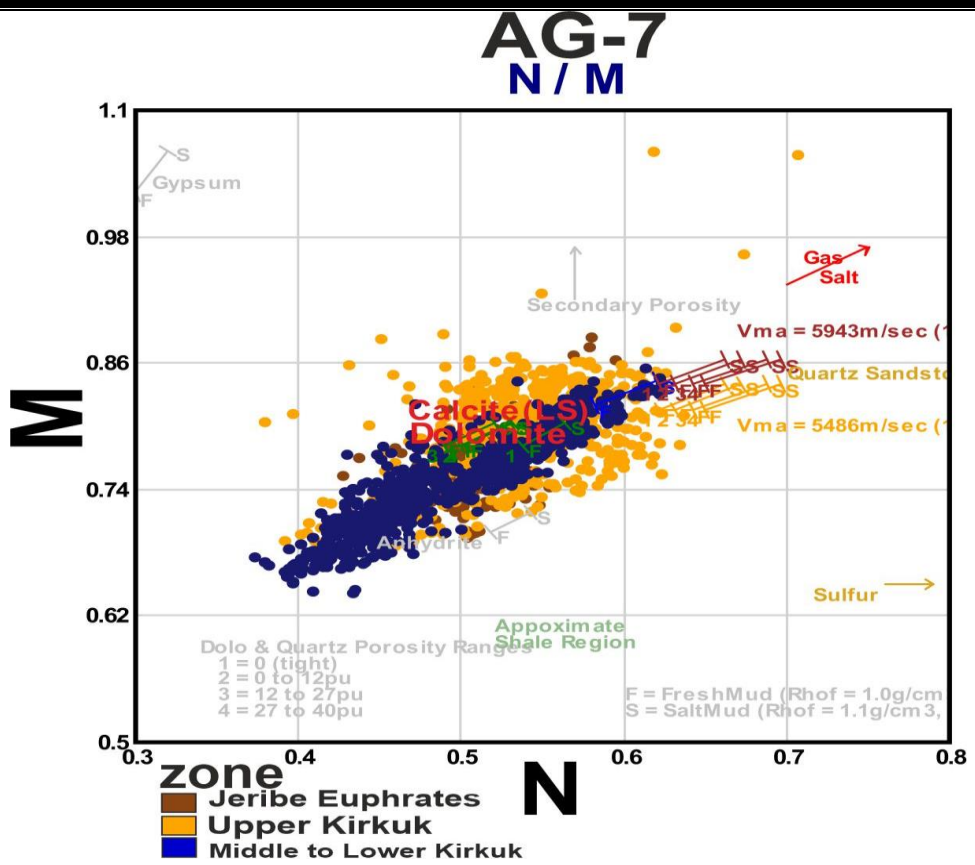

Figure (2-11): M – N cross plots of the reservoir for AG-7

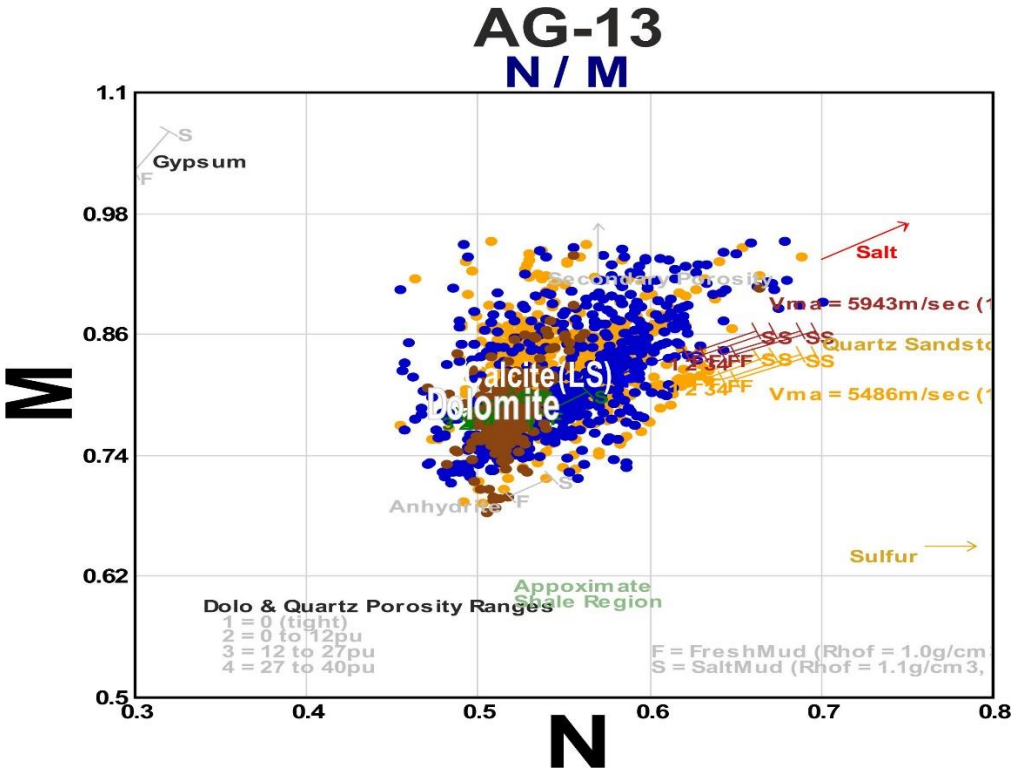

Figure (2-12): M – N cross plots of the reservoir for AG-13

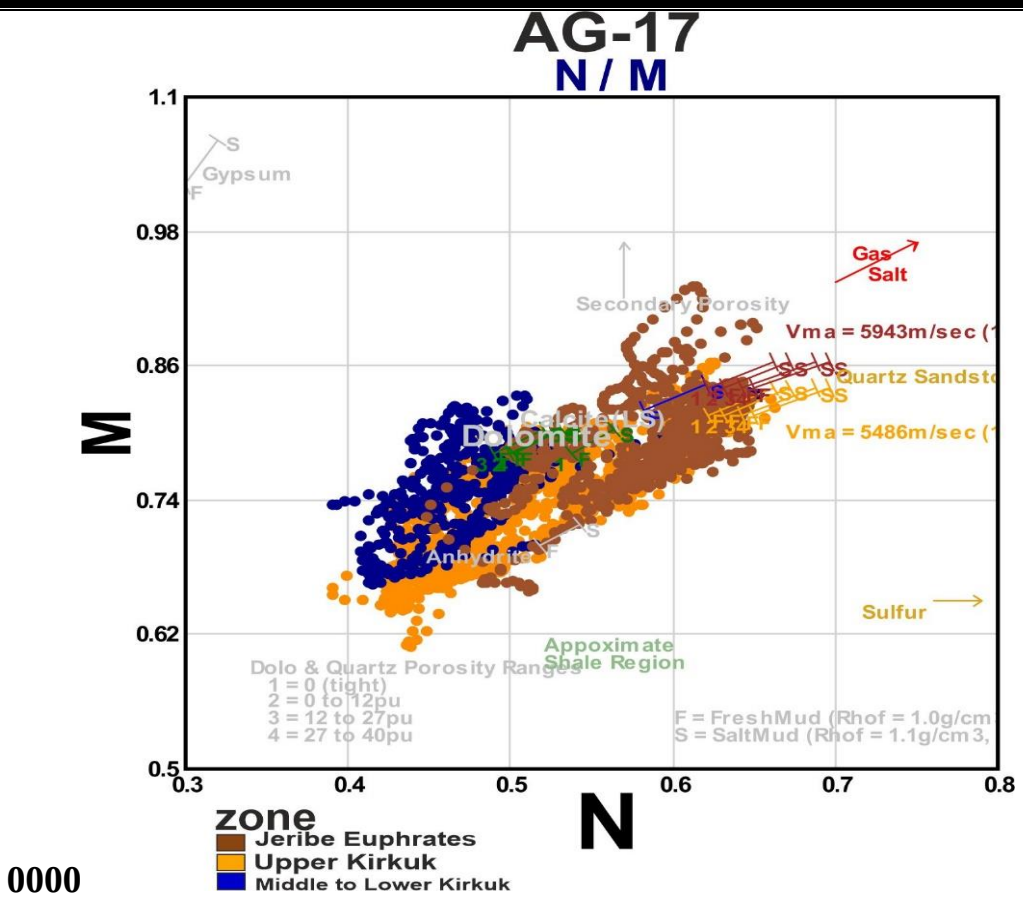

0000

Figure (2-13): M – N cross plots of the reservoir for AG-17

2.4.1.3. Matrix identification (MID) cross plot

The matrix identification (MID) cross plot may also be used to determine lithology, gas, and secondary porosity . The apparent transit time in rock matrix (Δtma) may easily be used to determine lithology. Three logs are required to utilize the MID cross plot: sonic, neutron, and density logs. The lithology of these logs is important (Asquith & Krygowski, 2004). The obtained neutron density must be used to calculate the apparent total porosity (Øta). According to Schlumberger (2005), the apparent density of matrix (ρmaa) and apparent transit time (Δtmaa) is calculated using the following equations:

$$RHOmaa = \frac{\rho b - \emptyset ta.\rho f}{1 - \emptyset ta} \quad \ldots\ldots(2\text{-}9)$$

$$\Delta tmaa = \frac{\Delta tlog - \emptyset ta.\Delta tf}{1 - \emptyset ta} \quad \ldots\ldots(2\text{-}10)$$

Where:

- ***RHOmaa* :** density of matrix (gm/cc).
- ***Δtmaa* :** transit time in rock matrix (µsec/ft).
- ***Øta* :** is the apparent total porosity.

The figures (2-14, 15, 16,17, and 18) of MID cross plot show the type of matrix in Asmari Formation in the Abu Ghirab field that is represented by mainly calcite and dolomite with few points falling in quartz

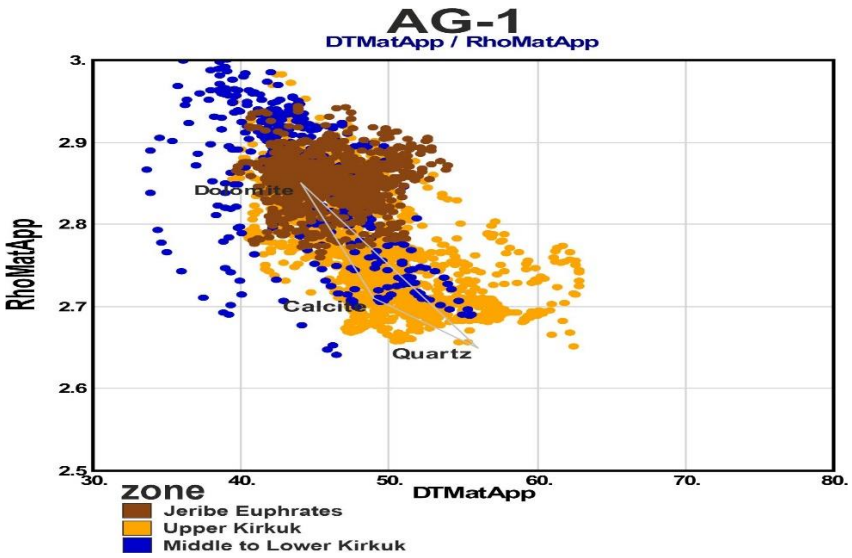

Figure (2-14): MID cross plot for AG-1

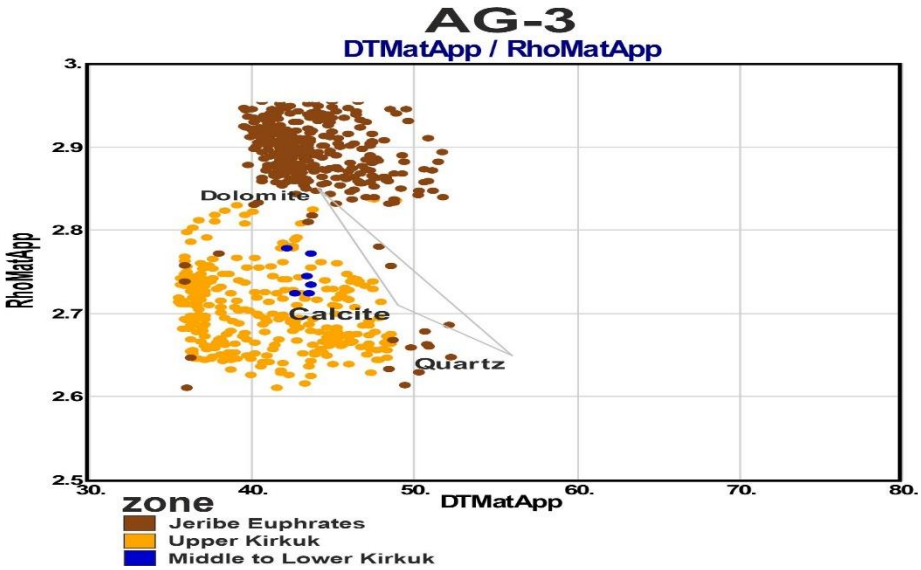

Figure (2-15): MID cross plot for AG-3

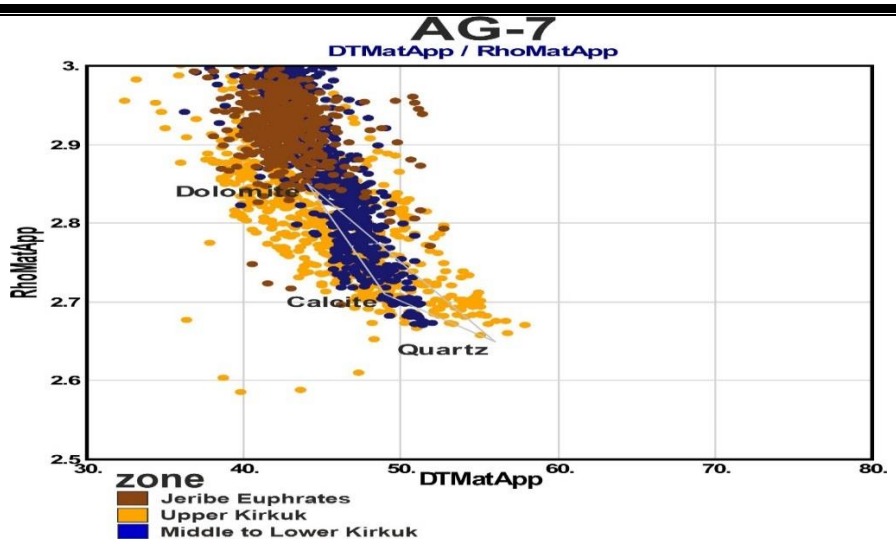

Figure (2-16): MID cross plot for AG-7

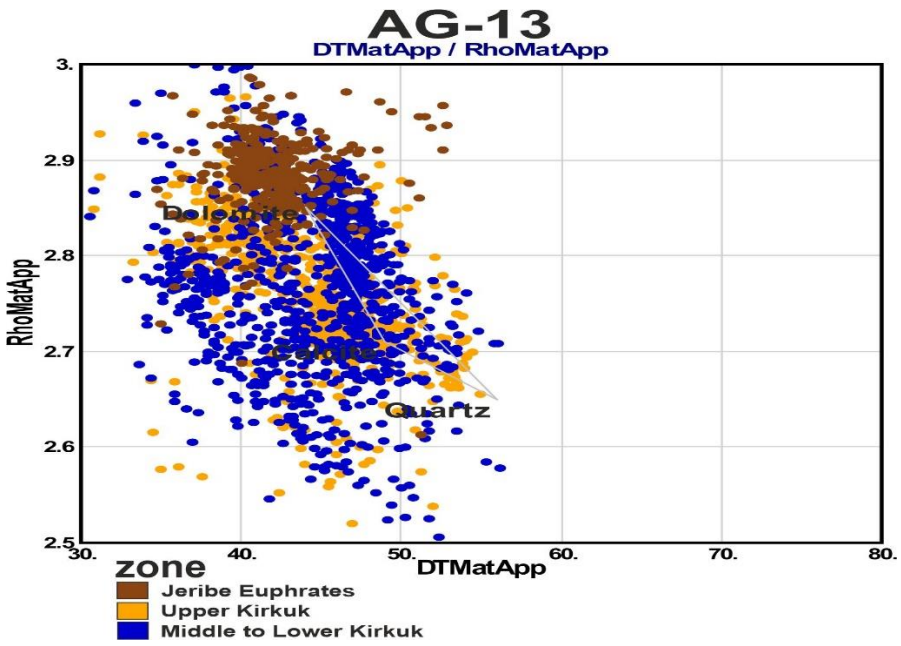

Figure (2-17): MID cross plot for AG-13

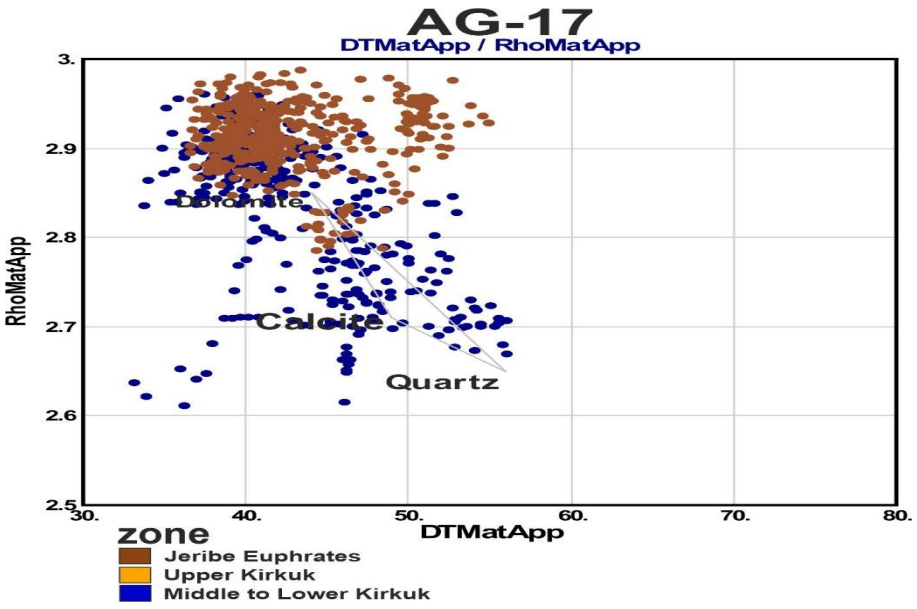

Figure (2-18): MID cross plot for AG-17

2.4.2. Calculation of Shale Volume (Vsh)

Shale is more radioactive than sand or carbonate, therefore gamma-ray logs can be used to estimate its volume in porous reservoirs (Asquith and Gibson, 1982). The first step in determining the volume of shale from a gamma ray log is to calculate the gamma-ray index (the following formula from Schlumberger, 1974).

$$I_{GR} = \frac{(GR\,log - GRmin)}{(GR\,max - GRmin)} \quad \ldots\ldots(2\text{-}11)$$

Where:

I_{GR} = index of gamma-ray.

GR_{log} = Gamma-Ray (API).

GR_{min} = Gamma-Ray minimum (carbonate or clean sand).

GR_{max} = Gamma-Ray maximum (shale).

In the study of this work, the formula of Larionov (Larionov v.v. 1969) for Tertiary rocks was used to determine the shale volume

$$Vsh = 0.83 * (2^{3.7 * IGR} - 1) \quad \ldots\ldots \quad (2\text{-}12)$$

Where:

Vsh = volume of shale.

IGR= gamma ray index.

ShaleVolume (Vsh) was calculated using an Interactive Petrophysics program by determining the maximum value of the shale and the minimum value of the shale as in (fig. 2-19,20).

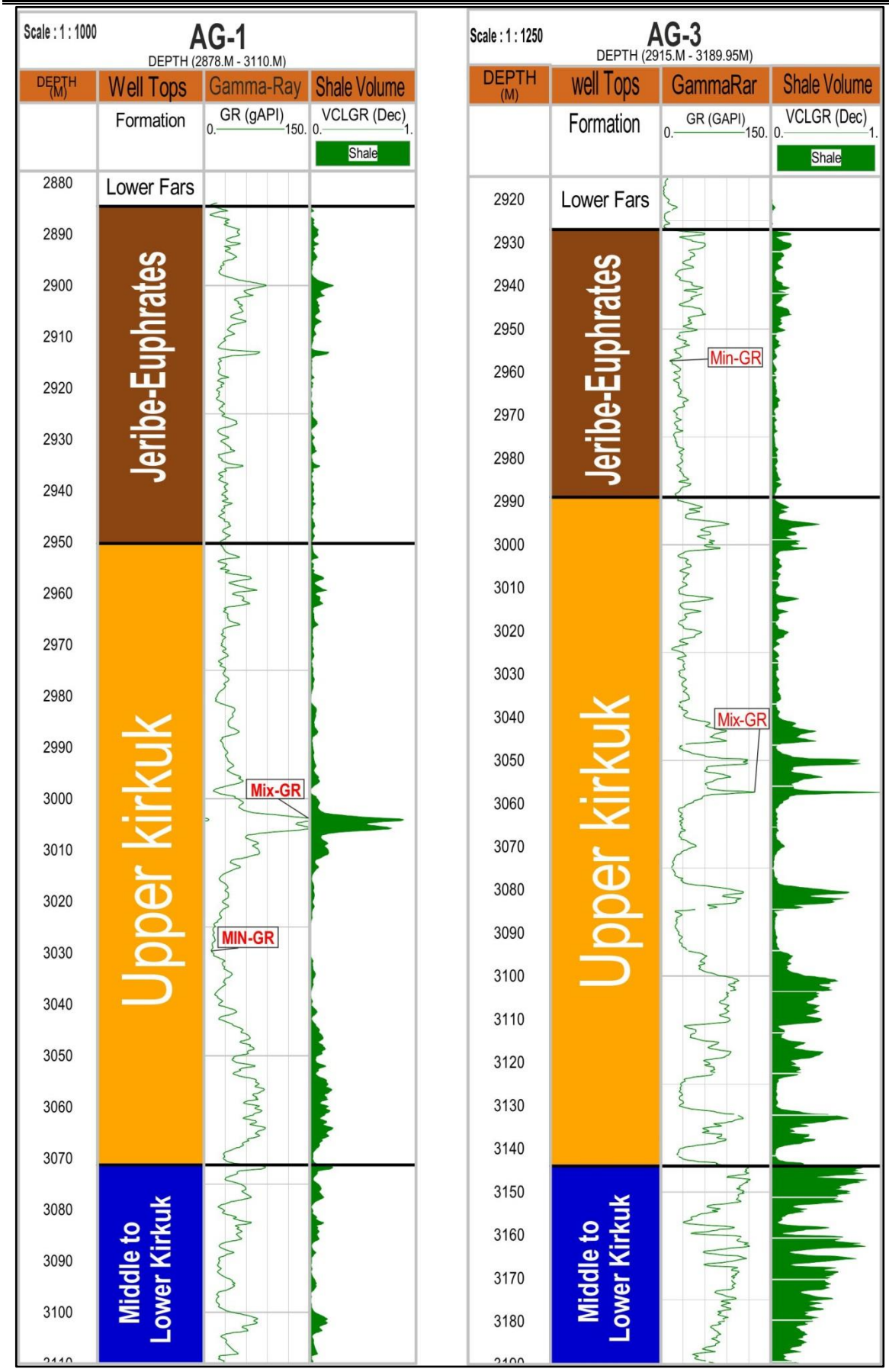

Figure (2-19): Shale volume of studied wells for AG-1 and AG-3

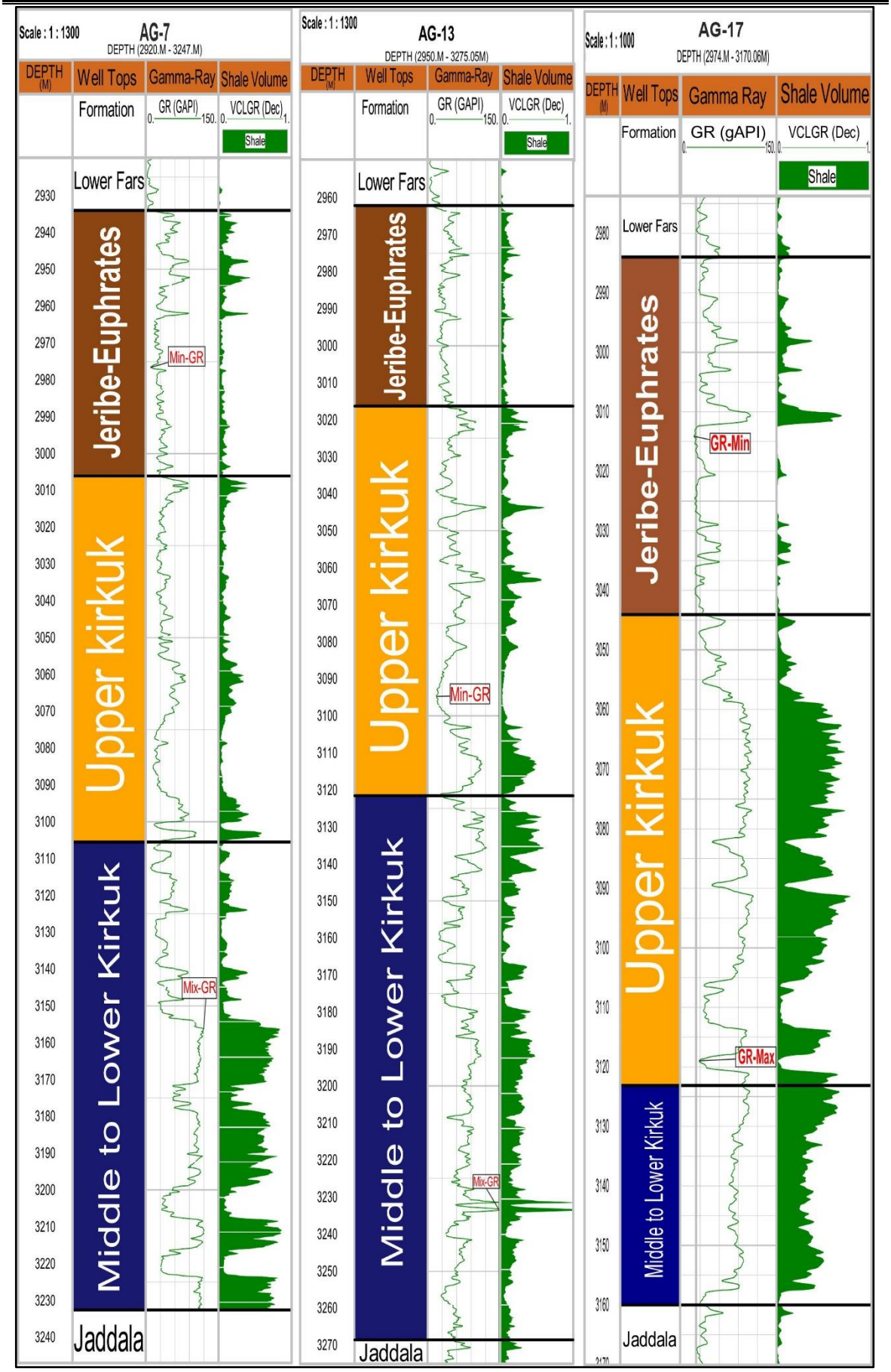

Figure (2-20): Shale volume of studied wells for AG-7, AG-13 and AG-17

2.4.3. Porosity Calculation

The ratio of pore volume to the bulk volume of a substance is known as porosity. In oil and gas reservoirs, pore volume refers to the amount of space accessible for the storage of hydrocarbons and water. It is commonly symbolized by the Greek letter Phi (Φ), Porosity is measured as a percentage of bulk volume and is denoted by (Bowen, 2003).

$$\Phi = (vp/vt) * 100 \quad \text{.....(2-13)}$$

Where:

Φ = Porosity

v_p= Pore volume.

v_t= Total rock sample volume.

And based on the percentage the porosity of the rock is classified according to (Leverson, 1972)

Table (2-3): the classification porosity according to (Leverson, 1972)

Porosity Φ	Type of Porosity
>5	Negligible
5 - 10	Poor
10 - 15	Fair
15 - 20	Good
20 - 25	Very good
>25	Excellent

It's critical to comprehend the many sorts of porosity.

2.4.3.1. Total Porosity

Regardless of whether or not all pores are linked, it total prosity computed by dividing the volume of all pores by the volume of the bulk material (Bowen, 2003). Schlumberger (1974) presented an equation that can be written and may be used to calculate the total porosity using neutron and density logs.

$$\Phi N.D = \frac{\Phi N + \Phi D}{2} \quad \ldots\ldots(2\text{-}14)$$

Where:

ΦN.D = Combination of neutron and density porosities (total porosity Φt).

ΦN = porosity from neutron.

ΦD = porosity from density.

2.4.3.2. Effective porosity

Effective porosity is the total volume of reservoir rock divided by the number of linked pores (Bowen, 2003). Total porosity minus clay-bound water and water retained in the porosity of clays (Darlling, 2005). The formula for calculating the effective porosity is (Schlumberger, 1972).

$$\boldsymbol{\Phi e = \Phi t * (1 - Vsh)} \quad \ldots\ldots(2\text{-}15)$$

Where:

Φ_e= effective porosity.

Φ_t= total porosity (Φ N.D).

2.4.3.3. Primary porosity

Is the number of pores existing or created in sediment at the moment of sedimentation. The amount of space between rocks determines how grains develop (Halliburton, 2001). The sonic porosity represents the main (intergranular) porosity (Asquith and Gibson, 1982). Primary porosity is calculated through this study by the sonic log, as in the equation.

$$\boldsymbol{\Phi c = \Phi s * Bhc} \quad \ldots\ldots(2\text{-}16)$$

That is where:

Φc: porosity corrected the effect of hydrocarbons.

Bhc = Effect of hydrocarbons coefficient of 0.7 compensates for the gas and 0.9 for oil.

2.4.3.4.Secondary porosity

Is the porosity that occurs as a result of digenesis processes such as deposition, re-crystallization, and dolomitization, or as a result of rock fracture following deposition (Tiab and Donaldson, 2004). whereas equation was used in reservoir studies with greater than 10% shale content (Schlumberger, 1997).

$$\boldsymbol{SPI = \Phi N.D - \Phi Sc} \quad \text{.....(2-17)}$$

Where:

SPI: Secondary porosity index coefficient.

ΦSc: corrected sonic–derived porosity.

ΦN.D: neutron–density properties combination (total porosity).

The figures (2-21 and 22) show the total, secondary and effective porosity in studied wells. Leverson (1972) classified porosity in the manner depicted in the table (2-4), porosity ranges from fair to good in the Asmari Formation, and the unit Upper Kirkuk is good Effective porosity.

In most intervals of the Asmari reservoir, the secondary porosity is minimal and generally less than the total porosity. Despite being somewhat greater in some Asmari Formation periods, particularly in AG-1 and AG-17, the overall porosity remains the greatest. These areas of increased secondary porosity indicate that dolomitization and dissolution, two diagenesis processes, have had an impact on the porosity of the Asmari Formation.

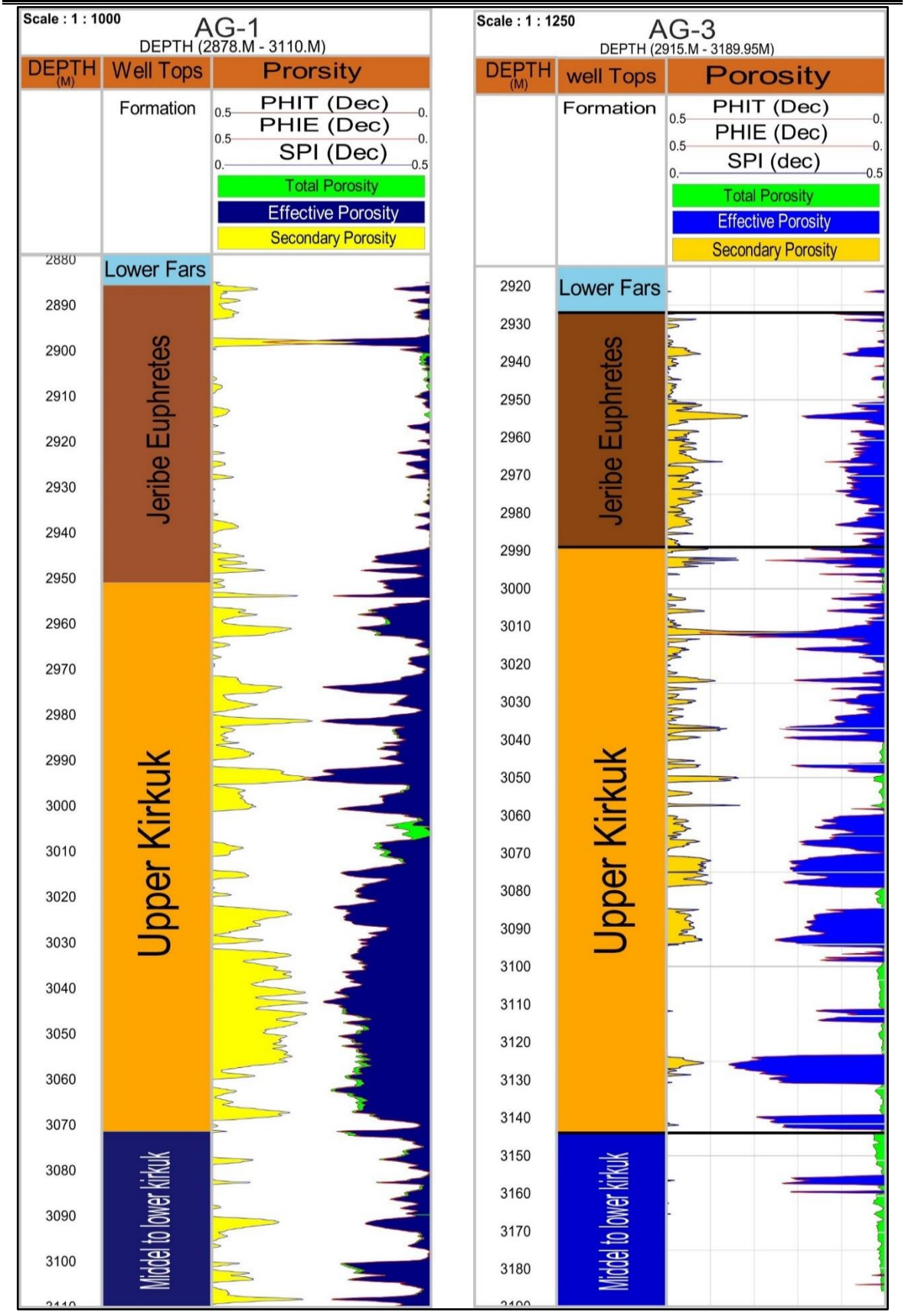

Figure (2-21): Porosity types (Total, Secondary and Effective) of Asmari Formation in Abu Ghirab field of AG1, AG-3

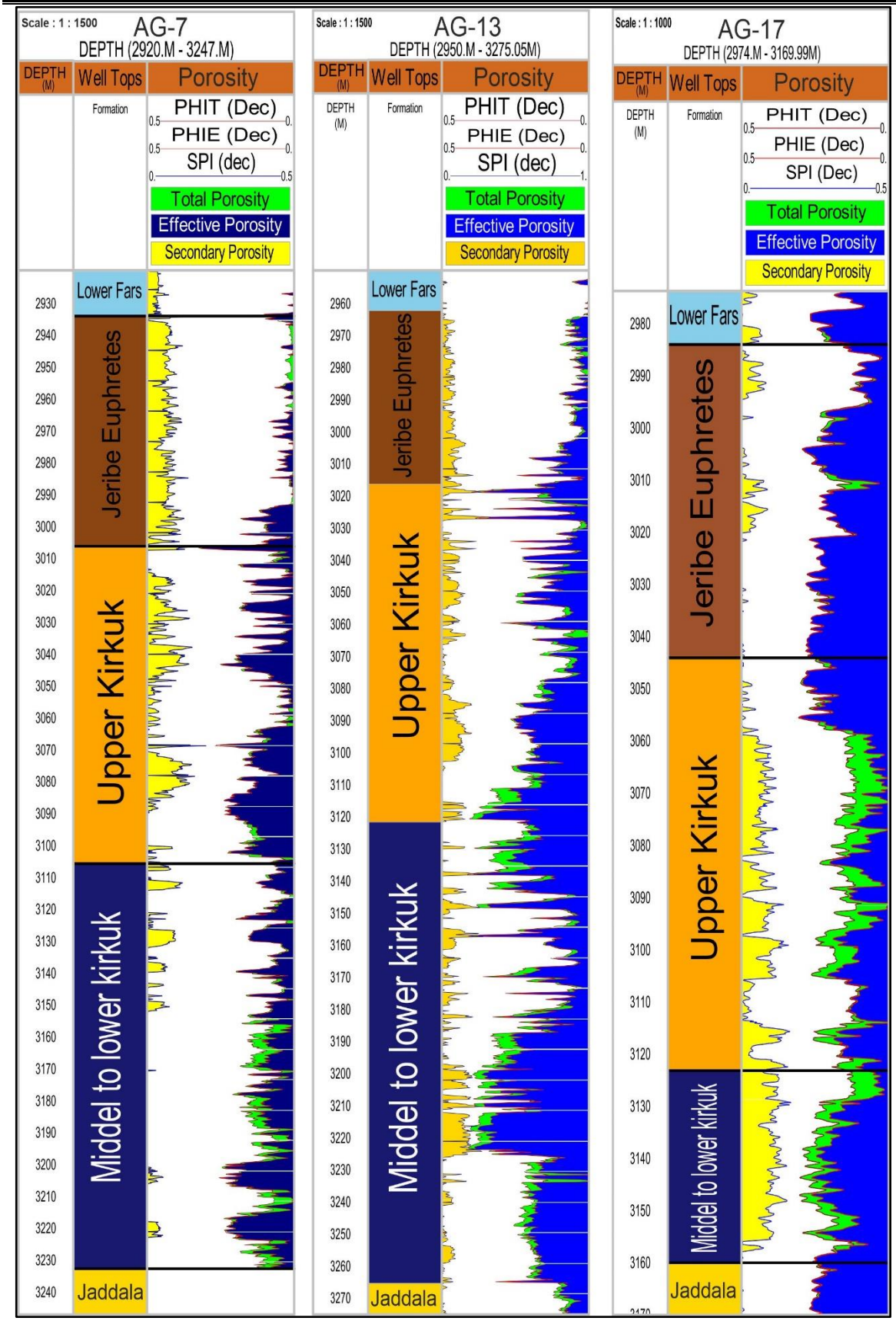

Figure (2-22): Porosity types (Total, Secondary and Effective) of Asmari Formation in Abu Ghirab field of AG7, AG-13 and AG-17

2.4.4. Determination of Archie's Parameters (m, n, & a) and Rw from well logs Using Pickett Plot

One of the most straightforward and efficient cross-plot techniques in use is the Pickett crossplot (Pickett, 1972). In addition to providing estimates of water saturation, this method can assist in determining:1- Formation Water Resistivity 2- cementation factor (m) 3-matrix parameters for porosity logs (Δt_{ma} and ρt_{ma}) (Asquith, 1982). Utilize Interactive Petrophysics software (V.3.5) Archie's parameters were determined from the well log using Pickett's plot. To determine (m) and/or (a) from well logs, Pickett (1966) proposed a technique that relies on a cross plot between resistivity vs. porosity.

$$\boldsymbol{Rt = \frac{a*Rw}{\Phi^{m}*S_w^n}} \text{ .....(2-18)}$$

Where

Sw: Water Saturation (fraction)

Rw: Water Resistivity (ohm-m)

Φ: is porosity (fraction)

Rt: Formation Resistivity (ohm-m)

a,m,n: Archie's parameters (dimensionless)

According to (Toby, 2005) .In the m measurements, the plugs will have been flushed with brine that is the same salinity as that anticipated in the reservoir, and the resistivity will have been measured. By graphing the formation factor's logarithm, which is determined by:

$$\boldsymbol{Log\ F = Log\ \left(\frac{Ro}{Rw}\right)} \text{……(2-19)}$$

against log porosity, according to Archie:

$$\boldsymbol{Log\ F = -m * Log(\emptyset)} \text{…..(2-20)}$$

As a result, m is given by the line's gradient. Be aware that the computed water saturations, Sw, will increase with increasing m values and vice versa. To get measurements of genuine resistivity, Rt, vs. Sw, the plugs were flushed with brine and subsequently desaturated (either with air or kerosene). Using the resistivity index's logarithm, which is represented by:

$$\boldsymbol{Log\ (I) = Log\ (\frac{Rt}{Ro})}\ldots\ldots(2\text{-}21)$$

against log (Sw), according to Archie:

$$\boldsymbol{Log\ (I) = -n * Log(Sw)}\ldots\ldots(2\text{-}22)$$

As a result, n is given by the line's gradient. Be aware that the Sw will be higher when a higher n number is utilized, and vice versa. Anomaly high n values (over 2.5) can be a sign of a mixed or oil-wet system and call for more research. Water-wet porous rock of high grade has lower values of n.

The equation is an equation of a straight line on a log-log plot, where m is the slope and (a*Rw) is the intercept at Φ =1. In a water-bearing zone, Sw = 1, and Equation is an equation of a straight line. Given what is known about Rw from other sources, (a) can be quickly located.

$$\boldsymbol{Log\ Rt = -mLog\Phi + Log(a * Rw) - nLog(Sw)}\ldots..(2\text{-}23)$$

This equation may be simplified to: in a zone Sw1 that is water-bearing:

$$\boldsymbol{Log\ Rt = -mLog\Phi + Log(a * Rw)}\ldots..(2\text{-}24)$$

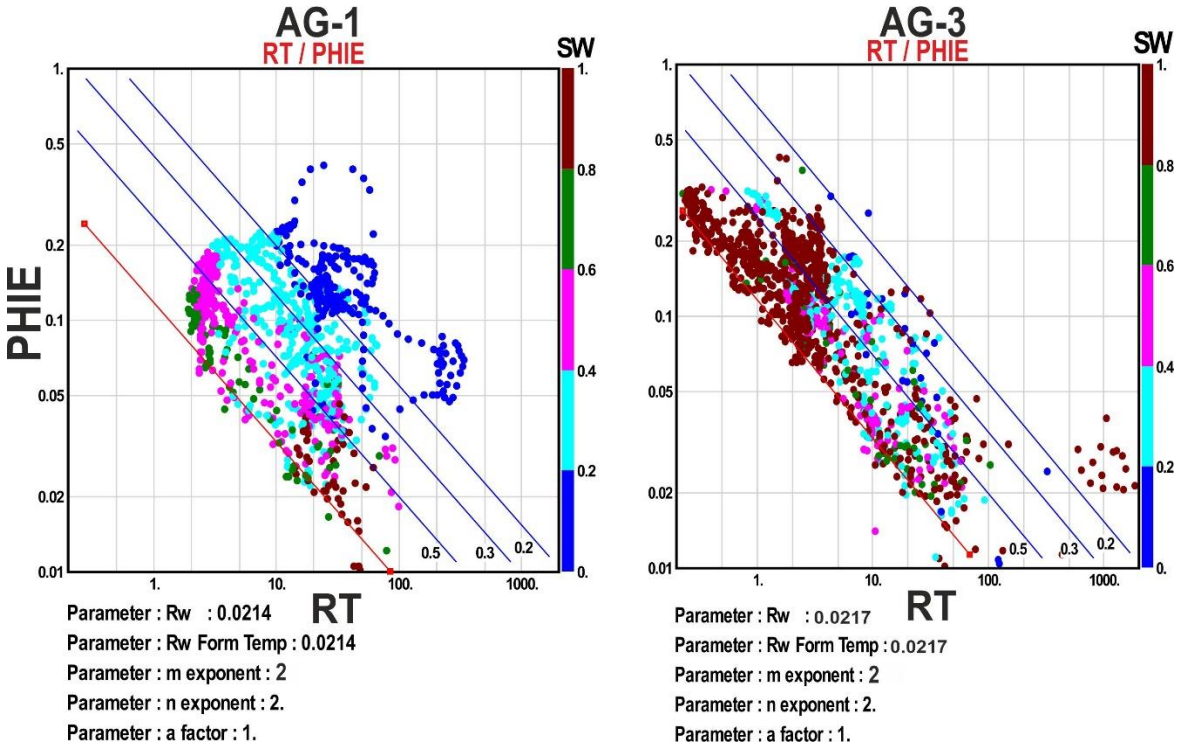

Figure (2-23): Pickett plot for well AG-1, AG-3**.**

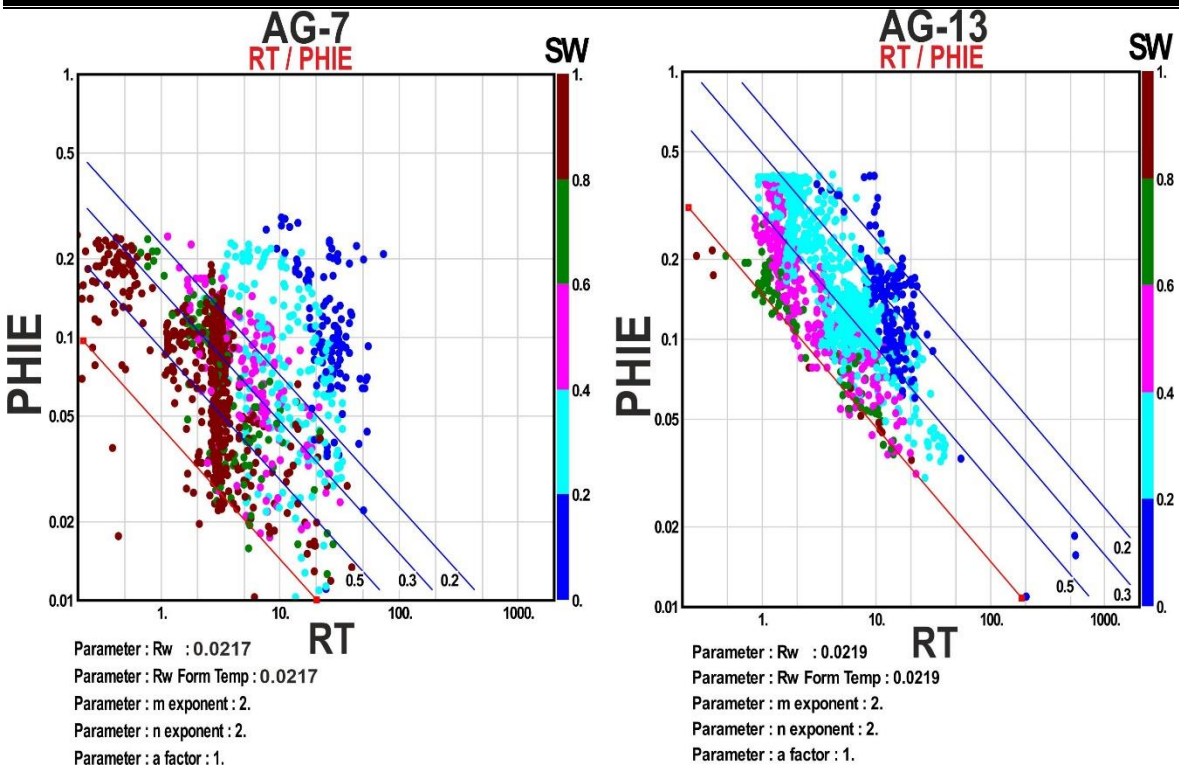

Figure (2-24): Pickett plot for well AG-7, AG-13**.**

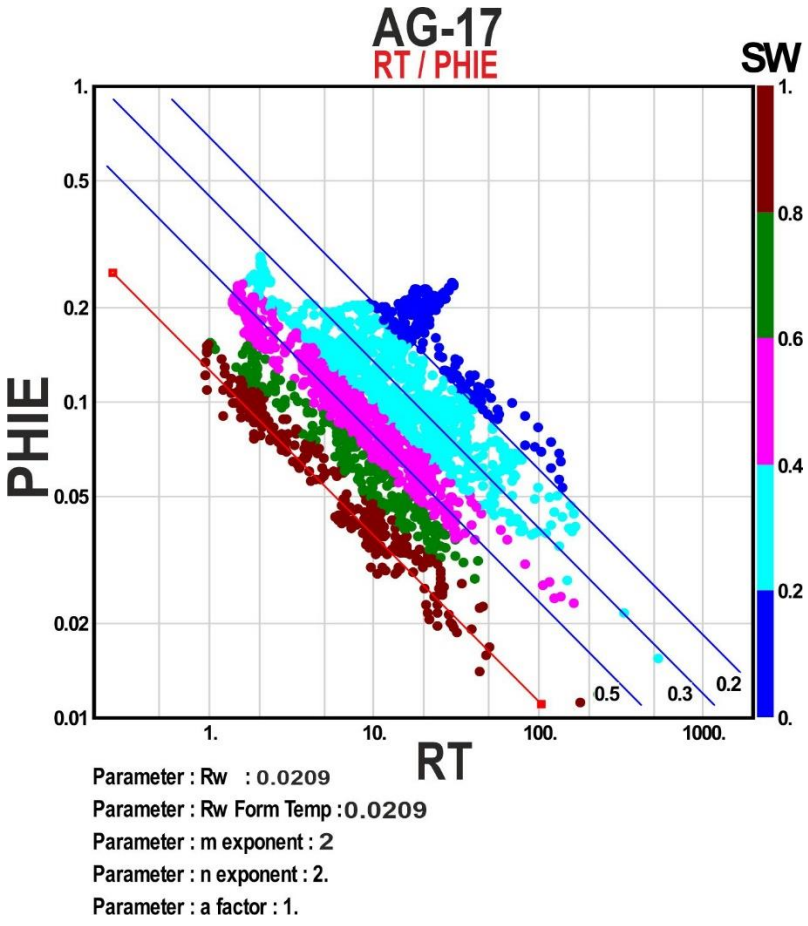

Figure (2-25): Pickett plot for well AG-17.

Table (2-4): The numerical values of the picket plot analysis for the studied wells displays the formation water resistivity (Rw) and the Archi parameters: saturation exponent (n), cementation factor (m), and tortuosity factor (a).

Well No.	Tortuosity Factor (a)	Cementation Exponent (m)	Saturation Exponent (n)	Rw
AG-1	**1**	**2**	**2**	**0.0211**
AG-3	**1**	**1.9**	**2**	**0.0212**
AG-7	**1**	**2**	**2**	**0.022**
AG-13	**1**	**2**	**2**	**0.0217**
AG-17	**1**	**1.9**	**2**	**0.0209**

2.4.5. Fluid and Formation Analysis

2.4.5.1. The Water and Hydrocarbon Saturations Calculation

The ratio of water-filled voids in the rock, stated as a percentage and symbolized by the symbol (SW %), is referred to as "water saturation" (Asquith & Gibson, 1982).

$$S_W = \frac{\boldsymbol{formation\ water\ occuping\ pores}}{\boldsymbol{total\ pore\ space\ in\ the\ rock}} \quad \text{……(2-25)}$$

The following two equations (Archie, 1942) can be used to compute water saturation in the uninvaded zone (Sw) and the invaded zone (Sxo).

$$\boldsymbol{Sw = \{(a.Rw)/(Rt.\Phi t^m)\}^{\frac{1}{n}}} \quad \text{.....(2-26)}$$

$$\boldsymbol{sxo = \{(a.Rmf)/(Rxo.\Phi t^m)\}^{\frac{1}{n}}} \quad \text{.....(2-27)}$$

Where:

Sw = water saturation of uninvaded zone.

Sxo = Water saturation of the invaded zone.

F = Formation factor.

Rw = Resistivity of water formation.

Rt= True formation resistivity.

n = Saturation exponent (assumed to be 2.0).

Rmf = Resistivity of mud filtrate at formation temperature.

Rxo = Resistivity of the invaded zone.

The water saturation of the uninvaded zone (Sw) and the water saturation of the invaded zone (Sxo) are calculated using the previously obtained parameters, and the results are given in figures (2-23) and the results of the other wells are given in Appendix (B).

The following equations (Asquith and Krygowski, 2004) can be used to estimate the residual hydrocarbon saturation (Shr) and the movable hydrocarbon saturation (Shm) from the water saturation of the uninvaded zone (Sw) and the water saturation of the invaded zone (Sxo):

$$\boldsymbol{Shr = 1 - Sxo} \ldots\ldots \text{(2-28)}$$

$$\boldsymbol{Shm = Sxo - Sw} \ldots\ldots \textbf{(2-29)}$$

Where:

Shr = residual hydrocarbon saturation

Shm = movable hydrocarbon saturation

Sxo = water saturation in the invaded zone

Sw = water saturation of uninvaded zone

To determine the hydrocarbon saturation (Sh), which is defined as the portion of the pore volume that is not filled with water (Serra, 1984). Sh may be calculated using the (Schlumberger, 1987) formula:

$$\boldsymbol{Sh = 1 - Sw} \ldots\ldots (2-30)$$

Calculating hydrocarbon movability using the water saturation of the flushed (invaded) zone (Sxo). Invading drilling fluids (Rmf) have likely transported or flushed hydrocarbons in the flushed zone out of the zone closest to the borehole if Sxo was greater than Sw (G. B. Asquith *et al*., 2004). To apply the above-mentioned equations to calculate water saturation, the following variables must be known and how to determine them:

a. **Formation Factor (F):** A rock containing oil and/or gas will have a larger resistance than a rock saturated with formation water, and the lower the formation resistivity, the greater the connate water saturation. The formation resistivity factor is an effective metric for detecting hydrocarbon zones because of its link to saturation (Tiab and

Donaldson, 2004). Archie (1942) demonstrated that the resistivity of a water-filled formation (Ro) may be linked to the resistivity of the water filling the formation (Rw) by using a constant known as the formation resistivity factor (F).

$$Ro = F \times Rw \ldots..(2\text{-}31)$$

Archie also discovered that the following formula, which was applied in the current investigation, may be used to connect formation factor (F) to the porosity of formation:

$$F = \frac{a}{\emptyset^m} \ldots..(2-32)$$

Where:

a= tortuosity factor = (1) for carbonate rocks.

m= cementation factor (taple2-5)

∅= total porosity.

b. The resistivity of Mud Filtrate (Rmf) Determination

The borehole environment has an electrochemical effect on the drilling mud, grading its resistivity according to the borehole resistivity (Rm), the resistivity of mud filtrate (Rmf), and the resistivity of uninvaded formation water (Rw). The most crucial factor to take into account when determining water saturation is (Rmf). These resistivities are significantly impacted by the temperature variations between depths (Schlumberger, 1972). Before being utilized in any computations, the resistivity of the different liquids (Rm, Rmf, or Rw) must first be rectified to the temperature of the formation. A particular chart is used to rectify the resistivity; the chart closely resembles Arp's formula (Asquith and Krygowski, 2004):

$$\mathbf{RTF = Rtemp(Temp + 6.77)/((TF + 6.77)\ )\ldots\ldots(2\text{-}33)}$$

Where:

R_{TF}= resistivity at formation temperature.

Rtemp= resistivity at a temperature other than formation temperature.

Temp = temperature at which resistivity was measured.

Formation temperature (TF) is computed using the following formula (Arps, 1964):

$$\boldsymbol{TF = G.G * d + TS} \ldots\ldots (2\text{-}34)$$

Where:

TF = formation temperature.

G.G = geothermal gradient.

d= formation depth at the point where the *SSP* was read.

Ts= surface temperature.

To calculate geothermal gradient **the Arps (1964) formula** is used

$$\boldsymbol{G.G = (BHT - TS)/Dt} \ldots\ldots (2\text{-}35)$$

Where:

BHT = borehole temperature

Dt= Total depth of borehole (m)

The values of mud filtrate resistivity (Rmf) at formation temperature, geothermal gradient, and formation temperature for each well in the current research are computed using the preceding formulae, and the results are displayed in a table (2-6).

Table (2-5): Contains the findings of this study's calculations of the resistivity of mud filtrate (Rmf) at formation temperature and formation temperature (ft) for each well.

Well No.	DT(M)	BHT(F)	Ts (˚F)	Tf (˚F)	Rmf @Ts	Rmf @Tf
AG-1	3116	176	70	165	0.312	0.322
AG-3	3190	190	70	170	0.08	0.04
AG-7	3240	178	78	170	0.294	0.410
AG-13	3315	240	78	200	0.445	0.311
AG-17	4440	258	72	173	0.23	0.33

2.4.5.2. Analysis of Bulk Volume

The bulk volume of water (BVW) is the result of a formation's water saturation (Sw) and porosity (Φ). (Asquith and Gibson, 1982). On the other hand, the following formula may be used to calculate the bulk volume of water in the flushed zone: (Schlumberger, 1984)

$$\boldsymbol{B_{VW}} = \boldsymbol{Sw} * \Phi \ldots\ldots (2\text{-}36)$$

$$BVWXO = Sxo * \Phi \ldots\ldots (2\text{-}37)$$

Where

BVW: Bulk water volume in the uninvaded zone

BVWXO: Bulk water volume in the invaded zone.

The moveable hydrocarbon saturation (Shm) and residual hydrocarbon saturation (Shr) are represented by the hydrocarbon's bulk volume (unmovable). The following equation (Asquith and Krygowski, 2004) may be used to determine the bulk volume of a hydrocarbon:

$$\boldsymbol{Bvo} = \boldsymbol{Sh} * \Phi \ldots\ldots (2\text{-}38)$$

Where:

Bvo: bulk volume of hydrocarbon.

Sh: Saturation of hydrocarbons.

The fluids analysis track is divided into three categories in figure (2-26) and the results of the other wells are given in Appendix (B). effective porosity (PHIE), water-filled porosity in the flushed zone (BVWXo), and water-filled porosity in the uninvaded zone (BVW). The region between (BVWXo) and (BVW) represents the moveable hydrocarbon, whereas (PHIE) and (BVWXo) represent the residual hydrocarbon and (PHIE) and (BVW) represent the total hydrocarbon.

2.4.6. Permeability Computation

The permeability of a rock determines its ability to transfer liquids. It connects the fluid flow rate to the applied pressure gradient and the fluid viscosity. Permeability is controlled by the associated channels of the pore space (pore throats). The Darcy unit (d) or millidarcy unit (m) is used to measure permeability (mD). The permeability is measured using an indirect approach including wireline logs and a difficult interpretation. Depending on the fluid composition (Al-musawi & Nasser, 2019), a differentiation must be made:

a- Absolute permeability in laminar flow for a single non-reactive fluid.
b- Effective permeability for the flow of one fluid in the presence of another fluid.
c- Relative permeability is defined as the ratio of efficient to absolute permeability.

The permeability of petroleum reservoir rocks can range from 0.1 to 1000 millidarcies or more, and a reservoir's class can be classed as poor if K1, fair if 1K10, moderate if 10K50, good if 50K250, and very good if K>250 MD based on permeability. The permeability of a reservoir may be determined in three ways. On a larger scale, a drill stem or a production check can be employed to assess it (Selley, 2000).

The second approach for determining permeability is to use wireline logs, and the third method is to use a permeameter (Selley, 2000). In this work, the Timur formula was used to predict permeability using wireline logs, as shown in fig (2-26) and the results of the other wells are given in Appendix (B).

$$\boldsymbol{K = 0.136\frac{\Phi^{4.4}}{Swi^{2}}} \quad \text{.....(2-39)} \quad \text{(Timur, 1968).}$$

K = permeability in mD.

Swi =irreducible water saturation.

2.5. Evaluation of Reservoir Units

The Asmari Formation in the Abu Ghirab oil field consists of hard dolomite with thin layers of anhydrite in the upper part and limestone with layers of Sandston in the lower part. The reservoir was divided into three main units (Jeribe-Euphrates, Upper Kirkuk, Middle- Lower Kirkuk) and eight secondary units, figure (2-23) and the results of the other wells are given in Appendix (B), the computer process interpretation (CPI) of AG-1, AG-3, AG-7, AG-13 and AG-17 by utilizing Interactive Petrophysics (IP) software (v3.5). The CPI figures display the fluid analysis and petrophysical characteristics of reservoir units.

2.5.1. Jeribe-Euphrates

consist of interbedded of dolomite with anhydrite beds of the upper part, A shale barrier striations have been identified as separating a number of reservoir sub units. Particularly in this unit, the porosity effective average declines except a well AG-17 which are considered from Negligible to poor. The Permeability is rang between (5-12%) Shale Volume range between (0.04-0.07).Thikness of this uint rang (60-75m).This uint the oil show is fair and shown in the bottom of the uint.

2.5.2. Upper Kirkuk

is the middle unit and it is considered the main unit of the reservoir due to the high hydrocarbon content and low water saturation. Also, this unit was divided into several sub-units depending on the sharp deviations of the gamma-ray log values and and content of Shale. The contact units are limestone with good to very good porosity and high porosity which shows the concentration of hydrocarbon content with the highest value which is in the B2 and B3 subunits. The reservoir's average volume of shale rang (0.12-0.15) except well AG-17 is 0.44.The total thickness of uint rang (90-150m).

2.5.3. Middle- Lower Kirkuk

This unit consists of thick layers of limestone with a high content of shale as well as a presence of small layers of sandstone. What distinguishes this unit is the high water saturation of the lower part of it to reaches in some parts of 100% except for the well AG13, where its water content is Lesser with clear petroleum marks and a layer of oil-bearing limestone. the porosity effective average fiar to good, except the bottom uint in the well AG-13.the Shale volume the rang (0.2-0.5).

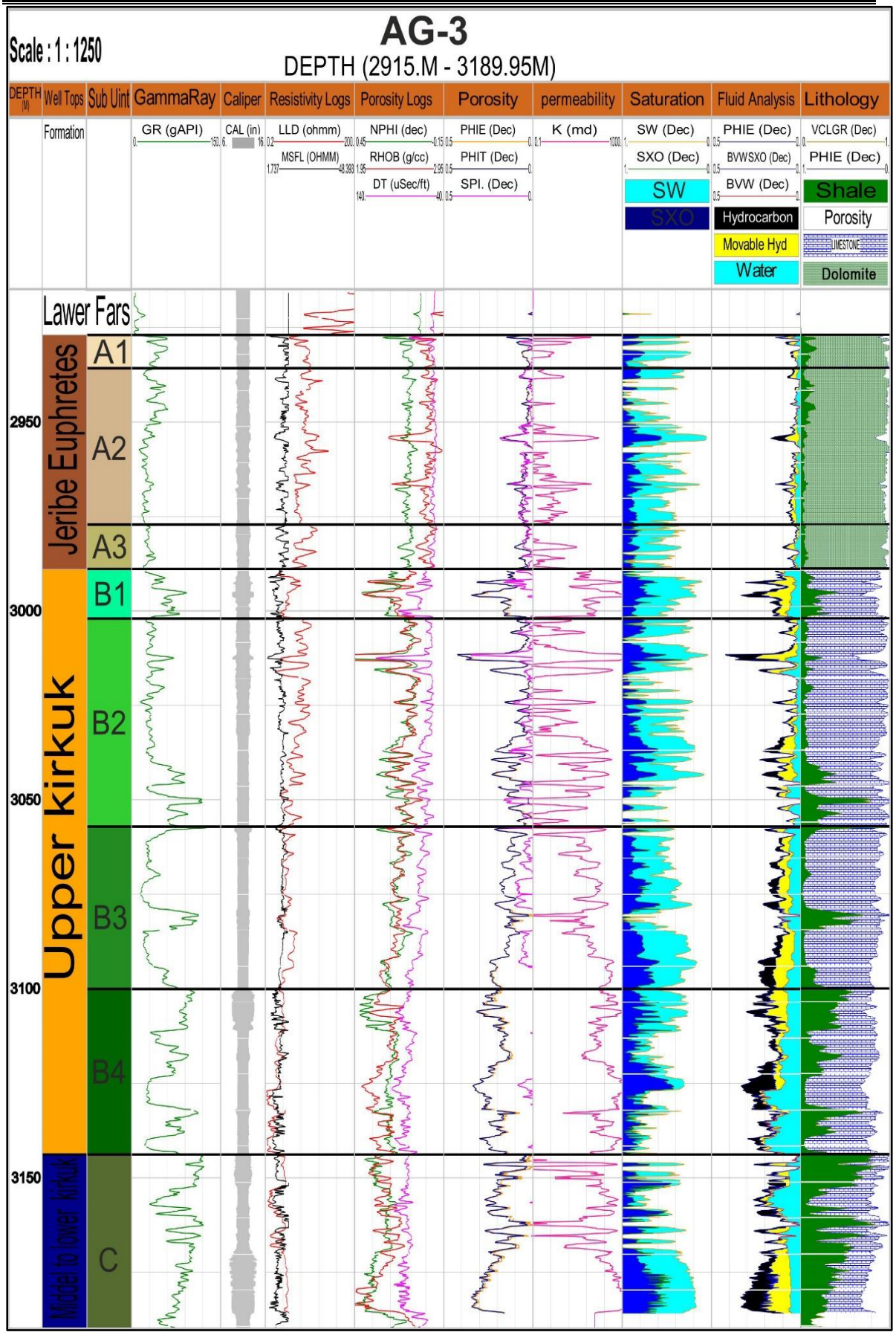

Figure (2-26): Computer Processes Interpretation (CPI) of Asmari reservoir in AG-3 well.

Table(2-6): Reservoir units' properties of Asmari Formation in well AG-1.

AG-1			Top	Bottom	Unit thickness	VCL%	PHIT	PHIE	K (D	SW	SH%
Reservoir	unit	Sub unit									
Asmari	Jeribe-Euphrates	A1	2884	2897	13	0.039	0.048	0.045	20.714	0.78	0.22
		A2	2897	2912	15	0.073	0.017	0.012	0.26	0.94	0.6
		A3	2912	2950	38	0.032	0.029	0.026	2.29	0.83	0.17
	Upper Kirkuk	B1	2950	3003	47	0.049	0.099	0.096	55.15	0.49	0.51
		B2	3003	3030	27	0.12	0.13	0.12	54.617	0.31	0.69
		B3	3030	3050	20	0.052	0.18	0.17	125.23	0.27	0.73
		B4	3050	3071	21	0.12	0.15	0.14	71.46	0.57	0.43
	Middle-Lower Kirkuk	C	3071	3110	39	0.05	0.073	0.069	44.73	0.73	0.27

Table(2-7): Reservoir units' properties of Asmari Formation in well AG-3.

AG-3			Top	Bottom	Unit thickness	VCL%	PHIT	PHIE	K	SW%	SH%
Reservoir	unit	Sub unit									
Asmari	Jeribe-Euphrates	A1	2927	2935	8	0.1	0.43	0.039	2.12	0.92	0.8
		A2	2935	2977	42	0.061	0.046	0.044	2.34	0.62	0.38
		A3	2977	2988	12	0.06	0.044	0.042	1.12	0.88	0.12
	Upper Kirkuk	B1	2988	3002	14	0.16	0.16	0.15	98.5	0.57	0.43
		B2	3002	3057	55	0.13	0.092	0.088	29.5	0.67	0.33
		B3	3057	3100	43	0.13	0.14	0.14	81.6	0.62	0.38
		B4	3100	3143	43	0.26	0.21	0.20	286.7	0.72	0.28
	Middle-Lower Kirkuk	C	3143	3190	47	0.42	0.18	0.20	208.4	0.95	0.5

Table(2-8): Reservoir units' properties of Asmari Formation in well AG-7.

AG-7			Top	Bottom	Unit thickness	VCL%	PHIT	PHIE	K	SW%	SH%
Reservoir	unit	Sub unit									
Asmari	Jeribe-Euphrates	A1	2933	2952	19	0.11	0.024	0.015	0.6	0.90	0.10
		A2	2952	2964	13	0.15	0.019	0.008	0.04	0.64	0.36
		A3	2964	3006	42	0.06	0.046	0.041	7.34	0.71	0.29
	Upper Kirkuk	B1	3006	3054	48	0.09	0.099	0.092	36.16	0.53	0.47
		B2	3054	3085	31	0.12	0.11	0.10	60.02	0.42	0.58
		B3	3085	3100	15	0.16	0.18	0.16	173.96	0.49	0.51
		B4	3100	3105	5	0.24	0.13	0.11	57.93	0.60	0.40
	Middle-Lower Kirkuk	C	3105	3232	127	0.35	0.11	0.09	25.811	0.84	0.16

Table(2-9): Reservoir units' properties of Asmari Formation in well AG-13.

AG-13			Top	Bottom	Unit thickness	VCL%	PHIE	PHIT	K	SW%	SH%
Reservoir	unit	Sub unit									
Asmari	Jeribe-Euphrates	A1	2962	2975	13	0.09	0.036	0.05	0.82	0.35	0.65
		A2	2975	2990	15	0.07	0.027	0.039	2.02	0.60	0.40
		A3	2990	3016	26	0.06	0.069	0.079	25.22	0.44	0.56
	Upper Kirkuk	B1	3016	3039	23	0.12	0.11	0.13	81.09	0.51	0.49
		B2	3039	3058	19	0.12	0.13	0.14	159.81	0.29	0.71
		B3	3058	3102	44	0.12	0.14	0.16	197.37	0.40	0.60
		B4	3102	3121	19	0.26	0.23	0.27	148	0.44	0.56
	Middle-Lower Kirkuk	C	3121	3265	144	0.23	0.20	0.24	90.26	0.47	0.53

Table(2-10): Reservoir units' properties of Asmari Formation in well AG-17.

AG-17			Top	Bottom	Unit thickness	VCL%	PHIE	PHIT	K	SW%	SH%
Reservoir	unit	Sub unit									
Asmari	Jeribe-Euphrates	A1	2983	2997	14	0.06	0.09	0.10	0.18	0.47	0.53
		A2	2997	3020	23	0.12	0.19	0.21	220.93	0.49	0.51
		A3	3020	3044	24	0.036	0.23	0.24	418.12	0.45	0.55
	Upper Kirkuk	B1	3044	3055	10	0.096	0.24	0.25	440.99	0.44	0.56
		B2	3055	3082	27	0.6	0.07	0.14	28.19	0.77	0.23
		B3	3082	3107	25	0.5	0.11	0.17	32.07	0.56	0.44
		B4	3107	3123	16	0.31	0.11	0.15	20.17	0.44	0.56
	Middle-Lower Kirkuk	C	3123	3160	37	0.45	0.16	0.21	150.23	0.39	0.61

Chapter Three

3D Geological Modeling

Chapter Three

3D Geological Modeling

3.1 Introduction

With moderately geostatistical tools like Petrel modeling software, one of the most well-known modeling tools in the oil industry, a large number of reservoir models can be created instantly, but frequently, a limited number must be chosen for input to flow simulation due to computational time requirements (Branet et al., 2008.).

3D geological models were built for the Asmari Formation in Abu Ghirab oil field by petrel software. These models consist of structural models and reservoir properties models (Porosity, Water saturation and permeability) in three dimensions.

Geological modeling is the practice of utilizing computers to produce digital models of many facets of the Earth's crust, such as oil and gas reserves. Realistic geologic models are needed in the oil and gas sector to feed reservoir simulator programs, which forecast how rocks will behave in different hydrocarbon recovery scenarios. Reservoir engineers may determine which recovery solutions offer the safest and most economical, efficient, and successful development strategy for a certain reservoir by using reservoir simulation (Turner and Gable, 2008).

3.2. Data Import

There are several sorts of data that must be provided to the Petrel program in this study to create a 3D model. Among them are:

3.2.1. Well Tops

Well tops information includes markers designating critical places (well picks) along the well's journey, often a change in stratigraphy, the reservoir units of the Asmari that have been imported to Petrel, as well as the overall depth for each well under study.

3.2.2. Well heads

The position of each well (northern, eastern), its 3-dimensional location using the Rotary Table Kelly Bosh (RTKB), and its measured depth along the journey are all included in the well heads data.

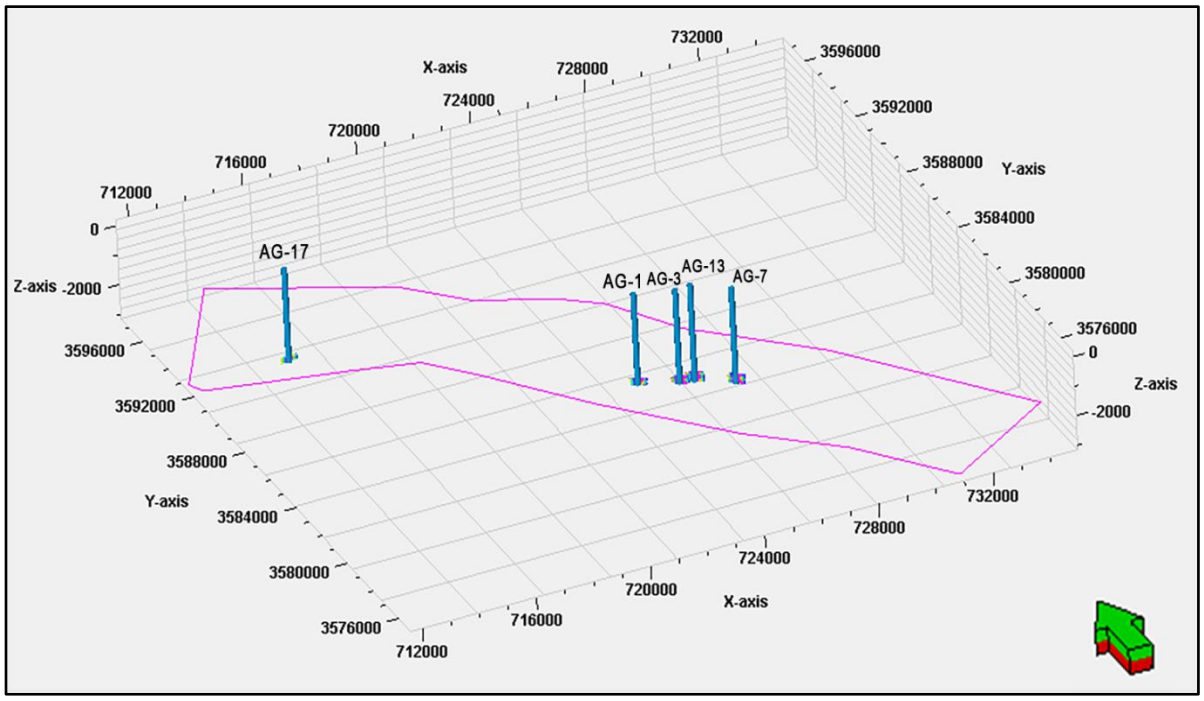

Figure (3-1): Well heads and well tops for the studied wells

3.2.3. Well logs

This sort of data comprised importing well logs from Interactive Petrophysics software (IP) (sonic, gamma ray, neutron, density, and resistivity logs) and CPI (permeability, porosity, and water saturation) for the examined wells (AG-1, AG-3, AG-7, AG-13 and AG-17) of Abu Ghirab oil field.

3.3. Well Correlation

Concepts for well correlation may provide information on the extent and thickness of various lithological units in reservoirs, as well as the distribution of petrophysical parameters (Schlumberger, 2008).

Well correlation has been used in this work as a very basic way to provide insight and enable straightforward visualization of the variations in the thickness within Asmari units.

With the aid of the Grapher program, correlation sections of the examined wells in Abu Ghirab oil field were created see Figure (3-2). The Asmari Formation investigated wells (AG-1, AG-3, AG7, AG-13 and AG-17) are shown in the first correlation segment in Figure (3-3). The sections below demonstrate how the thickness of the unit Asmari Formation.

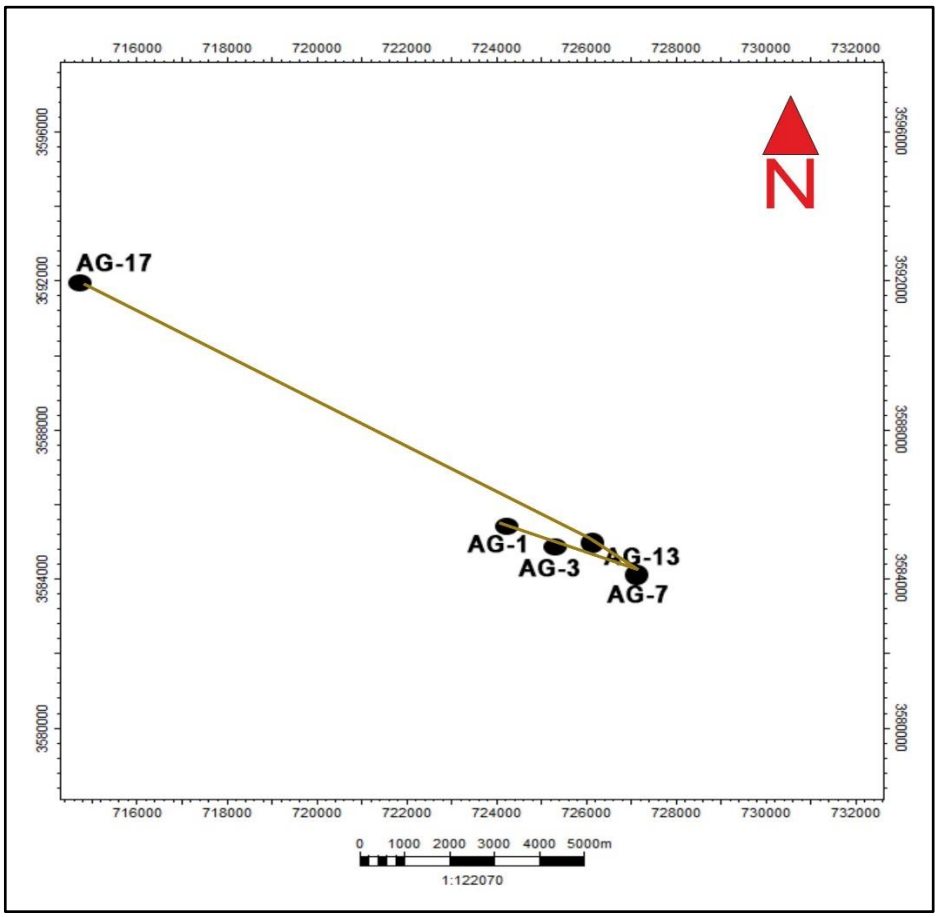

Figure (3-2): Distribution of correlation sections for the Abu Ghirab oil field

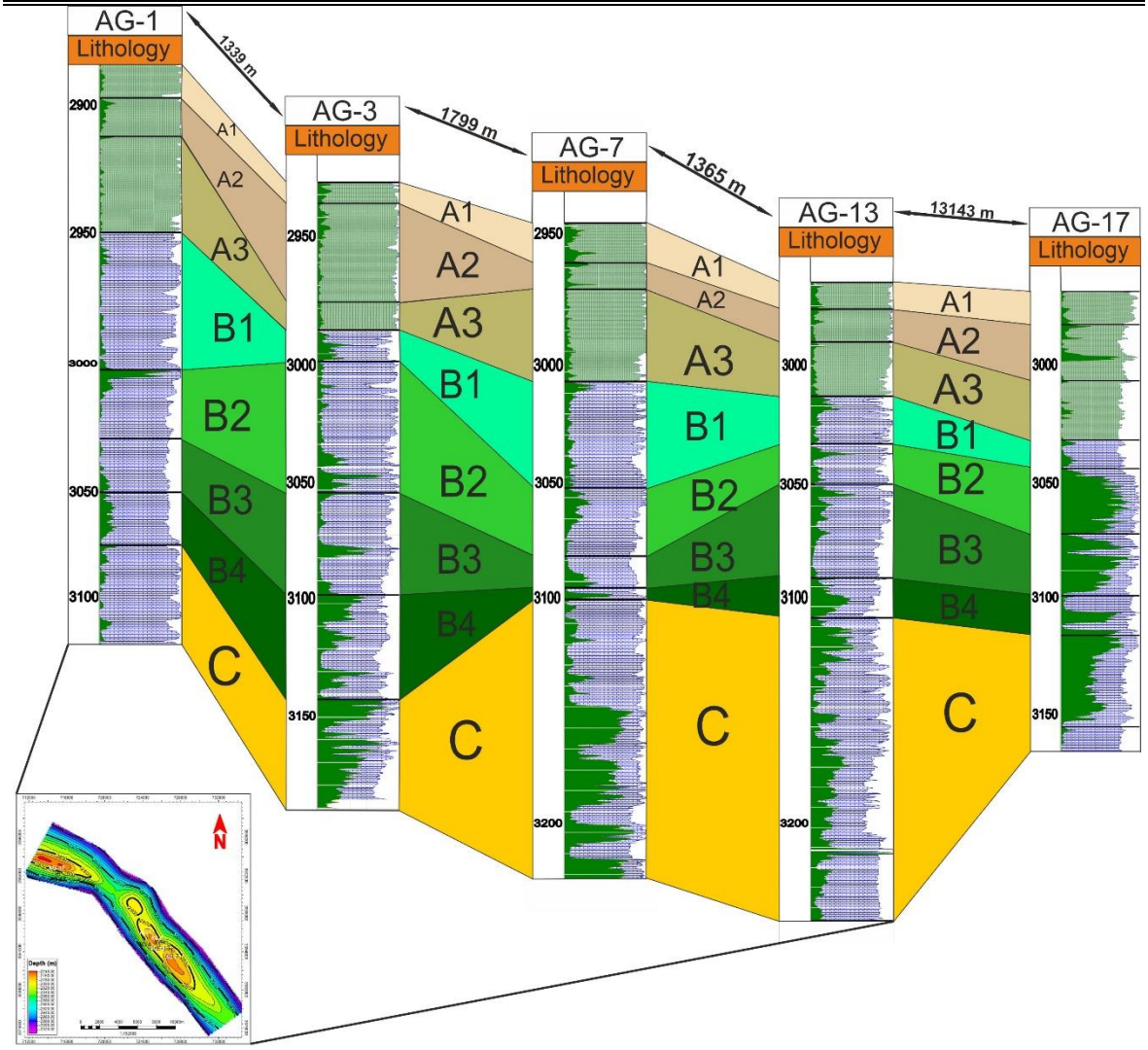

Figure (3-3): Correlation section between studied wells of the Asmari Formation.

3.4. 3D Grid Construction

A network of horizontal and vertical lines used to represent a three-dimensional geological model is known as a "3D grid." Petrel used a method called "Corner Point 3D Grid."

A 3D grid splits a model into boxes, or grid cells, each of which has a certain type of rock property as well as a specific value for water saturation, porosity, and other variables (Schlumberger, 2009). To put up a 3D model simply, a 3D grid structure is needed (Schlumberger, 2007).

The pillar making the skeletal structure is done by gridding. The skeleton is a grid made up of a Top, Mid, and Base skeleton grid that are each

tied to the Top, Mid, and Base points of the major pillars (Schlumberger, 2010).

The Asmari Formation in Abu Ghirab Field's 3D grid model has been created utilizing the Pillar Gridding technique. The top, middle, and base skeletons, as shown in the picture, are the major skeletons as a result of the Pillar Gridding fig(3-4).

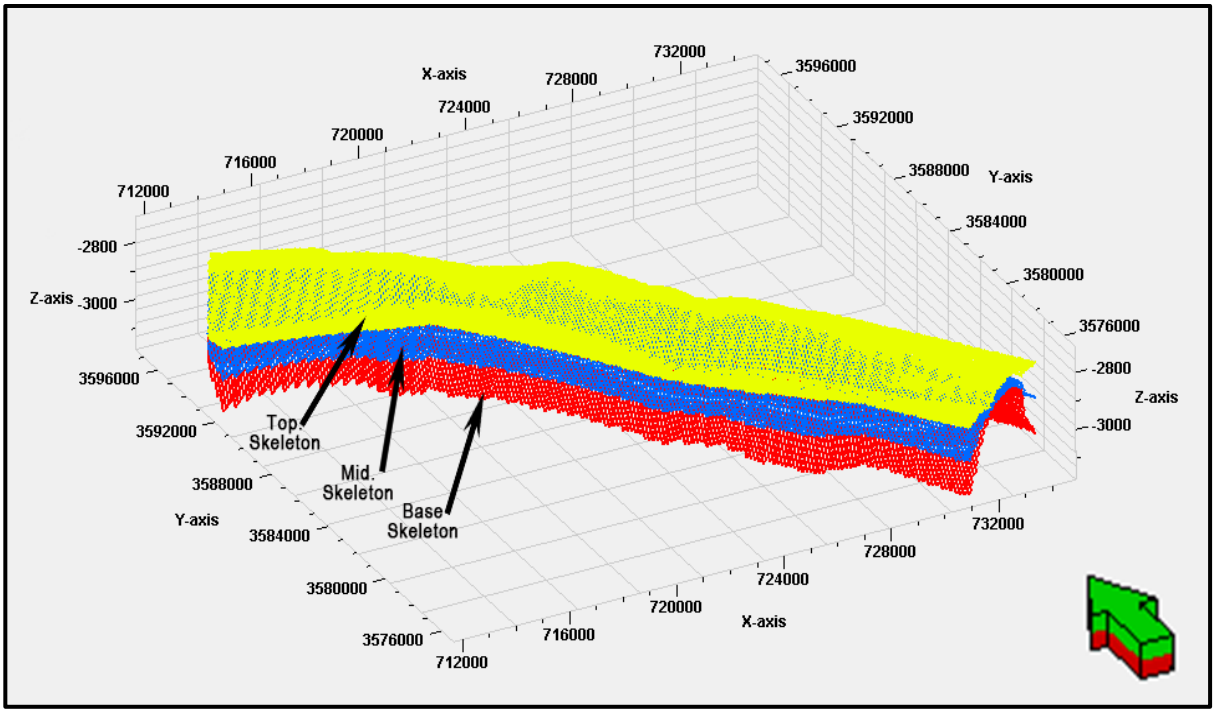

Figure (3-4): The Skeletons of Asmari Formation in Abu Ghirab field.

3.5. Structural Modeling

The structural contour map for each unit in the Asmari Formation is represented through structural modeling. The surface and linked borehole data may be used to create contour maps on a computer. Using Petrel software, the structural contour maps of the Asmari Formation barrier beds and all other units are calculated.fig (3-5)

Building a 3D structural model and creating a structural contour map for the top of each unit of the examined formations is known as structural

modeling. This was done for the Asmari Formatiom using Petrel software, as shown in Figures (3-6)

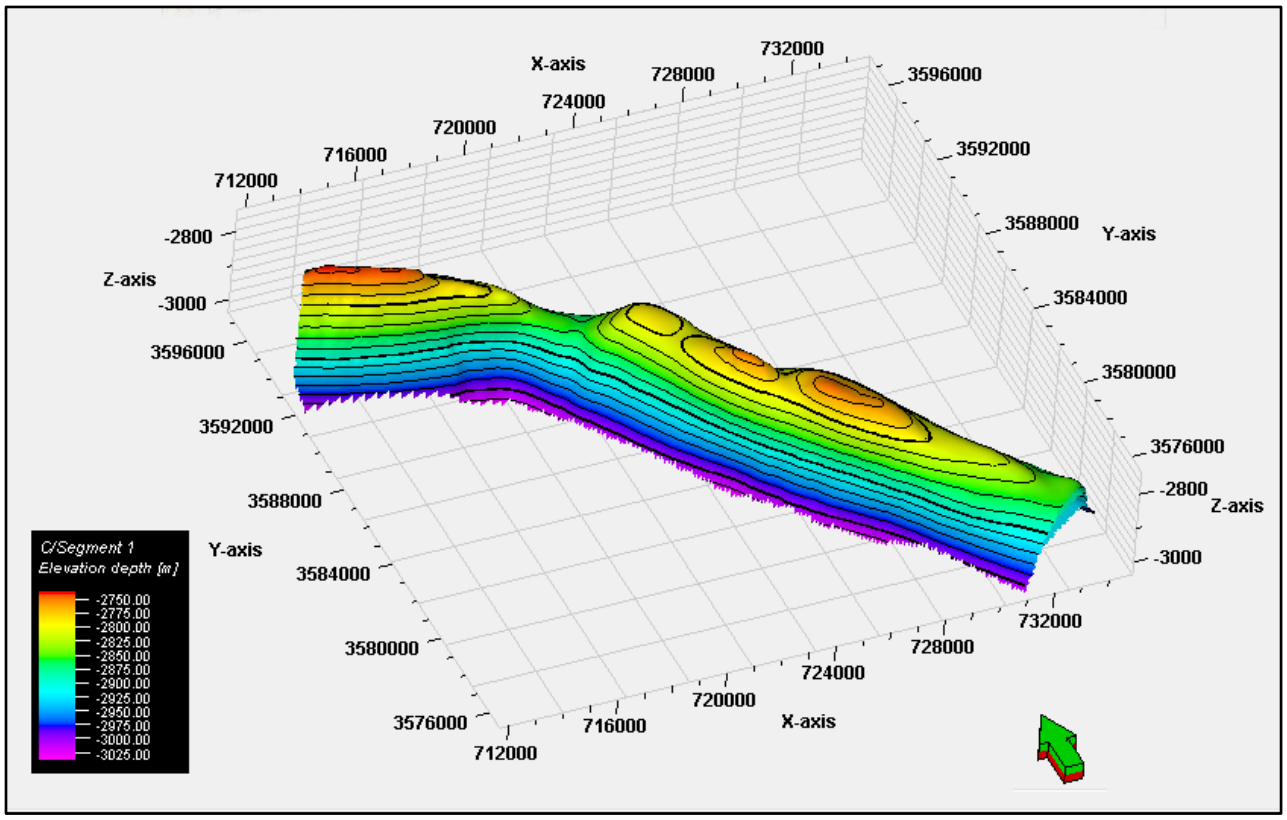

Figure (3-5):3D structural model of the Asmari Formation.

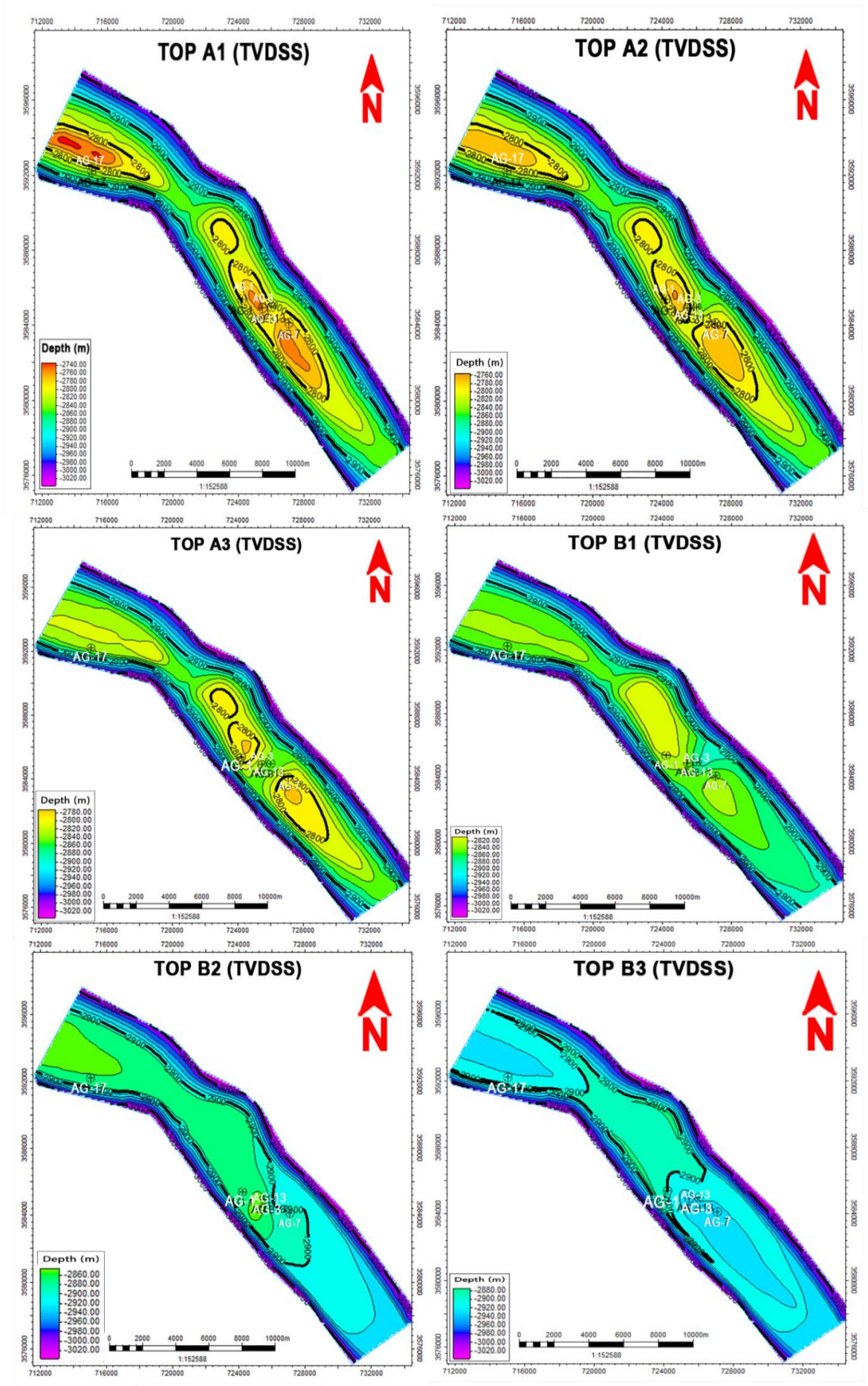
TOP A1 (TVDSS)
TOP A2 (TVDSS)
TOP A3 (TVDSS)
TOP B1 (TVDSS)
TOP B2 (TVDSS)
TOP B3 (TVDSS)
N
Depth (m)
AG-17
AG-13
AG-7
1:152588

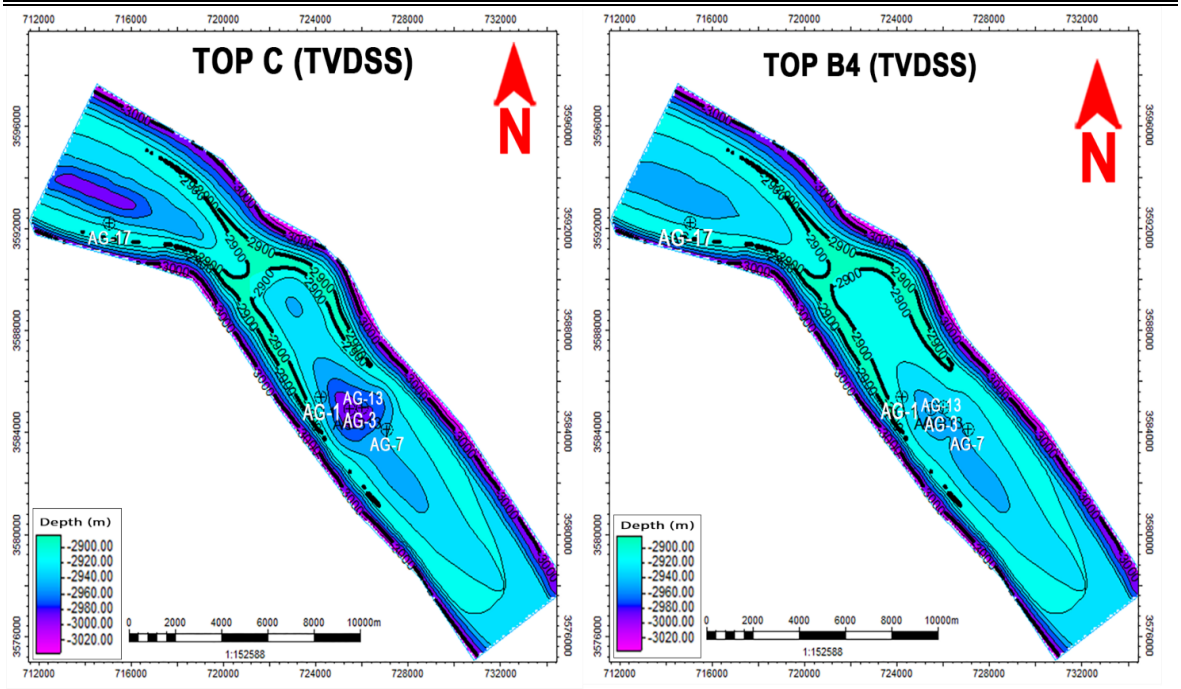

Figure (3-6): Structure contour maps of top of Asmari Formation units in Abu Ghirab oil field.

3.6. Make Horizons

The vertical stacking of the 3D grid in Petrel is defined by the Make Horizons process phase. Taking into consideration the linkages between the surfaces, obeying the fault model to assure accurate fault definitions in the surfaces, and maintaining the well control (well tops), this offered a real 3D approach in the development of 2D surfaces that were gridded in the same process (Schlumberger, 2005).

From X, Y, and Z input data, the contraction of horizons creates separate geological horizons; it also creates additional horizons by utilizing relative distance to current horizons (Schlumberger, 2009).

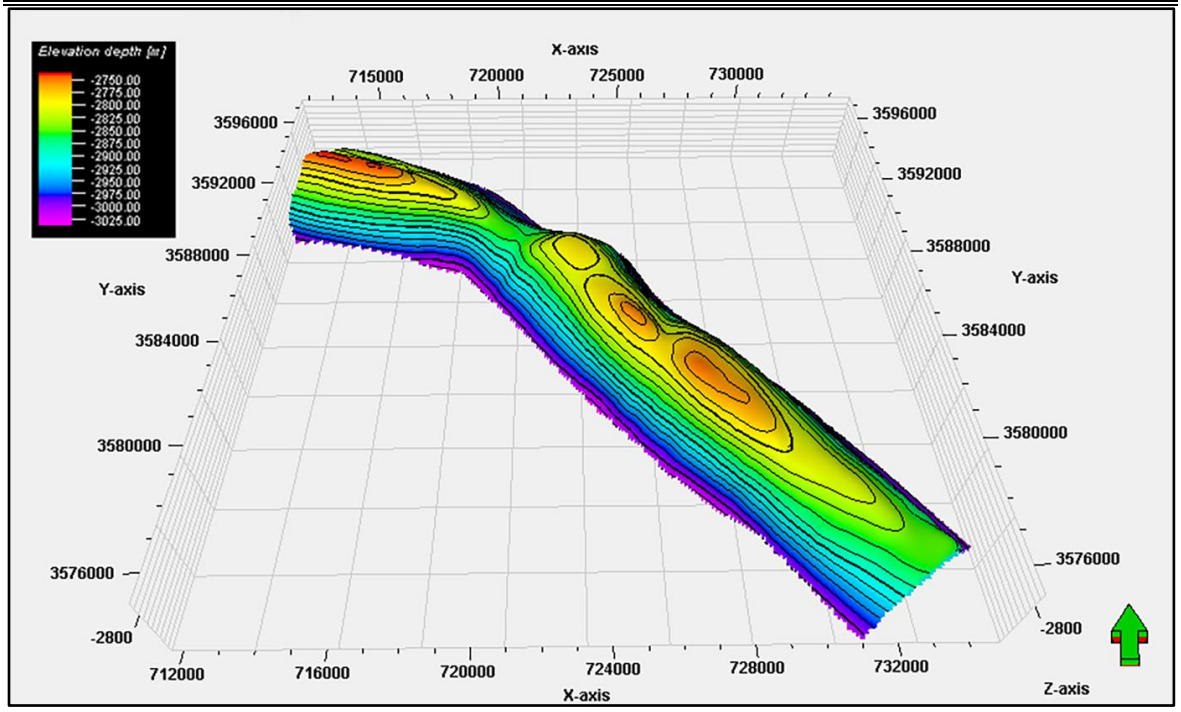

Figure (3-7): 3D model shows main horizons of The Asmari Formation

3.7. Scale up Well logs

This is the grid coarsening process made possible by the estimation of effective flow parameters using analytical (arithmetic, geometric, and harmonic averages) and numerical simulation. Permeability, porosity, and water saturation were among the characteristics that were taken into account throughout the scale-up process (Adaeze *et.al* .2016). The modeled region is divided up while modeling various features by creating a 3D grid. Each property's value is unique to each grid cell. Well log data must first be scaled up since the grid cells are typically significantly larger than the sample density for well logs. The blockage of the well logs is another name for this procedure (Schlumberger, 2009). To scale up permeability, water saturation levels, and porosity, arithmetic was applied. The scale-up well log arrangement used in Abu Ghirab oil field is shown in Figure (3-8).

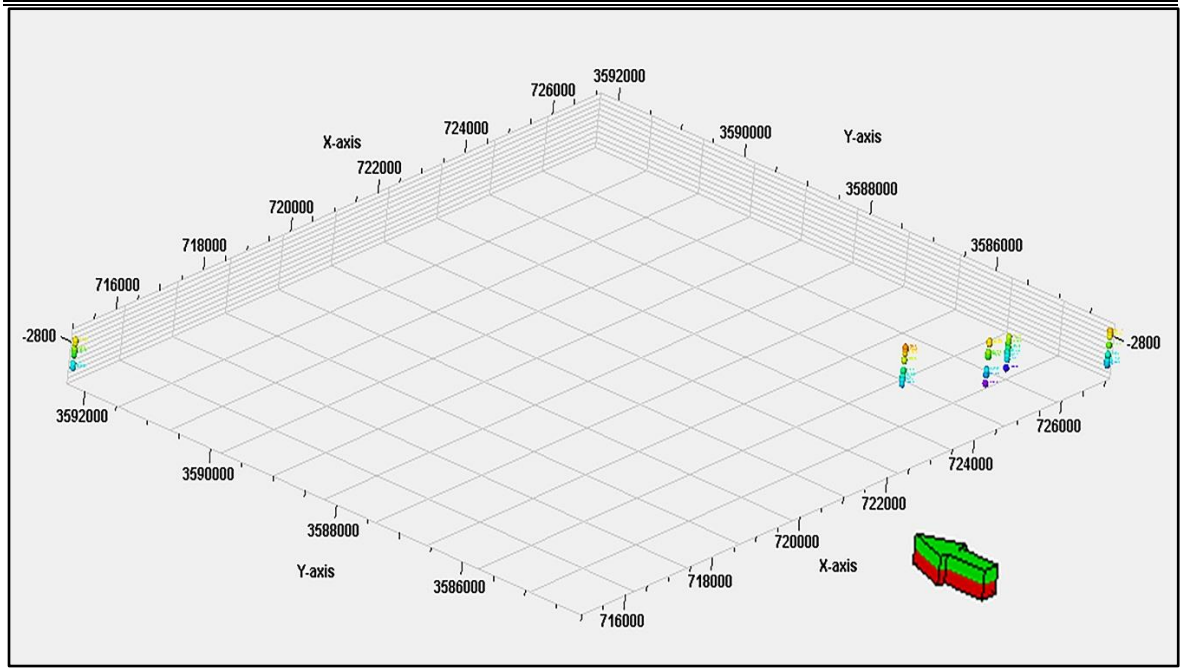

Figure (3-8): Scale up process of Abu Ghirab model.

3.8. Property Modeling

The process of giving each cell of the 3D grid a petrophysical property value, such as porosity or water saturation, is known as petrophysical property modeling. Property modeling is the act of adding petrophysics properties (porosity, permeability, and water saturation) to the grid cells to match well data and accurately retain reservoir heterogeneity fig (3-9).

The distribution of properties among the accessible wells is the goal of property modeling (Schlumberger, 2010). Well log data serve as the foundation for 3D property modeling, which entails computing solutions to difficult mathematical equations that include one or more 3D property models, or, more specifically, Sw transformations based on the porosity 3D model (Schlumberger, 2007).

A petrophysical model is a method for simulating the porosity, permeability, and water saturation of a reservoir. This method may be carried out using the Petrel program , which provides many methods for modeling the distribution of petrophysical parameters in a reservoir model (Schlumberger, 2009).

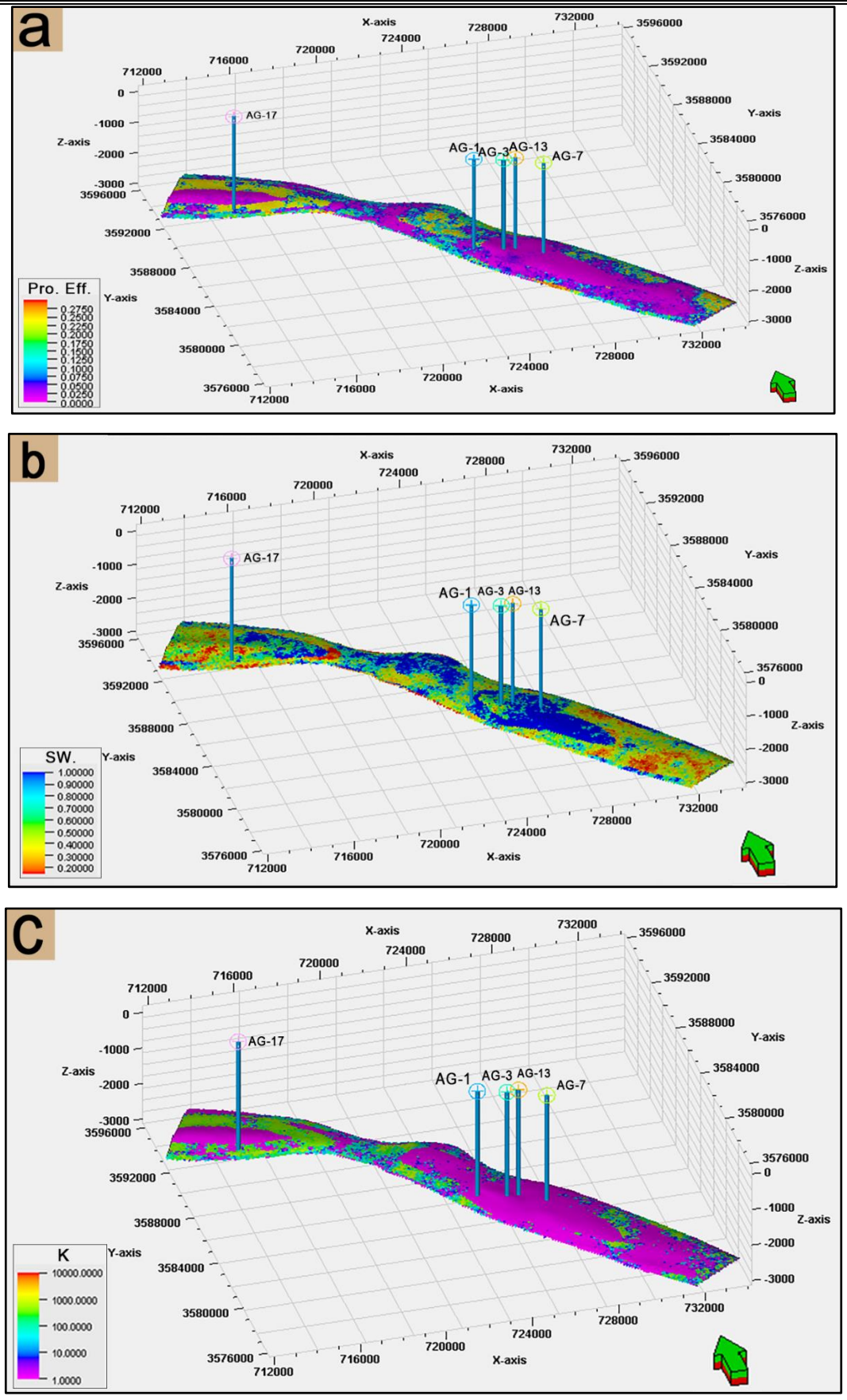

Figure (3-9): Petrophysical models of the reservoir Asmari (a) Porosity; (b) water saturation; (c) Permeability.

3.8.1 Porosity model

To distribute the porosity from the well log data to the grid cells in the 3D model as accurately as possible while keeping the variability of the geological subsurface, it is crucial to scale up the porosity from the well grid cells to the full model. The initial porosity distribution was converted into a stationary, normally distributed data set before the porosity could be modeled. Before modeling, trends were eliminated to ensure that the input data was stationary show in Figure (3-10, 11, 12).

A statistical approach that works with the volume of accessible data is the geostatistical algorithm (Statistical sequential Gaussian simulation technique) (Bellorini et al., 2003). The density, neutron, and sonic porosity logs are used to build the porosity model in the current study, which is then corrected and interpreted using IP software.

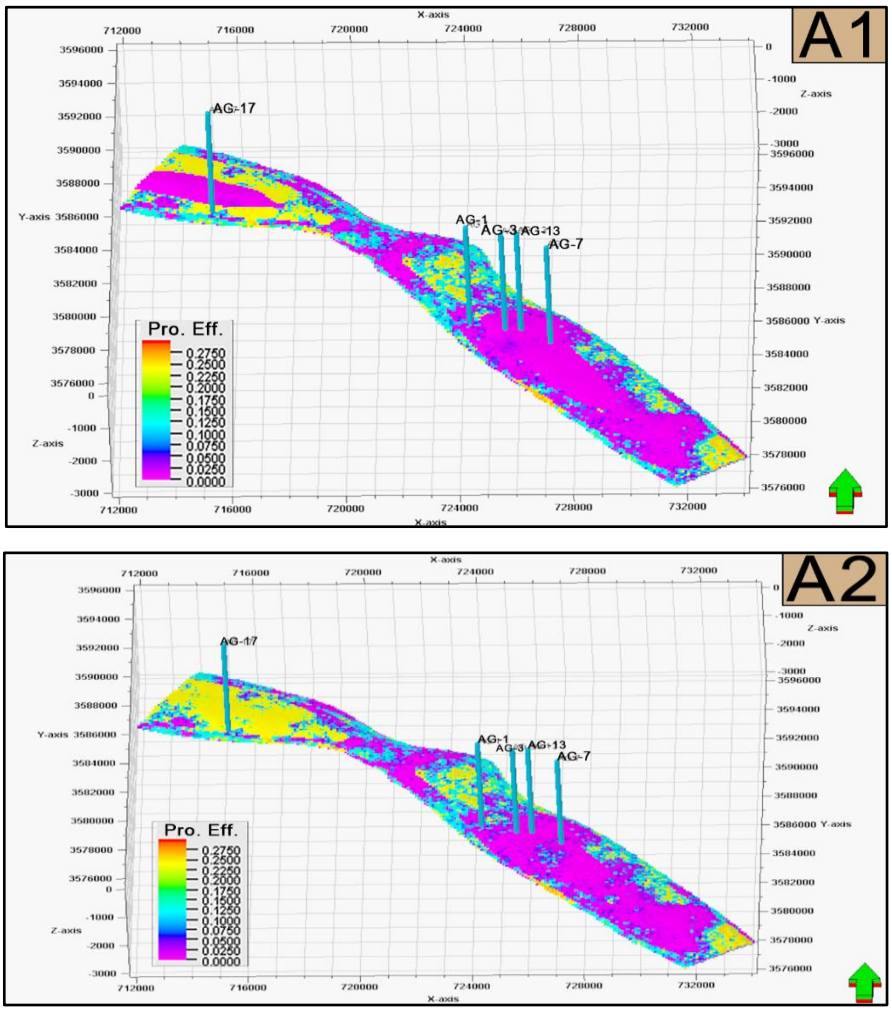

Figure (3-10): Porosity distribution models of Asmari Formation part unit (A1, A2)

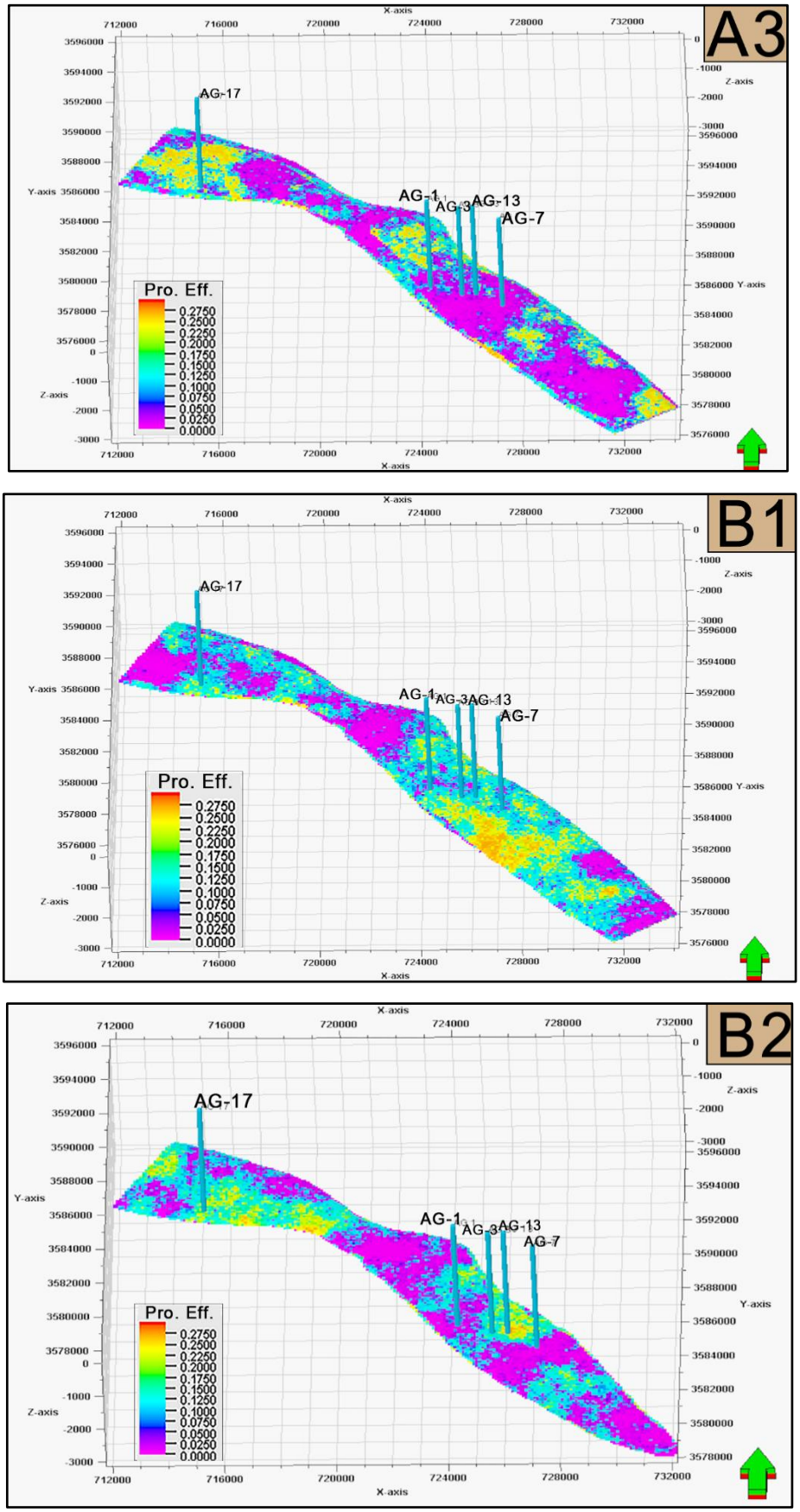

Figure (3-11): Porosity distribution models of Asmari Formation part unit (A3,B1,B2)

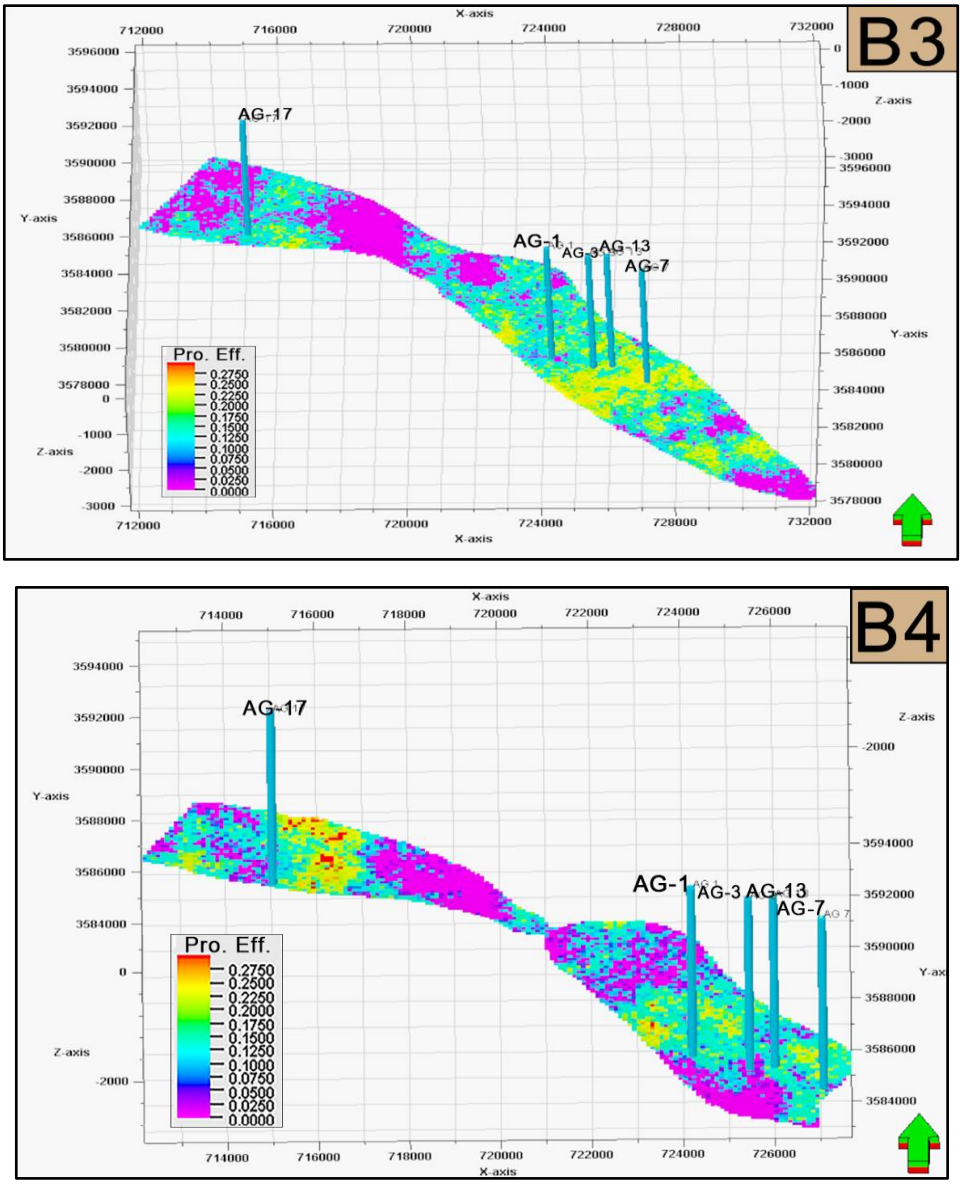

Figure (3-12): Porosity distribution models of Asmari Formation part unit (B3,B4)

3.8.2 Water Saturation Model

The water saturation model uses the same geostatistical approach as the porosity model (Statistical Sequential Gaussian Simulation Algorithm) and the available data on water saturation which are inferred using IP software.

The water saturation model for each reservoir unit in the reservoir portion of Asmari Formation is shown in the figures (3-13,14,15) below. Each unit is distinguished by a different water saturation distribution from the others.

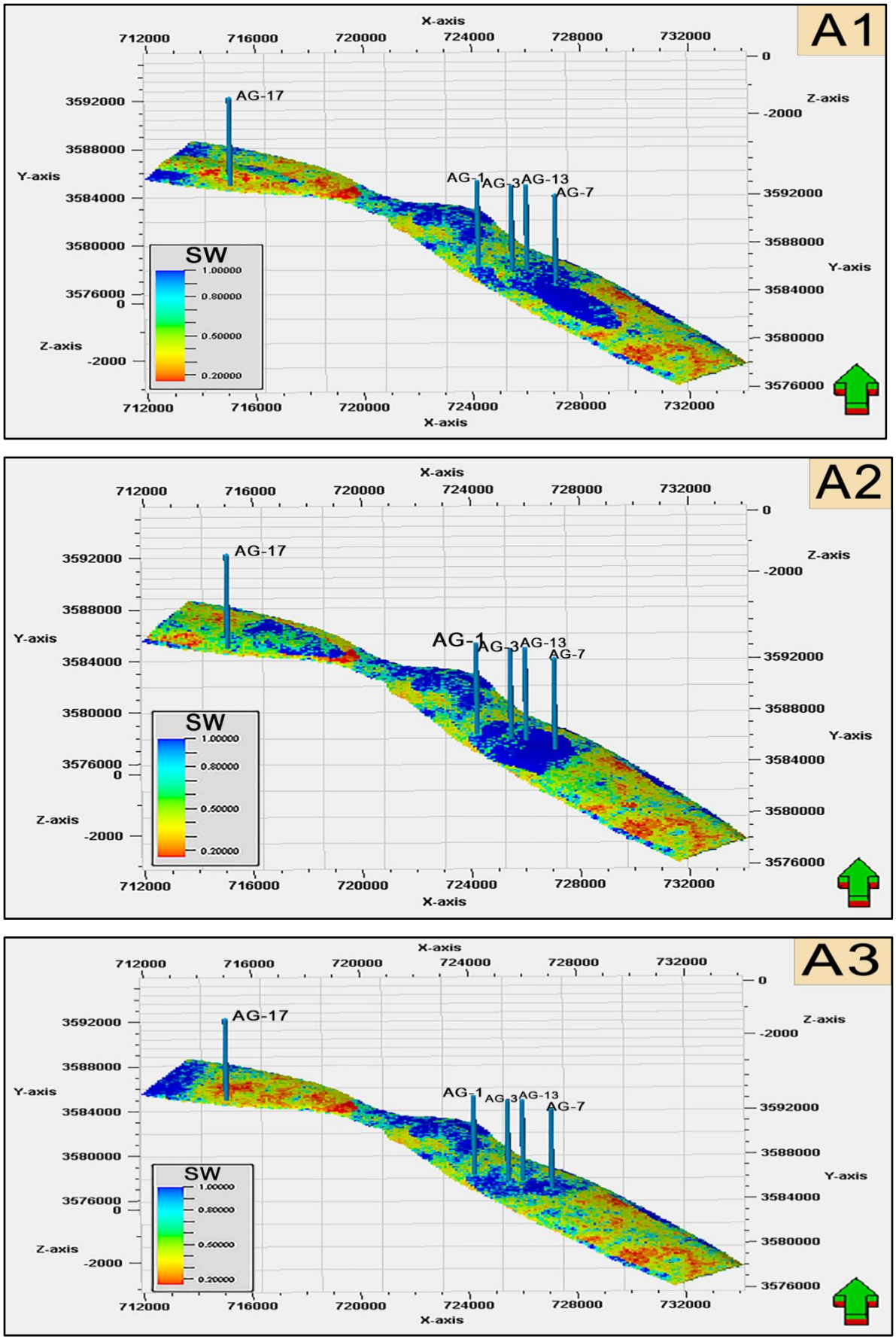

Figure (3-13): Water saturation model of Asmari Formation part unit (A1, A2, A3)

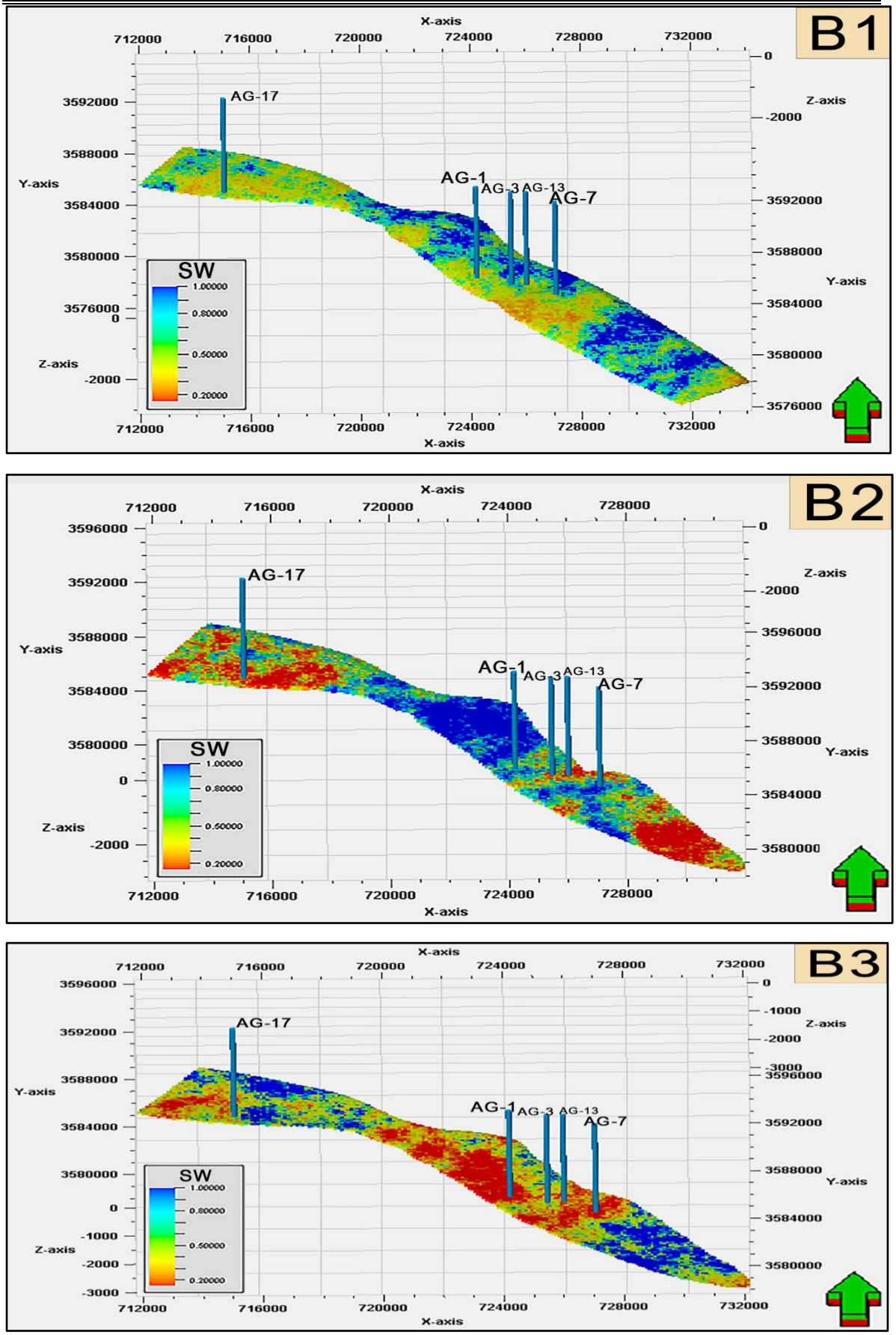

Figure (3-14): Water saturation model of Asmari Formation part unit (B1, B2, B3)

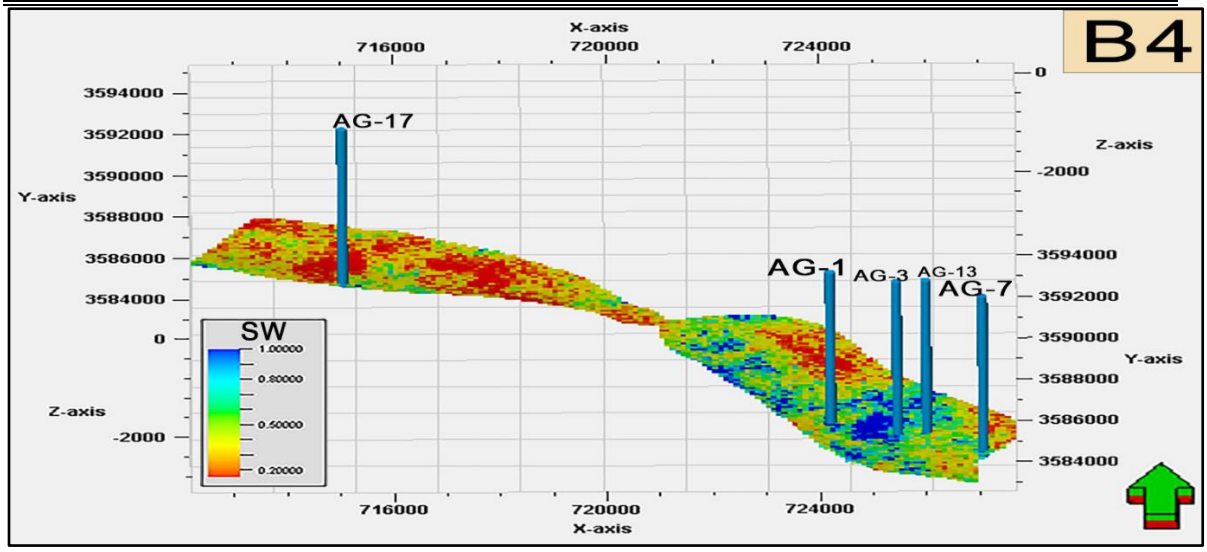

Figure (3-15): Water saturation model of Asmari Formation part unit (B4)

3.8.3. Permeability model

After scaling up the permeability that IP software exported for each reservoir unit Asmari, a permeability model was created. According to the information provided, the porosity and water saturation models have both been created using the same geostatistical technique, known as the Statistical Gaussian Simulation Algorithm.

The permeability models for each reservoir unit in the reservoir portion of Asmari are shown in the figures (3-16,17,18) below. Each unit of the investigated formations has a different permeability distribution.

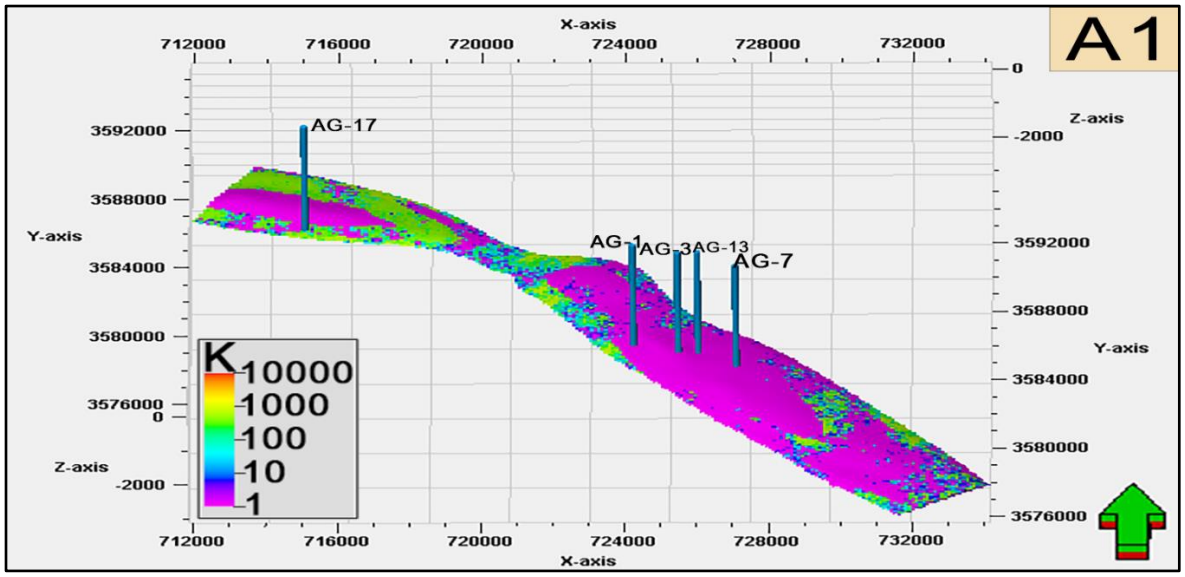

Figure (3-16): Permeability model of the reservoir Asmari part unit (A1)

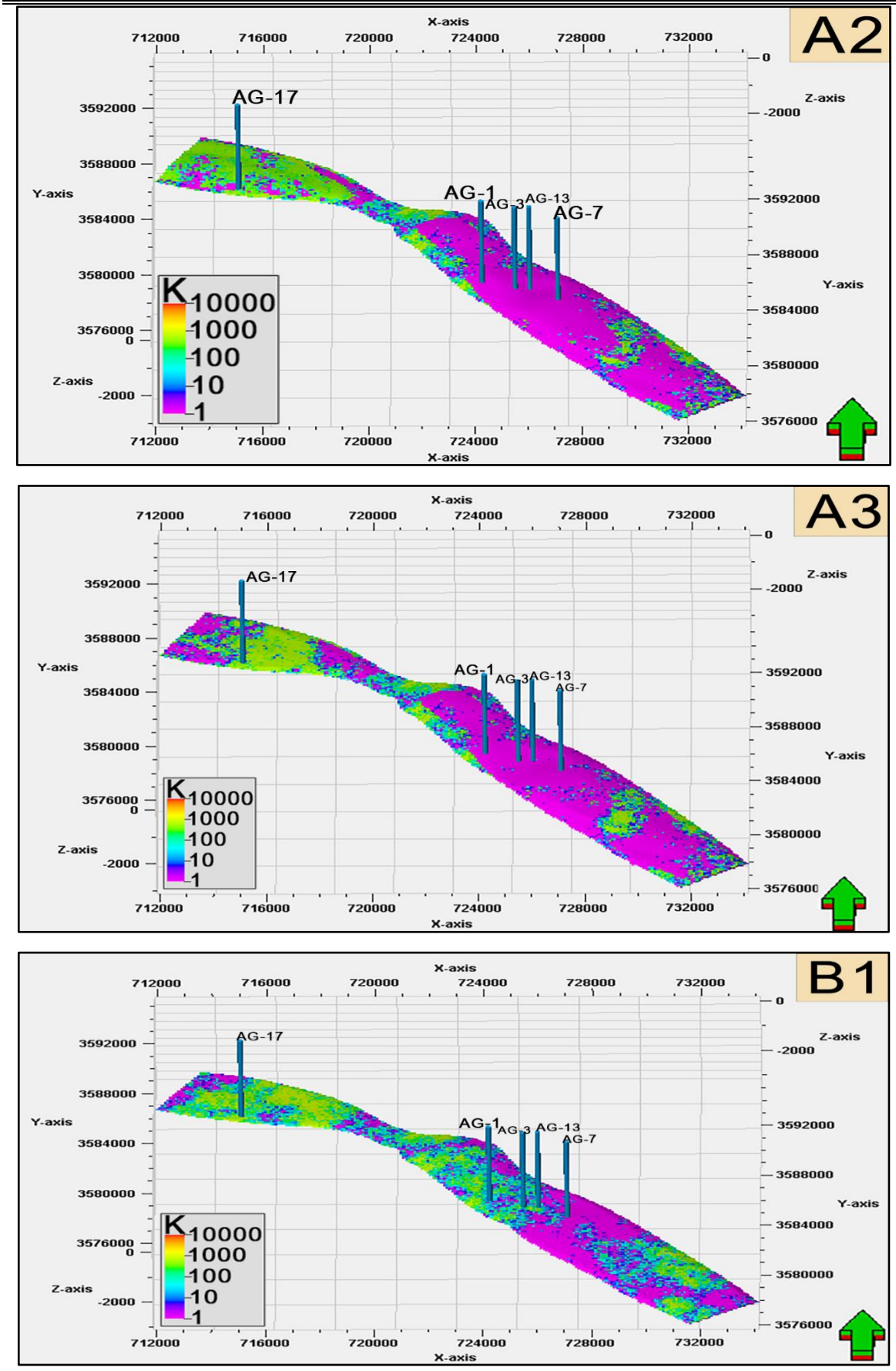

Figure (3-17): Permeability model of the reservoir Asmari part unit (A2, A3, B1)

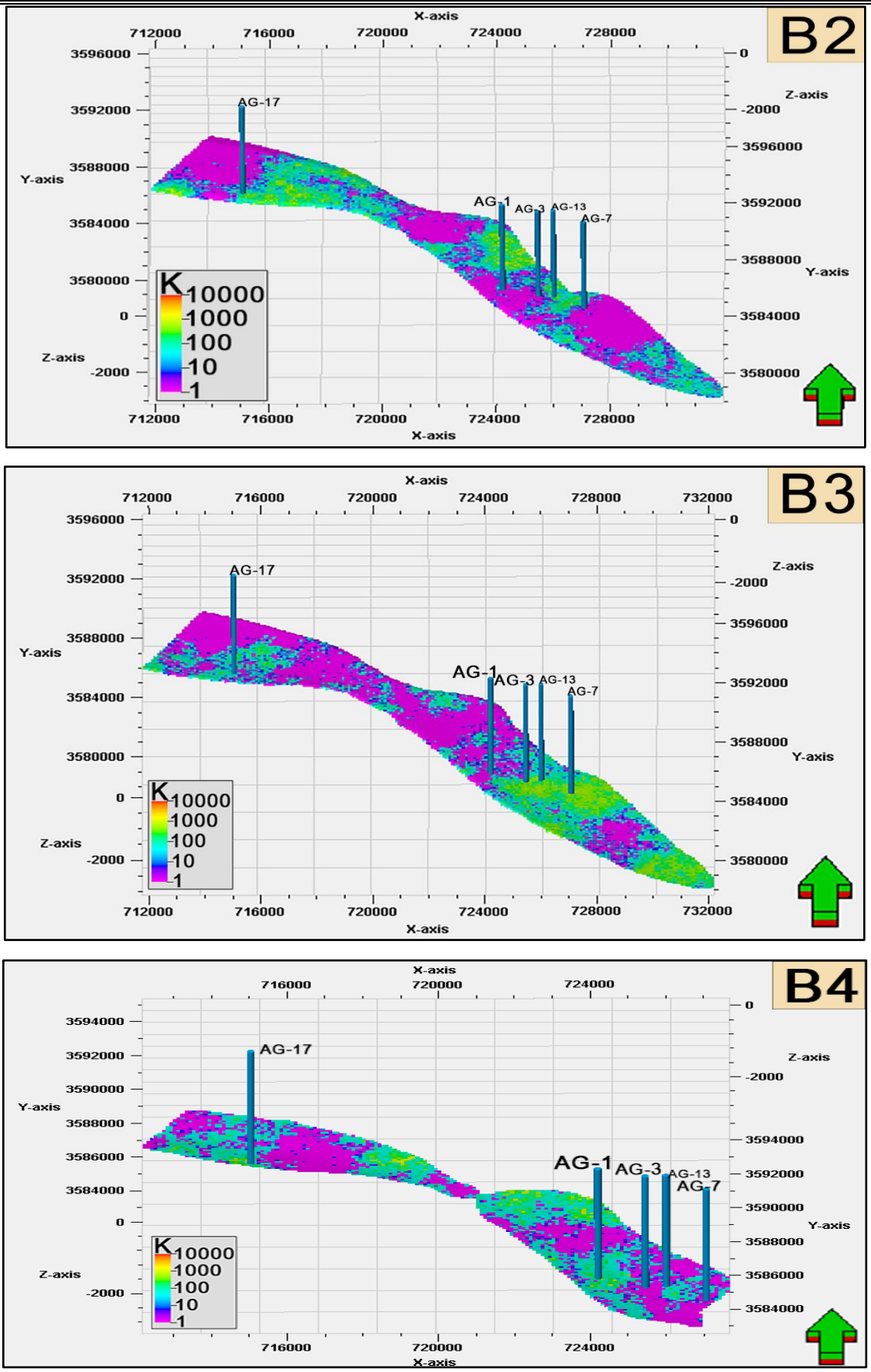

Figure (3-18): Permeability model of the reservoir Asmari part unit (B2, B3, B4)

3.9. Evaluation of 3D Asmari Model

3.9.1 Reservoir unit A1

This unit is the upper reservoir unit of the Asmari Formation reservoir section. The thickness of this unit of rang (10-20m). Average values for this unit's effective porosity (0.02-0.009) , water saturation (0.35-0.90) the high value of water Saturation, and permeability (0.2-20) because this unit is unable to serve as an oil reservoir due to its extremely low effective porosity.

3.9.2 Reservoir unit A2

The second unit of the reservoir portion of the Asmari formation is designated as A2. In the wells under study. The thickness of this unit is comparatively uniform (12-23m). Average values for this unit's effective porosity (0.012-0.027) , water saturation (0.40-0.60), and permeability (0.2-2) except the uint in AG-17. This unit exhibits poor petrophysical characteristics.

3.9.3 Reservoir unit A3

The reservoir portion of the Asmari Formation third unit is designated as A3. The thickness of this unit is comparatively uniform (12-40m). Average values for this unit effective porosity (0.029-0.2) , water saturation (0.40-0.80), and permeability (1-450). Its petrophysical characteristics are favorable especially in AG-13,AG-17 and contact oil in AG-17,AG-13.

3.9.4 Reservoir unit B1

The fourth unit in the reservoir section of the Asmari Formation is designated as B1.The thikness of this unit is rang (10-45m). Average values for this unit effective porosity (0.99-2) , water saturation (0.40-0.50), and permeability (50-120) except in AG-17 (4450). It has good petrophysical properties .

3.9.5 Reservoir unit B2

The fifth unit in the reservoir section of the Asmari Formation is designated as B2. The thickness of this unit is comparatively uniform (15-45m). Average values for this unit effective porosity (0.13-018) , water saturation (0.3-0.4), and permeability (80-170). The best oil reservoir unit is thought to be this unit due to its strong petrophysical characteristics.

3.9.6 Reservoir unit B3

The sixth unit in the reservoir section of the Asmari Formation is designated as B3. The thickness of this unit is comparatively uniform (20-40m). Average values for this unit effective porosity (0.12-0.18) , water saturation (0-20-0.45), and permeability (70-190). The best oil reservoir two unit is thought to be this unit due to its strong petrophysical characteristics.

3.9.7 Reservoir unit B4

The seventhunit in the reservoir section of the Asmari Formation is designated as B4. The thickness of this unit is comparatively uniform (20-40m). Average values for this unit effective porosity (0.11-0.22) , water saturation (0.40-0.70), and permeability (20-150). It has good petrophysical properties.

Chapter Four

Crude Oil Characterization

Chapter Four

Crude Oil Characterization

4.1. Introduction

Crude oil is a combination of hydrocarbons that existed in the liquid phase in natural subterranean reservoirs and that remain liquid at atmospheric pressure after passing through surface separating facilities. Crude oil can range in hue from straw yellow, green, and brown to dark brown or black (Peters *et al.*, 2005a). Surface oil has a higher viscosity than oil in heated subsurface reservoirs (Selley, 1998).

Crude oils are divided into fractions: n-alkanes, isoalkanes, cycloalkanes, mono-aromatics, di-aromatics, poly-aromatics, asphaltenes and resins. These are separated into saturated HC (hydrocarbon) and aromatic HC using benzothiophenes, and then evaluated with GC and GC/MS (Gas chromatography/Mass spectrometry) systems (Hunt, 1996) fig (4-6).

Crude oil is a complex mixture of hydrocarbons ranging from C_1 to C_{60}, with aliphatic, alicyclic, and aromatic hydrocarbons predominating. Small quantities of nitrogen, oxygen, and sulfur compounds, as well as certain organometallic complexes, particularly sulfur and vanadium, and dissolved gases, such as hydrogen sulphide, may be present (Akinlua *et al*.,2007).

A biomarker (or biological marker) is an organic geochemical instrument that may be used to determine the source of organic matter, the depositional environment, age, and the correlation between oils and source rocks (Hunt, 1996).

Geochemical techniques for characterizing crude oil include the use of bulk characteristics, stable isotope ratios, hydrocarbon contents, and biomarker signatures. Gas chromatography-mass spectrometry (GC-MS) is a practical method for analyzing chemicals found in oils in trace amounts (typically ppm), most of which are biomarkers (Peter and Moldowan, 1993).

In this study, crude oil samples were taken from three producing wells from Jeribe Euphrates, Upper Kirkuk and Middle Kirkuk Formation in Abu Ghirab Oil Field from well (AG-1, AG-7, AG-10). In the Geomark labs, these samples were examined using gas chromatography/mass spectrometry (GC/MS).

4.2. Crude oil geochemistry

The assessment of bulk characteristics, crude oil composition, and biomarkers is a typical approach to the geochemical characterization of crude oil. Oil is a complicated mixture having a huge number of chemical constituents that are closely linked. The type of the organic content in the source rock controls the chemicals present and their relative amounts at first (Tissot and Welte;1984).

4.2.1 Bulk properties:

Bulk properties are used to describe the physical and chemical qualities of crude oil in general. According to Tissot and Welte (1984) they are these measurements API gravity, sulfur compounds, nickel and vanadium compounds, light hydrocarbons (C15%), and stable carbon isotope composition (δ^{13}C%) that are the factors to consider.

1- API° gravity.
2- Sulphur content.
3- Organometallic compounds of (Ni, V).
4- Stable carbon isotopes.
5- Composition of crude oils

4.2.1.1 API gravity

The API gravity of oil is a bulk physical parameter that may be used to estimate thermal maturity. Because API gravity is inversely proportional to specific gravity. Also One key characteristic used to assess the quality of the oil is density (Peter *et al.*,2005; Dickson and Udoessien, 2012). A crude indication of thermal maturity, this measurement establishes the weight of a

crude oil per unit volume at 60°F. The following is an expression for the API gravity formula (Waples,1985; Wang *et al.*, 2000).:

$$API° \ gravity = (141.5/ SG) - 131.5$$

Where:

API: The Degrees API Gravity.

SG: Specific Gravity (at 60° F or 15.5°)

The heavy components in oil, such as NSO compounds, asphaltenes, and heavy saturated and aromatic compounds, crack more during thermal maturation,

According to general classifications, light crude oil is defined as having an API gravity of higher than 31, medium crude is defined as having an API gravity of 22 to 31, and heavy crude is defined as having an API gravity of 20 or less. According to (Tissot and Welte,1984), crude oils with API gravities less than 20o are immature, whereas oils with API gravities more than 20o are mature. According to (Waples,1985), the API gravity range for most crude oils is between 20 and 45, with less than 20 being typically biodegraded and more than 45 being condensates oil. All examined crude oil samples in the area under study range in API gravity from (20° -22° API) table (4-1), it is considered as medium oil and the well AG-10 heavy crude (19° API)

4.2.1.2 Sulfur Compounds (S):

Sulfur compounds are among petroleum's most significant nonhydrocarbon heteroatomic components. It is the third most prevalent atomic ingredient of crude oils, after carbon and hydrogen. It is found in both medium and heavy fractions of crude oils.

In contrast to nitrogen, sulfur concentration is not directly connected to crude oil's heaviest components. The majority of sulfur compounds in crude oil are generated early in the diagenesis process. Low–sulfur oil is generally connected with terrestrial classics, whereas high–sulfur oil is frequently associated with carbonate sequences. According to Tissot and Welte (1984),

whereas oils with high sulfur concentration (greater than unity) belong to the aromatic intermediate class, oils with low sulfur content (less than unity) are categorized as paraffinic, paraffinic - naphthenic, or naphthenic classes. Sulfur compounds are employed as paleoenvironmental markers, as well as for determining maturity, biodegradation, and crude oil correlations.

High sulfur oil is defined as oil that contains greater than 1% sulfur (Tissot and Welte, 1984). Sulfur content and maturity have an inverse relationship, with sulfur content decreasing as maturity increases (Tissot and Welte, 1984).

Sulfur content of oil of marine origin can be used as a source indication since it contains more than 0.5% percent sulfur. Oil with high sulfur content is generated from carbonate source rocks, while oil obtained from clastic source rocks has low sulfur content (peter *et.al.,* 2005a). All the examined reservoirs oils in the region had significant sulfur concentration, ranging from (4.11%- 4.36%) Table (4-1).

4.2.1.3 Stable carbon isotopes ($\delta\ ^{13}C\%$)

To identify genetic links between oil and bitumen, stable carbon isotopes are toms whose nuclei contain the same number of protons but differing numbers of neutrons. Carbon-12 (12C) and carbon-13(13C), generally known as the light and heavy isotopes, are two stable carbon isotopes that are employed for oil-oil and oil-source correlation. Because of its dominance and simplicity of analysis, it is the most commonly utilized (Peters *et al.,* 2005a).

The relative amounts of 13C and 12C in the sample are measured using mass spectrometers and compared to those in the Peedee Belemnite standard to determine the carbon isotope levels (PDB limestone).

$$\delta 13C\ (‰) = [(^{13}C/^{12}C\ sample - (\_^{13})C\ /^{12}C\ standard)\ /^{13}C/^{12}C\ standard \times 1000$$

….(4-1) (Peter,1984).

Sofer (1984) proposed that the isotope composition of oils could change owing to maturation and possibly migration effects due to minor

homogeneities in the source material. Zumberge (1993) utilized the connection between the carbon isotopes of the saturated fractions and those of aromatic to differentiate between marine and non-marine oils.

The following equation (Sofer, 1984) was used to distinguish between oils from marine and non-marine sources using the canonical variable relationship (CV):

$$CV = -2.53\,\delta^{13}C_{\text{sat}} + 2.22\,\delta^{13}C_{\text{aro}} - 11.6 \ldots\ldots (4-2)$$

A positive result indicates that the sample is richer in 13C isotope in comparison to the standard, and is referred to as 13C-enriched; a negative value indicates that the sample is depleted in 13C isotope in comparison to the standard, and is referred to as 13Cdepleted (Peter *et al.*, 2005).

The aromatic percentage ranges from -23.87 to -27.90 and the saturate fraction ranges from -24.55 to -27.74, indicating that the samples are marine oils (Denison *et al.*, 1990; Hunt, 1970; Tissot and Welte, 1978 and Rogers, 1980).

The oil samples computed canonical variable (CV) values, which varied from (-2.57 to -3.34), suggesting that the oils were non-waxy and came from carbonate marine sources, as shown by (Sofer,1984). The average stable carbon isotope ratio for the studied crude oil samples are (-27.52% - 27.72%) percent, the reservoir is Tertiary, so the source age according to this relation is Jurassic to Lower Cretaceous fig(4-4).

4.2.1.4 Composition of crude oil:

According to (Peter *et al.*, 2005), the organic compound of petroleum is subdivided into: -

A- Hydrocarbons: - compounds made up solely of carbon and hydrogen. They are split up into:

1- **Light Hydrocarbons (%C¹⁵):** Light hydrocarbons, which range from methane to octane and include regular, iso-, cyclic alkanes, and aromatic compounds, are gases that are volatile liquids at ordinary

temperature and pressure. Early-expelled oils with low maturities may have less than 15% of light hydrocarbons, and typical marine oils with mid-oil windows may contain 25% to 40% of light hydrocarbons as in the samples under study, and high-maturity condensates may contain almost 100% of light hydrocarbons.

2- **Saturated Hydrocarbons: -** compounds that are hydrogen-saturated could only have single carbon-carbon bonds including:

- **Normal-paraffins** refer to straight chains of various lengths.
- **Branched paraffin (branched alkanes)** are saturated hydrocarbons in which the carbon atoms form branched chains**.**
- **Cyclic paraffin**, also known as cyclic alkanes or naphthenes, are saturated cyclic compounds like steranes and triterpanes.

3- **Aromatic Hydrocarbons:-** Aromatic hydrocarbons are unsaturated substances with at least one benzene ring, a flat six-carbon ring in which each carbon atom shares its fourth bond with the rest of the ring. They may have side chains that are saturated and range in size.

B- Non-hydrocarbons:- They are organic molecules that also contain atoms of nitrogen, sulfur, and oxygen in addition to atoms of carbon and hydrogen. The majority of non-hydrocarbons also have straight chains and intricate cyclic configurations of double-bonded carbon atoms (Peter *et al.*, 2005). They are Subdivided into**:**

1- **Resins and Asphaltenes:** Most NSO Compounds (resins) molecules have less than 40 carbon atoms. Asphaltenes are complex compounds with more than 40 carbon atoms that are insoluble. Asphaltene addition to resin quantities range from 10 to 40 percent in aromatic intermediate oils but are typically under 10 percent in paraffinic oils and under 20 percent in paraffinicnaphthenic oils. Asphaltenes make up only 0 to 20 percent of the regular, undamaged oils (Tissot and Welte, 1984). The studied crude oil samples are primarily aromatic, with saturated hydrocarbon percentages ranging from 21.1% - 23.4%, aromatic from

48% - 49%, and NSO and resin compounds from 14.7-16 (table 4-2). By plotting these data on a ternary hydrocarbon plot of aromatic HC, saturated HC, and NSO compounds, one can determine a typical crude oil for the studied samples with no degradation and abundant hydrocarbons .

2- **Organometallic Compounds (Nickel and Vanadium):** It is possible to compare oil samples using nickel and vanadium metals (Hedberg, 1968; Barwise, 1990; Galarraga *et al.*, 2008). Vanadium is often more abundant than a nickel in oil (Hunt, 1996). The majority of crude oil samples taken from maritime environments have been associated with high amounts of Ni and V. This is typical for marine source rocks where there is a significant input of porphyrins, which are precursors to chlorophylls and are produced by bacteria and algae to the organic matter (Dickson and Udoessien,2012). As the age of the oils grew older, the V/Ni ratio decreased. Oils from marine carbonates or siliciclastics have low wax content, moderate to high sulfur, high amounts of nickel and vanadium, and low nickel/vanadium (1) ratios. Oils from lacustrine source rocks have high wax, low sulfur, moderate amounts of metals, and high Nickel/Vanadium (>2) levels. Non-marine oils are derived from higher plant organic matter, which shows high wax, low sulfur, and extremely low metals (Peter *et al.*, 2005). Ni/V ratios for the examined crude oil samples varied from (42-103), pointing to marine carbonate source rock (table 4-1).

4.2.2. Bulk Parameters Relationship

- The results of bulk properties of the studied sample crude oil are listed in tables (4-1) and (4-2).
- All of the investigated crude oil samples had high sulfur content (4.11% to 4.36%), which is related to the marine environment (Peter and Moldowan, 1993).

- All samples' API Gravities, which ranged from (19-22 API), reflected middle oils (Peter *et al.*, 2005). Different thermal maturities may produce variations in API gravity, although low API values indicate lower thermal maturity (Peter *et al.*, 2005). Additionally, as the proportion of aromatic and naphthenic hydrocarbons grows relative to paraffin and as the proportion of NSO compounds increases, crude oil gets heavier and its API gravity decreases (Hunt, 1996). It indicates a favorable association between the saturated-to-aromatic ratio and the percentage of hydrocarbons C15 (Hunt, 1996).
- The wide range of Ni and V trace element values and the high ratios of V/ (V Ni) in the oil sample, along with the presence of a significant amount of sulfur, point to anoxic environmental conditions. The variations in the sulfur concentration and API gravity can be used to account for the discrepancies in oil samples' thermal maturities. Because of this, the oils were therefore less mature fig. (4-2) (4-3)
- When related to thermal maturity, all samples from the analyzed fields had light hydrocarbon percentages (C15) that ranged from (25-28) and displayed the typical mid-oil window marine oils (Peter *et al.*, 2005).
- All of the samples were analyzed, and the Nickel/Vanadium ratios ranged from (42-103), indicating a marine environment (Peter *et al.*, 2005).
- The graph (4-1)shown represents a comparison of the carbon-isotope levels of the aromatic and saturated fractions of the crude oil samples under study (fig.4-1). These plots can be used to identify oil families and determine whether sources are marine (non-waxy) or terrestrial (waxy) Sofer's (1984). Additionally, it was suggested that the age of the source rock is between the Jurassic and lower Cretaceous by depending on the average of the stable isotope ratios for the examined oil samples versus age. Low CV values, which varied from (-2.57 to -3.34), show that the marine environment is carbonate.

Table (4-1): Bulk properties, gross compositional parameters, and stable carbon isotope composition of the studied crude oil fields

Well No.	Depth (m)	Formation	API	%S	$<C^{15}$	Ni(ppm)	V(ppm)	Carbon isotope PDB		
								%Sat	%Aro	Cv
AG-1	3030	Middle Kirkuk	21	4.11	25.8	49	112	-27.72	-27.57	-2.57
AG-7	2949	Upper Kirkuk	22.4	4.24	26.5	39	98	-27.64	-27.62	-3.04
AG-10	2941	Jeribe Euphrates	19.8	4.36	28.1	40	101	-27.52	-27.62	-3.34

Table (4-2): The percentages of Saturates, Aromatics, Resins and Asphaltene in the studied crude oil samples

Well no.	Formation	**Saturate%**	**Aromatic%**	NSO%	**Asph. %**
AG-1	Middle Kirkuk	21.1	49	16	14.9
AG7	Upper Kirkuk	23.1	48.2	15.5	13.2
AG-10	Jeribe-Euphrates	23.4	49	14.7	12.9

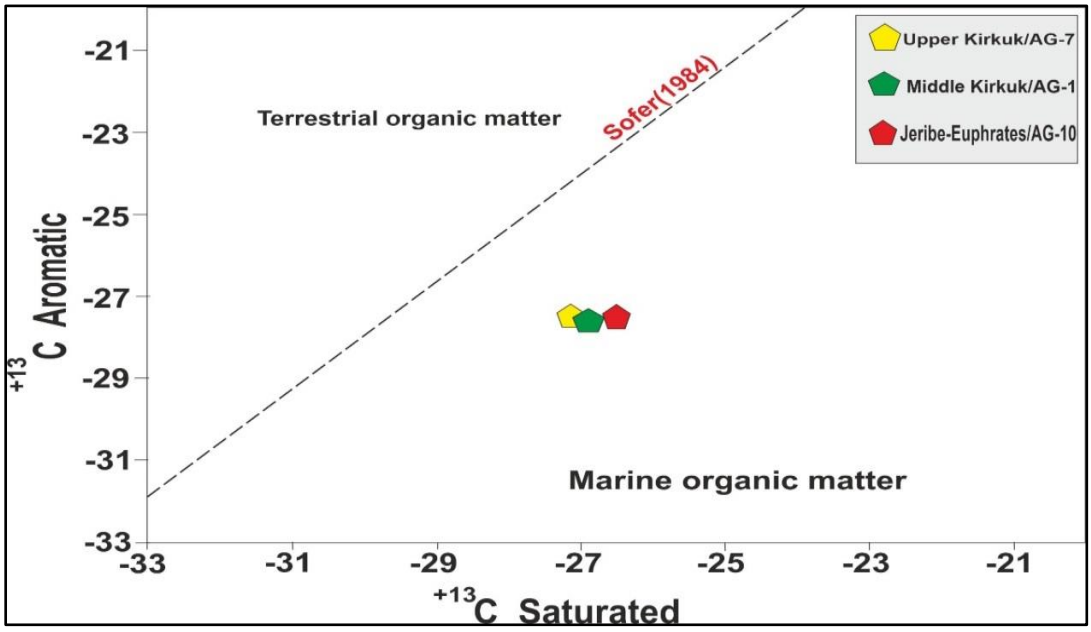

Figure (4-1): Cross plot of the analyzed crude oil samples' saturated vs aromatic hydrocarbon carbon-13 isotope ratios (Sofer,1984).

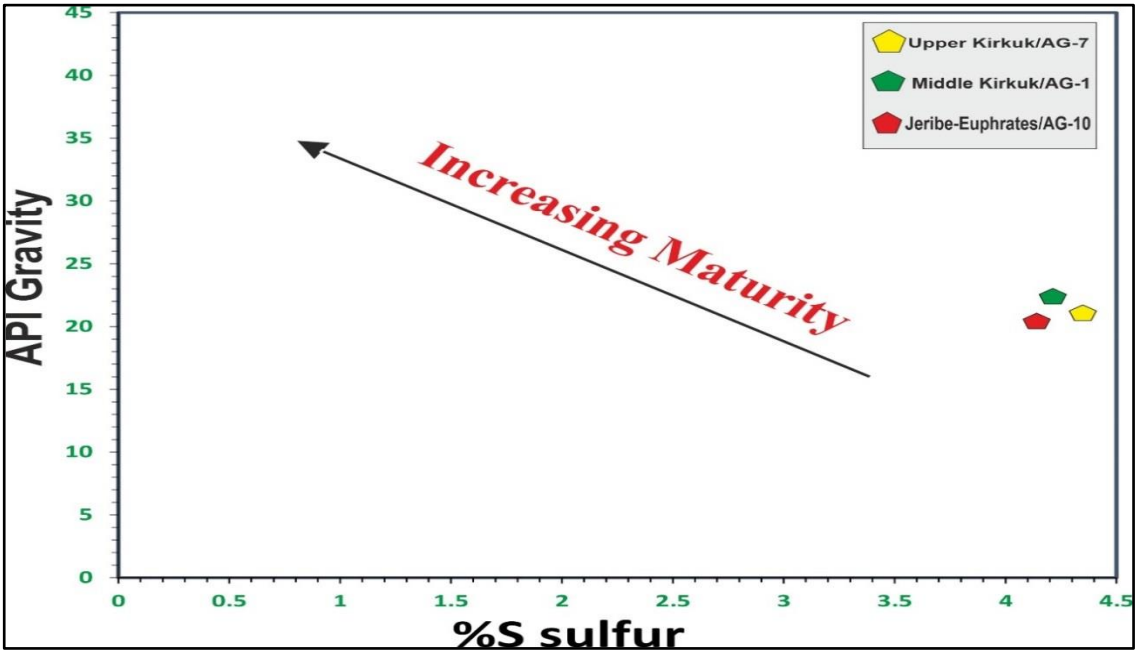

Figure(4-2): Plot of API gravity versus (wt. %) Sulphur for crude oil samples of Abu Ghirab oil field.

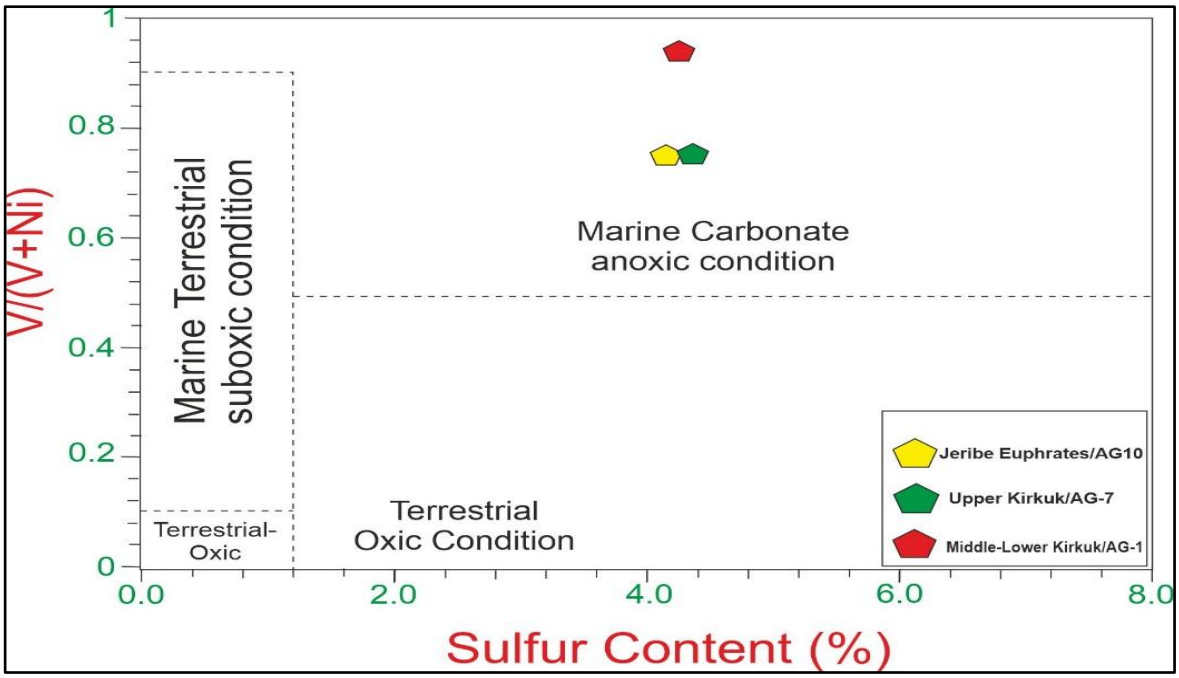

Figure (4-3): Cross plot of V/(V / Ni) versus sulfur content after (Peters *et al.*, 1999).

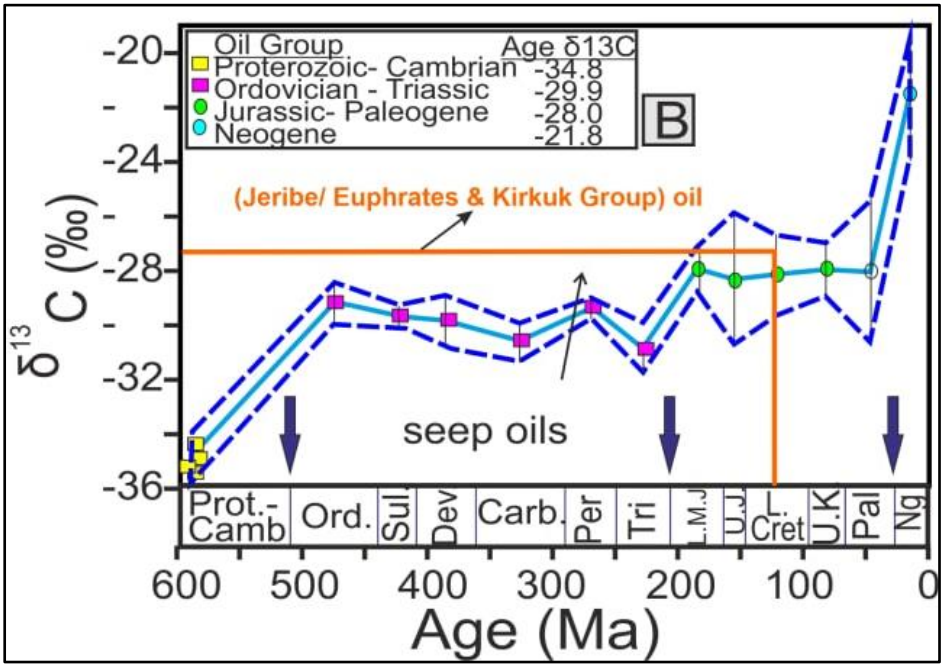

Figure (4-4): Average stable carbon isotopic ratios for C15+ saturated fractions oil versus age for crude oil sample of Halfaya oil field after (Andrusevich et al., 1998).

4.3. Gas chromatography-mass spectrometry analysis

Gas chromatography (GC) is an analytical intended to separate organic molecules as they pass through the column based on their respective propensity to partition into the stationary (high-molecular-weight liquid) or mobile (inert carrier gas) phases. As these components elute from the column, a variety of detectors can be utilized to quantify them.

Gas chromatography represents another screening method, which determines the content and concentration of light hydrocarbons (oil and gas) emitted from formation cuttings during drilling (Noble, 1991). The full crude oil is analyzed using the GC method to extract the normal alkane and acyclic isoprenoids. Fine-grained formation cuts, such as those formed by source rocks, can retain hydrocarbons long after they reach the surface, making them ideal samples for this sort of study.

Mass spectrometry is a technique for determining the molecular structure of chemicals, particularly biomarkers, by monitoring the ions at m/z 191 and m/z 217, respectively. The gas chromatography technique can be performed at the well site or in a laboratory under strictly controlled

conditions (McCarthy *et al.*, 2011). A gas chromatograph analyses and records distinct peaks for methane (C1), ethane (C2), propane (C3), isobutene (iC4), and normal butane (nC4) freed throughout the drilling operation.

For pentanes (iC5 and nC5) and heavier hydrocarbons (C5+), a single peak is usually observed. By analyzing the composition and concentration of these gases, geoscientists may assess the sorts of hydrocarbons that may be generated inside a potential resource (McCarthy *et al.*, 2011).

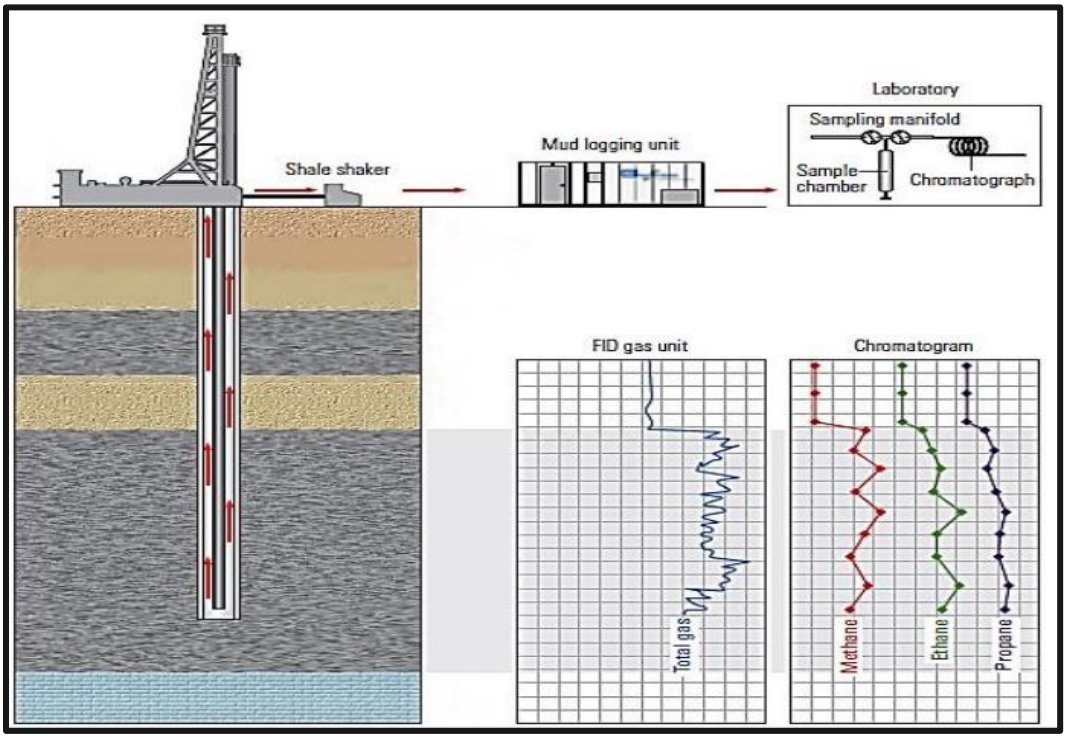

Figure (4-5): Illustrating formation cuttings analysis using gas chromatography technique. After (McCarthy *et al.*, 2011).

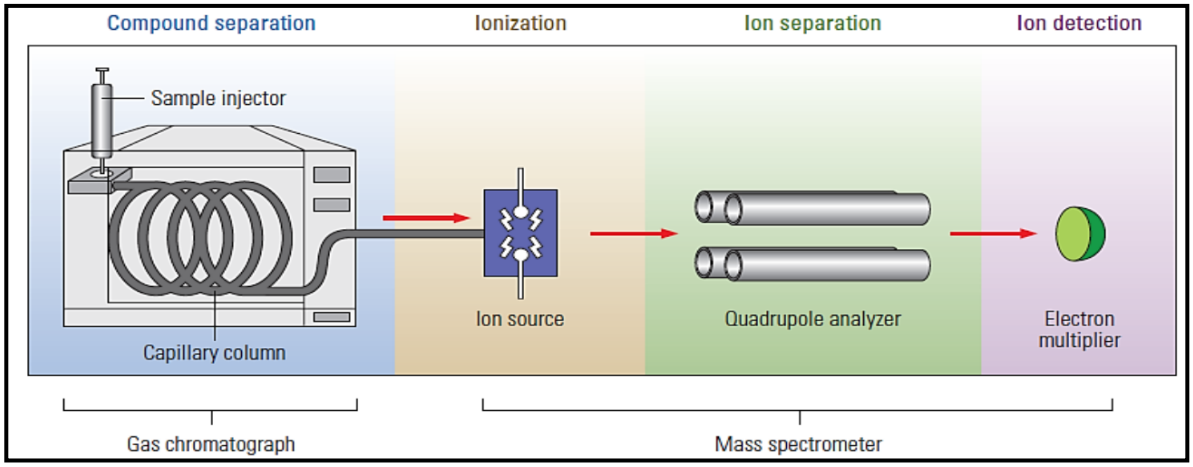

Figure(4-6): Biomarker analysis using GCMS technique. After (McCarthy *et al.*, 2011)

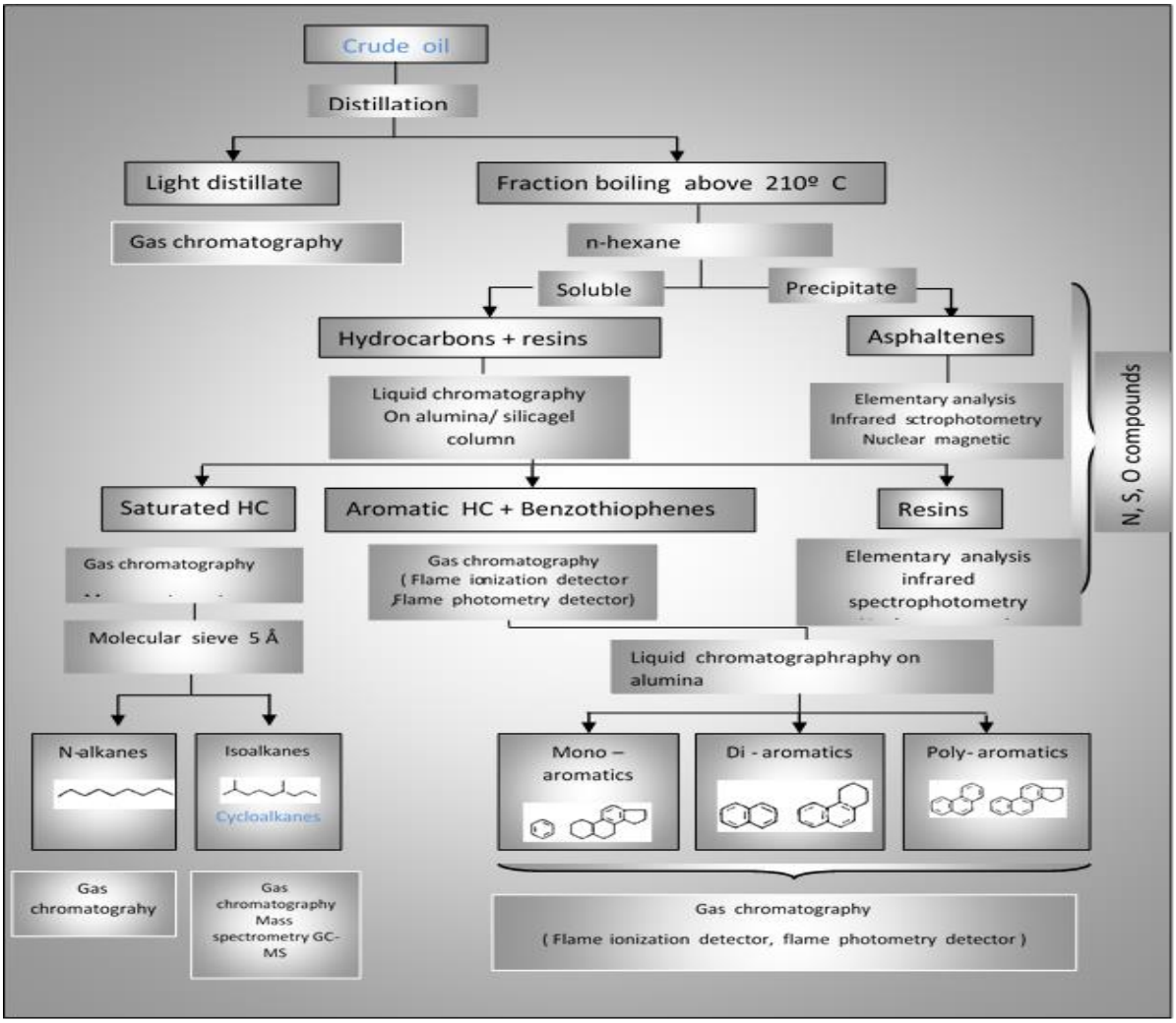

Figure(4-7): Flow chart of crude oil and source rock bitumen analysis by gas chromatography and mass spectrometry after (Tissot and Welte, 1984).

4.4. Biomarkers

Biomarkers are complex organic compounds made up of carbon, hydrogen, and other elements found in petroleum, rocks, and sediments that are structurally similar to their parent organic molecules in living creatures. Total ion chromatograms (TIC) are used to identify these substances, which are normally quantified by selective ion monitoring (SIM/GCMS) and their distribution computed using regions beneath the peaks.

Most but not all, biomarkers are isoprenoids, composed of isoprene subunits. Phytane, sterane, triterpenes, and porphyrins are among them (Peters *et al.*, 2005b). Biomarkers are also helpful because they can offer information on the organic matter in the source rock, environmental circumstances during

depositional and burial, the rock or oil's thermal maturity, the degree of biodegradation, some features of the source rock lithology, and age (Peters *et al.*, 2005b). Biomarker parameters are arranged by groups of related compounds; alkanes and, cyclic isoprenoids, sterans, terpenes, aromatic steroids, and porphyrins.

4.4.1. Alkanes and Acyclic Isoprenoid Ratios

The gas chromatograms apparatus provides alkanes and acyclic isoprenoids figure (4-7,8,9).

4.4.1.1. n-alkenes ratio

In crude oil, the n-alkanes range from n C15 to n C35. Their distribution in crude oil can be utilized to determine the source of organic materials (Duan and Ma, 2001). For example, the shift from n-C15 to n-C20 suggests that marine organic matter contributes to biomass via algae and plankton (Peters and Moldowan, 1993). The consistency of n-alkane distribution patterns in oil samples suggests that they are linked and have had comparable histories with no evidence of biodegradation (Moustafa and Rania,2012).

a- Extended tricyclic terpene ratio (ETR):

To identify Triassic from Jurassic oil samples, use an age-related characteristic. m/z chromatogram used to measure. The extended tricyclic ratio can be used to lessen the impact of thermal maturity on source interpretation (Holba *et al.*,2001):

$$ETR=(C_{28}+C_{29})/(C_{28}+C_{29}+TS)\ldots.(4\text{-}3)$$

The examined crude oil samples show an ETR value that (0.9), which is less than 1.2 (table 4-3), which may suggest that these oils were produced in the middle to late Jurassic. ETR declines with age.

b- Carbon Preference Index (CPI) and Odd-to Even Preference (OEP):

The Carbon Preference Index (CPI) is defined as concentrations of the ratio of odd to even carbon number n-alkane. It's the ratio obtained by dividing the

amount of odd-numbered alkanes by the sum of even-numbered alkanes. According to Hunt 1996, this equation may be used to estimate CPI values:

CPI= 1/2[(C25- C33) / (C24- C32) + (C25-C33) / (C26- C34)]….(4-4)

CPI is influenced by both source and maturity of crude oils (Tissot and Welte, 1984). It was the first crude oil maturity indicator, and it is lower as maturity increases. Immature rocks showed high CPI values (>1.5) regularly, but mature oils' CPI values were frequently below 1.0. Some of the numbers are close to 1.0, indicating that the crude oils are nearing maturity (Onojake *et al.*, 2015).

The high CPI values imply poor maturity and a continental environment, but the CPI~1 values for oils and source rocks indicate a marine environment and higher thermal maturity, and the ratio CPI<1 indicates a hypersaline environment, indicating a redox paleoenvironment (Fagbote and Olanipekun,2012). Odd/even preponderance (OEP) is frequently used as a marker for the presence of terrestrial plant waxes in geological and environmental materials. On the other hand, recent sediments containing organic matter input from phytoplanktonic organisms such as diatoms and certain bacteria have been linked to an even/odd preponderance (Ekpo .,2012).

The OEP can be altered to include any range of carbon values, and it was calculated using the following formula:

$$OEP(1) = (C21 + 6\,C23 + C25) / (4\,C22 + 4\,C24) \quad (4\text{-}5)$$

$$OEP(2) = (C25 + 6\,C27 + C29) / (4\,C26 + 4\,C28) \quad (4\text{-}6)$$

In immature samples, the carbon preference index (CPI) and odd/even preponderance (OEP) are excellent predictors of OM type, with a greater abundance of C16–18 n-alkanes indicating aquatic OM and a C27–33 odd abundance of n-alkanes indicating terrigenous OM (Hunt, 1995). In typical mature crude oils, n-alkane abundance varies considerably as OM matures, and CPI and OEP trend to 1(Asif *et al.*,2012). The CPI and OEP values for the examined crude oil samples were approximately (less than 1), except for

the previously described sample of AG-1, all of the examined samples shared immaturity and a more reducing environment (table 4-3).

4.4.1.2. Pristane and Phytane (Pr/Ph):

These chemicals are produced during a sedimentary deposition when the phytyl side-chain of chlorophyll breaks down. According to a theory, in anaerobic sedimentary conditions, phytol degradation causes the creation of phytane rather than pristane to occur more frequently. To assess the redox paleo conditions, Pr/Ph ratios might be utilized.

The Pr/Ph ratios of about 1.2 show that fossil fuel pollution developed throughout geologic time by sediment deposition in somewhat aerobic water column environments, such as the ocean or open marine (Payet *et al.*, 1999).

In conclusion, significant caution must be used when interpreting the Pr/Ph ratio as a sign of depositional settings (Philp, 2003a). Without supporting evidence, the Pr/Ph ratios in the range of 0.8 to 3.0 are taken to represent unique paleoenvironmental conditions. Less than 0.8 suggests salty to hypersaline conditions linked with evaporite and carbonate deposition, whereas Pr/Ph more than 3.0 shows terrigenous plants supply deposited under oxic to suboxic conditions (Peters *et al.*, 2005).

Pr/Ph ratios were typically low and ranged from 0.9 to 0.94, Pr/Ph <1, the oil samples produced from source carbonate and anoxic environment, indicate anoxic source rock deposition, particularly when accompanied by high sulfur content figure (4-10).

Table (4-3): Ratios of the studied samples' Pr/Ph, Pr/nC17, Ph/nC18, and Carbon Preference Index (CPI) values.

Well No.	Pr/Ph	Pr/n-C17	Ph/n-C18	n-C27/n-C17	CPI	ETR
AG-1	0.9	0.26	0.36	0.14	1.02	0.9
AG-7	0.84	0.25	0.36	0.18	0.87	0.9
AG-10	0.94	0.27	0.36	0.15	0.95	0.9

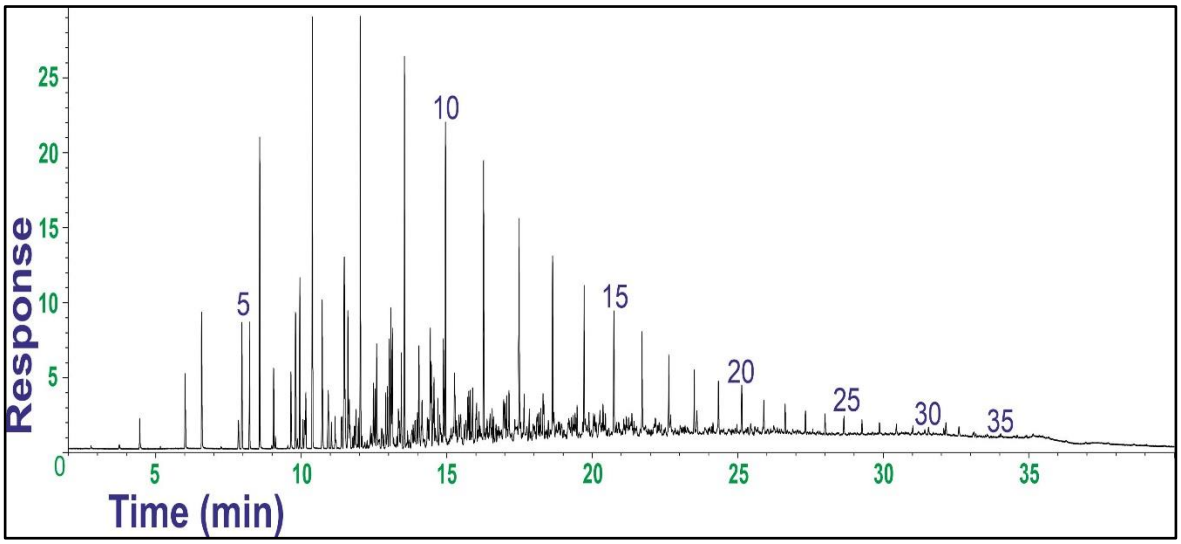

Figure (4-8): Whole crude chromatograms for AG-1.

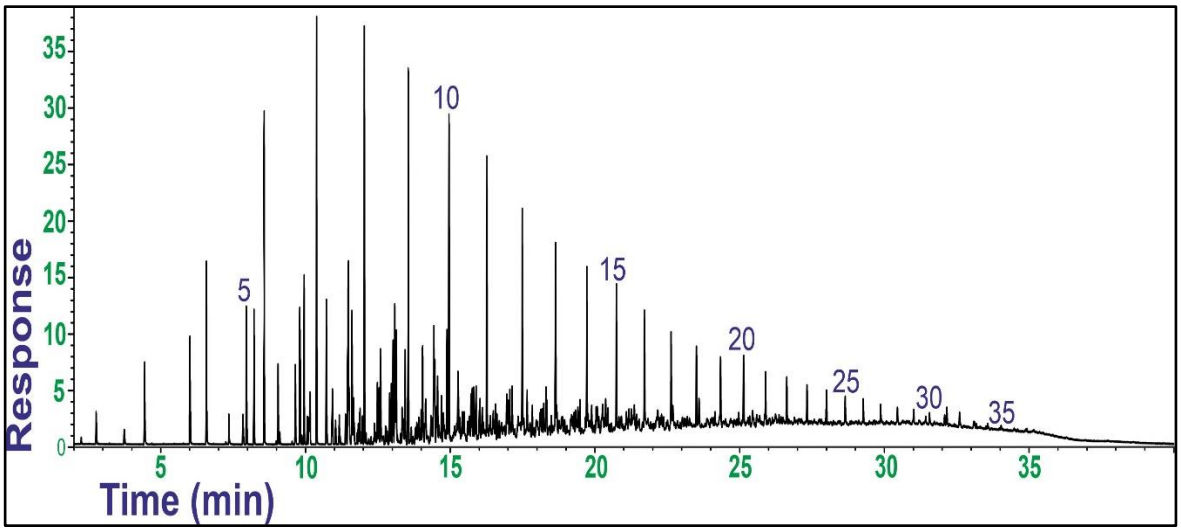

Figure (4-9): Whole crude chromatograms for AG-7.

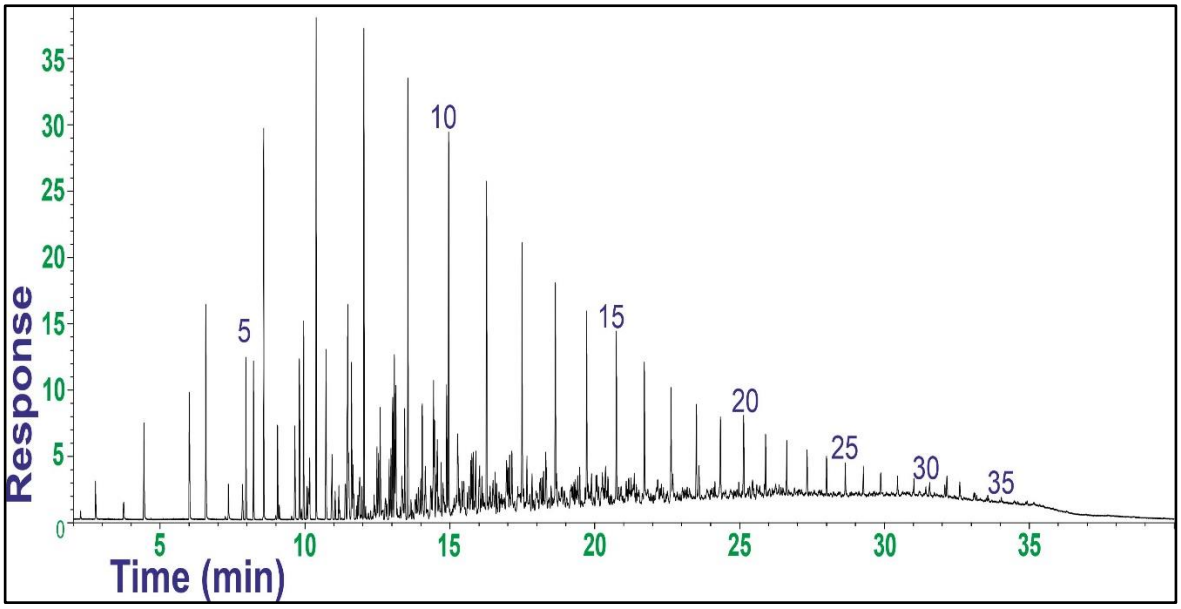

Figure (4-10): Whole crude chromatograms for AG-10.

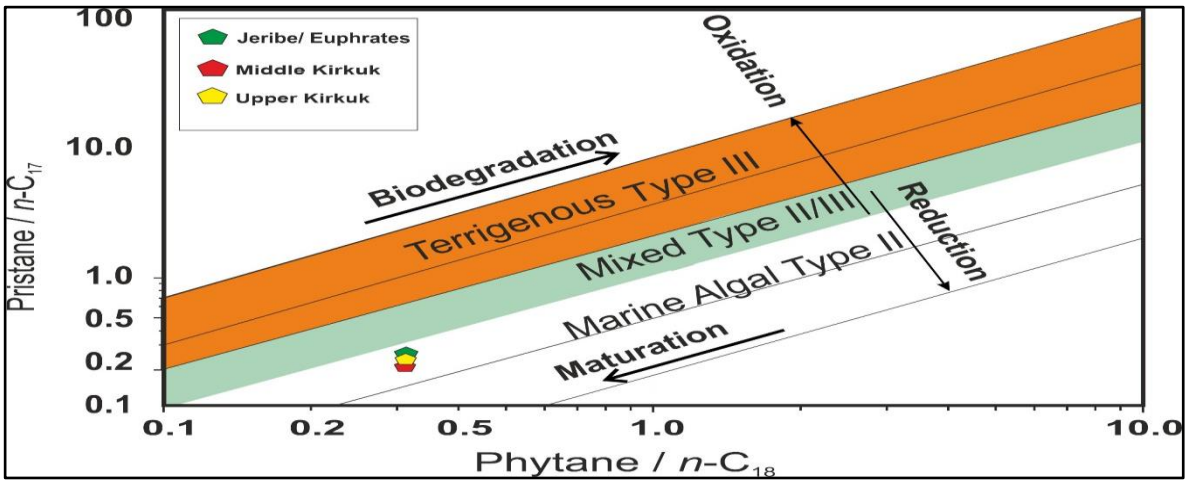

Figure (4-11): Pristane/ nC17 Versus Phytane/ nC18 for studies Sample crude oil (after Peters, 1999).

4.4.2. Terpanes similar compound

Many terpanes found in petroleum are derived from lipids found in bacterial (prokaryotic) membranes (Ourisson *et al.*, 1982). These homologous series of cyclic, bicyclic (drimanes), tricyclic, tetracyclic, and pentacyclic chemicals that make up these bacterial terpanes are frequently observed utilizing m/z 191 mass chromatograms (Peter *et al.*, 2005) fig (4-11,12,13). The following terpenes compounds are used to identify the source of crude oils:

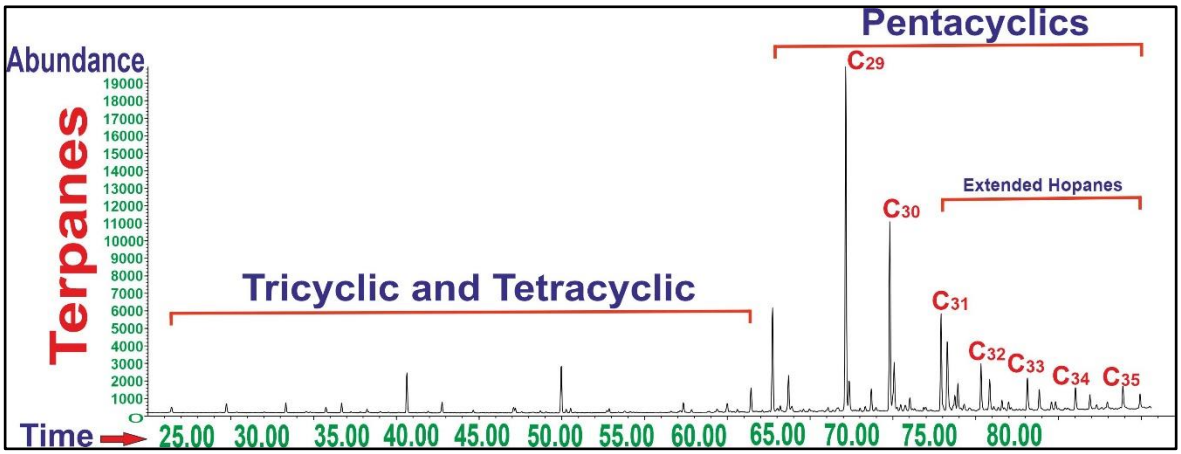

Figure (4-12): GC/MS showing terpanes peaks of AG-1

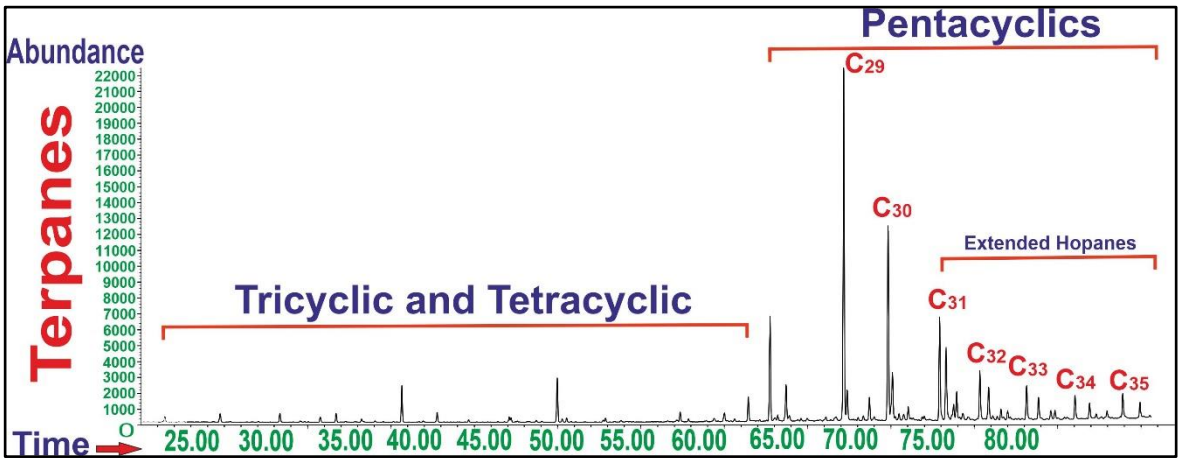

Figure (4-13): GC/MS showing terpanes peaks of AG-7

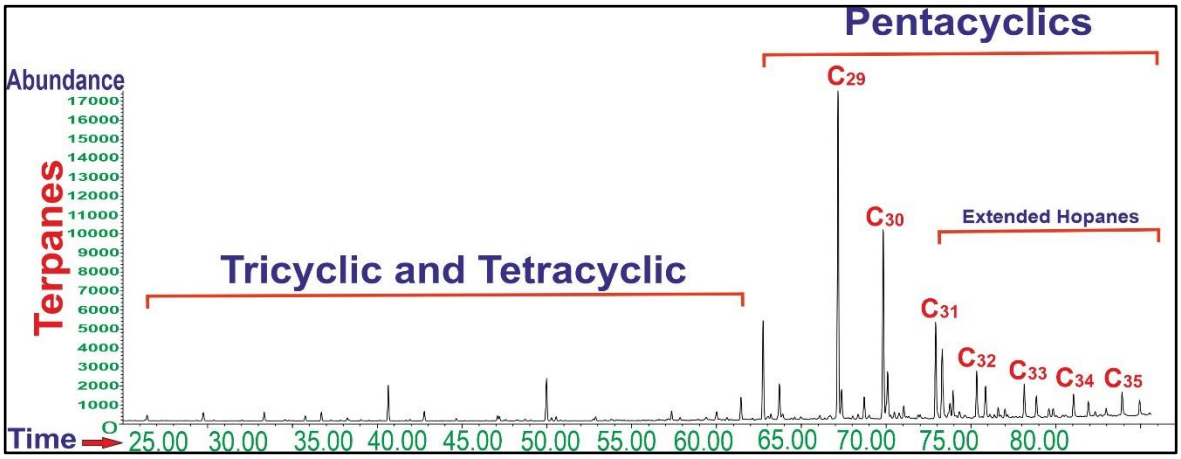

Figure (4-14): GC/MS showing terpanes peaks of AG-10

4.4.2.1 Tricyclic terpane ratios

The tricyclic terpanes include the ratios of C22/C21 and C24/C23 tricyclic terpanes. When employing m/z 191, the ratio of different tricyclic terpanes to carbon numbers can be used to discriminate between marine, carbonate, lacustrine, paralic, coal/resins, and evaporitic oils. The tricyclic terpane ratios C22/C21 and C24/C23 aid in identifying crude oils and extracts originating from carbon-bearing source rocks.

Lacustrine and marine oil can be differentiated using the C26/C25 tricyclic terpane ratio (peters *et al.,* 2005b). The crude oil samples are likely made from marine carbonate source rocks, as evidenced by the high C22/C21 ratio in all study crude oils and the low C24/C23 ratio (table 4-5).

4.4.2.2. The C_{26}/C_{25} tricyclic terpane ratio

The ratio of C26 tricyclic terpane to C25 tricyclic terpane can be used to distinguish marine from lacustrine source rocks When cross-plotted with C31/C30hopane (Peters *et al*., 2005; Volk *et al.*, 2005) This association for the examined crude oil samples shows a marine source carbonate environment (fig. 4–17), (table 4-5).

4.4.2.3. C24 Tetracyclic terpane ratio

Most oil and rock extracts contain tetracyclic terpanes that range in size from 24 to 27, and there is strong evidence that they can also contain homologs up to C35 (Hunt,1996). On the m/z 191 chromatograms, some of these substances are identifiable. More mature source rocks and oils exhibit higher ratios of tetracyclic terpanes to hopanes. Tetracyclic terpanes, in contrast to hopane, are more resistant to biodegradation (Aquino Neto *et al.*, 1983).

The presence of C24 tetracyclic terpane (also known as C24Tet/hopane, C24Tet/C23, and C24Tet/C26 tricyclic) in large quantities in petroleum appears to indicate a carbonate and evaporate source-rock context (Lewan,1984). The values of this ratio in the samples of crude oil that were tested show high proximity (table 4-5), suggesting that these samples are low mature and from carbonate marine sources.

4.4.2.4. C_{31}/C_{30} hopane

Useful for differentiating between the habitats where source rocks were deposited—marine vs lacustrine. Also known as C31R/H or C31 22R/C30 hopane. Oils from marine shale carbonate and marl source rocks typically exhibit high C31 values more than 0.25, in contrast to crude oils from lacustrine source rocks.

When combined with other criteria such as the C30 n-propylcholestane and C26/C25 tricyclic terpanes and the canonical variable from stable carbon isotope studies, marine and lacustrine crude oils may be separated most effectively (Peters *et al.*, 2005b). The C31/C30hopane value for the crude oil

samples under investigation is 0.36, indicating a carbonate marine source rock table (4-5).

4.4.2.5. (30-Norhopane/hopane):

Anoxic carbonate or marl source rocks and oils typically have high 30-norhopane/hopane levels. When this ratio is greater than 1.0, it can also be represented as C29/C30 hopane (C29/H), which indicates oil produced under anoxic carbonate or marl source rocks. At higher temperatures of thermal maturity, norhopane is more stable than hopane. This means that within a set of related oils, 30-norhopane/hopane might rise with thermal maturity (Peters *et al.,* 2005b). The analyzed samples are all more than 1.0 and correspond to anoxic carbonate source rocks (Table 4-5).

4.4.2.6. Oleanane/30 Hopane (Oleanane index)

Oleanane, which can be found in crude oils and rock extracts, is a very specific indicator of higher-plant input from Cretaceous or younger rocks (Peters et al., 2005b). It can also be written as OL/ H or OL/ (OL + H), and it typically elutes before the C30 hopane.

Oleanane is difficult to identify if its ratio is low due to interference from other components with comparable retention durations as they exit various columns of mass spectrometry (GC/MS), but it is more precisely done using GC/MS m/z -190 (Peter *et al.*,2005). According to Moldowan *et al*.,(1994)'s hypothesis, crude oils extracted from Tertiary-aged rocks have an oleanane index greater than 0.3.

Oleanane is prevalent in Middle/Late Cretaceous to younger sediments but not in Jurassic or older layers, according to Peter & Moldowan (1993). In crude oil samples, the oleanane index (table 4-5), which is almost zero as shown by GCMS, indicates that the input from organic matter connected to angiosperms was very low. Additionally, the lack of oleanane may be a reliable sign of a carbonate marine environment.

4.4.2.7. Ts/Tm Ratio

Ts (trisnorneohopane) and Tm (trisnorhopane) are specific types of trisnorneohopane (Peters *et al.,* 2005). This ratio is widely utilized as a maturity indicator, as the abundance of the less stable Tm isomer decreases as a function of burial depth compared to the more stable Ts isomer during cantagenesis (Seifert and Moldowan, 1981) and (Peter *et al.,* 2005).

The ratio Ts/Tm [also written as Ts/(Ts+Tm)] decrease with depth (Peter *et al.,* 2005). Otherwise, the relative role of lithology and oxicity of the depositional environment in influencing this ratio is unknown, while some findings imply that they have a significant impact. Ts/Tm appears to be sensitive to clay-catalyzed reactions; for example, oils from carbonate source rocks have a lower Ts/Tm ratio than those from shale (Rullkotter *et al.,* 1984).

The oil sample of the study well shows low values of TS/TM this could be because oil from carbonate source rocks appears to have lower Ts/Ts+Tm ratios than oil from shale (Hunt, 1996; Peter *et al.,* 2005) table (4-5).

4.4.2.8. Gammacerane Index:

Gammacerane, a six-membered pentacyclic triterpane with the composition C30H52, is a facies-controlled triterpane. Gammacerane, formerly assumed to be a hypersalinity marker (SinninghеDamste *et al.,* 1995), is associated with increasing salinity in both marine and lacustrine habitats (Waples and Machihara, 1991; and Peters and Moldowan, 1993).

It is commonly recognized as a pointer of the salinity-stratified water column and a probable marker for photic zone anoxia in this manner. They are often low, implying a sedimentological environment with typical salinity. This component can be found in large amounts in the marine oils found in carbonate source rocks (Moldowan *et al.,*1991).

The gammacerane index ratio for the examined oil samples is (0.21) table (4-5). They often refer to a sedimentological environment with normal salinity and are low. This component is prevalent in marine oils found in carbonate source rocks (Moldowan *et al.,*1991).

4.4.3. Steranes and Diasteranes:

Stermes are a kind of saturated tetracyclic biomarker made up of six isoprene subunits. They are derived from sterols, which are abundant in higher plants and algae but rare or nonexistent in prokaryotic species (Waples and Machihara, 1991), while Diasteranes (rearranged steranes) are the result of the rearrangement of sterol precursors.

The existence of diasteraness reveals information on the SR's lithologies as well as the depositional environment (Philp, 2003b). Diasteranes are low in clay-poor carbonate source rock and associated oils, and they grow to steranes with thermal maturity **(**Peters *et al.*, 2005).

Steranes and terpanes are frequently found to be unaffected by biodegradation figure (4-14,15,16) (Welte *et al.*, 1982), and hence are still appropriate for correlation in these circumstances (Tissot and Welte, 1984). The relevance of algal-derived organic matter may be demonstrated by the dispersion of steranes. The existence of the four primary steranes is commonly linked to a marine depositional environment. The presence of diasteranes is frequently considered as proof that the oil came from clastic source rocks containing clay (Bacon *et al.*, 2000).

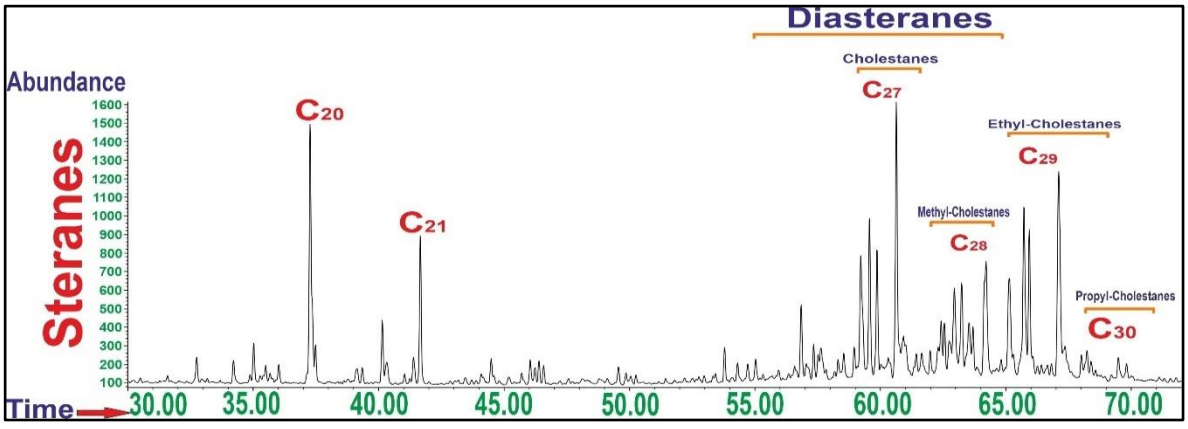

Figure (4-15): GC/MS showing steranes peaks of AG-1

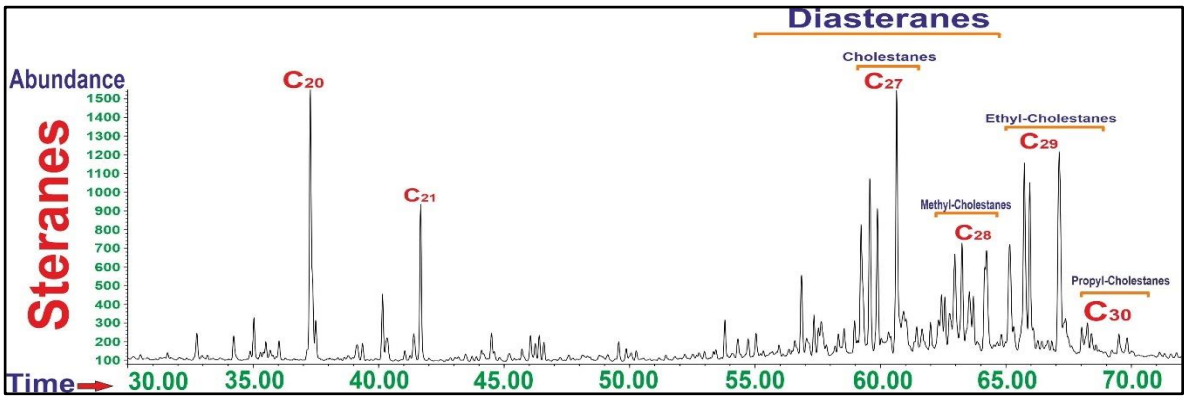

Figure (4-16): GC/MS showing steranes peaks of AG-7

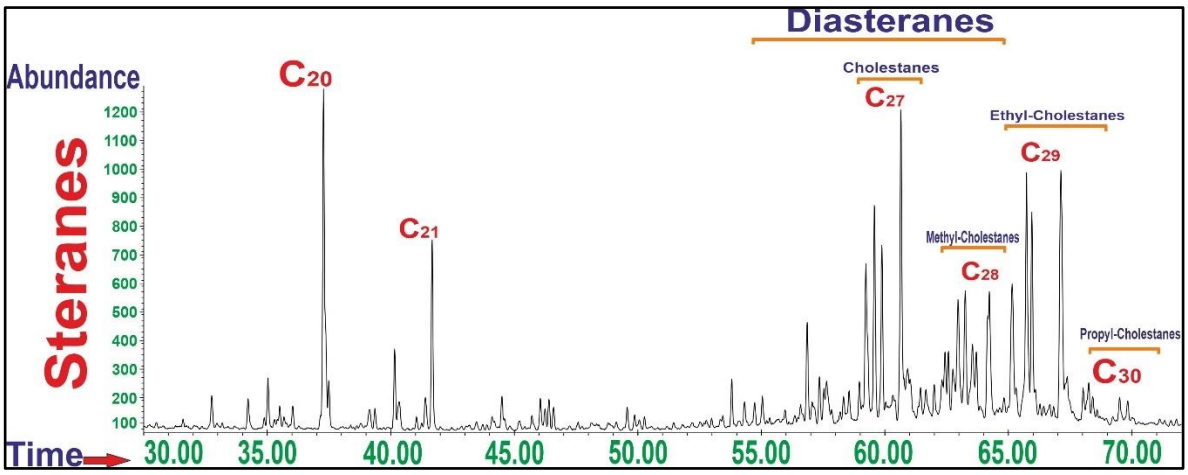

Figure (4-17): GC/MS showing steranes peaks of AG-10.

4.4.3.1. Regular Steranes (C_{27}, C_{28}, C_{29}):

The distribution of C27, C28, and C29 sterol homologs on a ternary diagram, according to Huang and Meinschein (1979), might be used to distinguish ecosystems. This ternary diagram of C27-C28-C29 steranes is used to distinguish between crude oil groups extracted from diverse source rocks. They also claimed that C27 sterols (steranes) are mostly obtained from algae, whereas C29 sterols are more commonly associated with terrestrial plants.

It is widely agreed that the relative amounts of C27-C29 steranes can be used to indicate source differences. For example, the presence of C28, C29, and C30 steranes indicates that the oils were derived primarily from a mix of terrestrial and marine organic sources, whereas oils with a slightly lower abundance of C28 and C29 and relatively higher concentrations of C27 steranes

indicate that the oils were derived primarily from a marine organic source (Moustafa and Morsi,2012).

The values of C27, C28, and C29 sterane were calculated from the Gas Chromatography-Mass Spectrum of the crude oil in the analyzed samples and projected on the sterane ternary diagram to indicate related to the carbonate marine environment for its source rocks (Moldowan *et al.,* 1985) (table 4-4). (fig. 4-17).

4.4.3.2. C_{28} / C_{29} steranes

Through geologic time, the relative substance of C28 steranes increases while the relative substance of C29 steranes decreases in marine petroleum. In the Jurassic and Cretaceous eras, the growth of C28 might be linked to an increased variety of phytoplankton assemblages, such as diatoms, coccolithophares, and dinoflagellates. Although this method is not perfect for determining the age of the source rock for oil, it can distinguish Upper Cretaceous and Tertiary oils from Paleozoic or earlier oil (Grantham and Wakefield, 1988 in Peter *et al.,* 2005).

The C28/C29 steranes were seen to be less than 0.5 for Lower Paleozoic and older oils, 0.4 to 0.7 for Upper Paleozoic to Middle Jurassic oils, and greater than or equal to 0.7 for Upper Jurassic to Miocene oils. It is generally that the C28/C29 values for the examined oil samples range from 0.57 to 0.58, and that this range corresponds to the Middle Jurassic to Cretaceous (Figure 4-20). (table 4-4).

4.4.3.3. Diasteranes/Steranes:

Diasteranes/steranes ratios are commonly used to distinguish petroleum from carbonate versus clastic source rocks, and they may also be used to distinguish immature from mature oils (Peters *et al.,* 2005; Younes and Philp, 2005).

Anoxic clay-poor or carbonate source rocks are indicated by low diasteranes/steranes ratios (mass/charge 217) in oils. High diasteranes/steranes ratios are common in petroleum obtained from clay-rich

source rocks, and high thermal maturity (Seifert & Moldowan, 1979 in Peters *et al.*, 2005) and/or heavy biodegradation can induce them in some crude oils (Peters *et al.*, 2005).

The studied crude oil samples' low values ratios demonstrate that the oils come from anoxic, clay-poor, or carbonate source rocks, and the closed values reflect that the samples all have the same degree of thermal maturity (table 4-4)

Table (4-4): The percentage of the C27, C28 and C29 steranes for the analyzed oils and extract samples.

Sample NO.	Well NO.	Formation	C_{27}%	C_{28}%	C_{29}%	C_{28}/C_{29}	C_{29} 20S/R
1	AG-1	Middle Kirkuk	34.6	24.2	41.9	0.57	0.44
2	AG-7	Upper Kirkuk	34.2	24.4	41.4	0.58	0.52
3	AG-10	Jeribe Euphrates	34.2	23.9	41.9	0.57	0.53

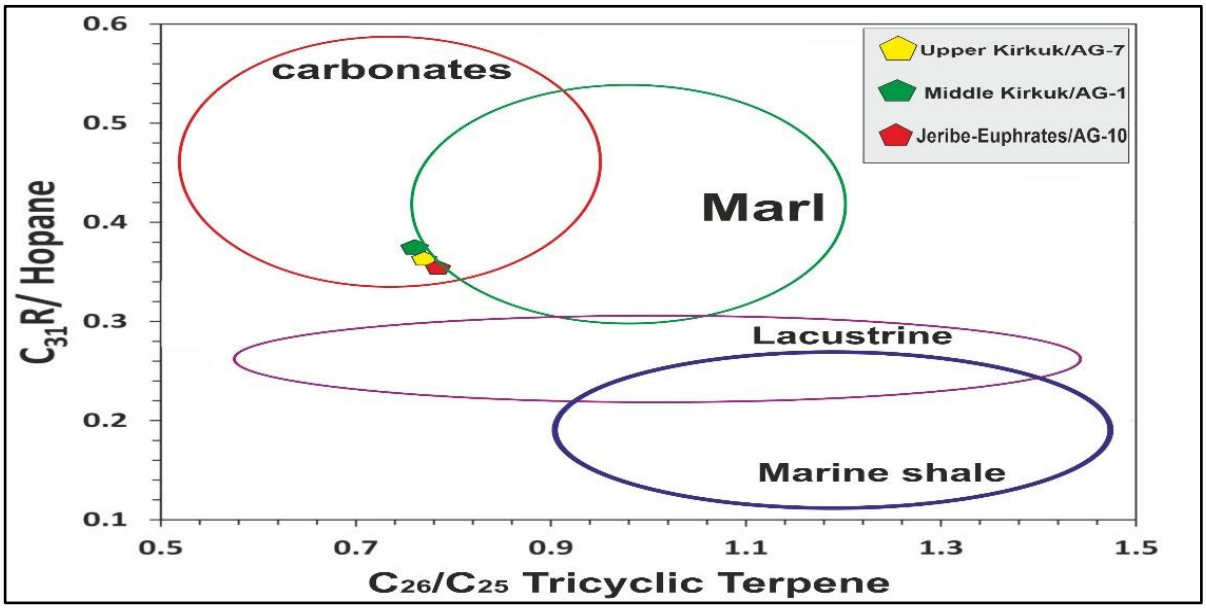

Figure (4-18): Cross plot of C31/C30hopane and C26/C25 tricyclic terpane of crude oil sample after (Zumberg, 2000).

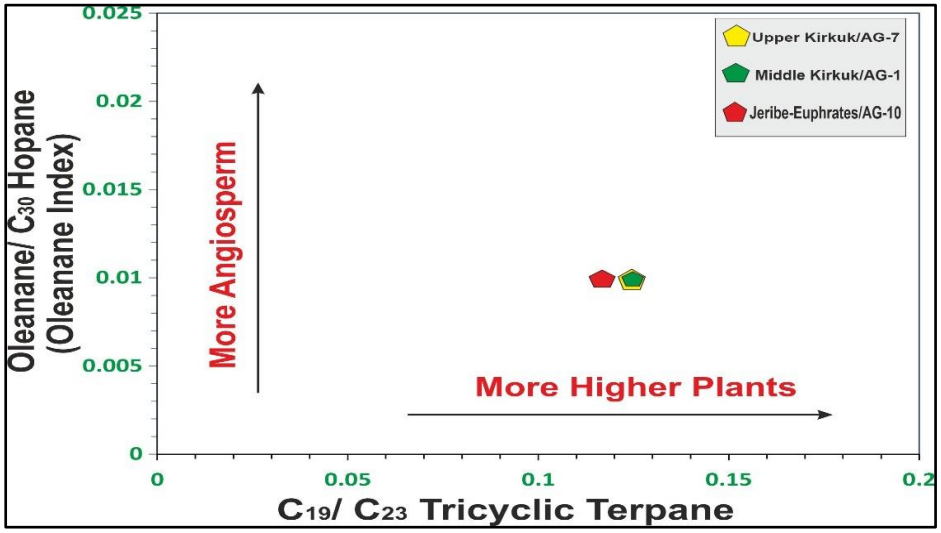

Figure (4-19): Cross plot of oleanane/C19/C20 tricyclic terpane of crude oil sample after (Zumberg, 2000).

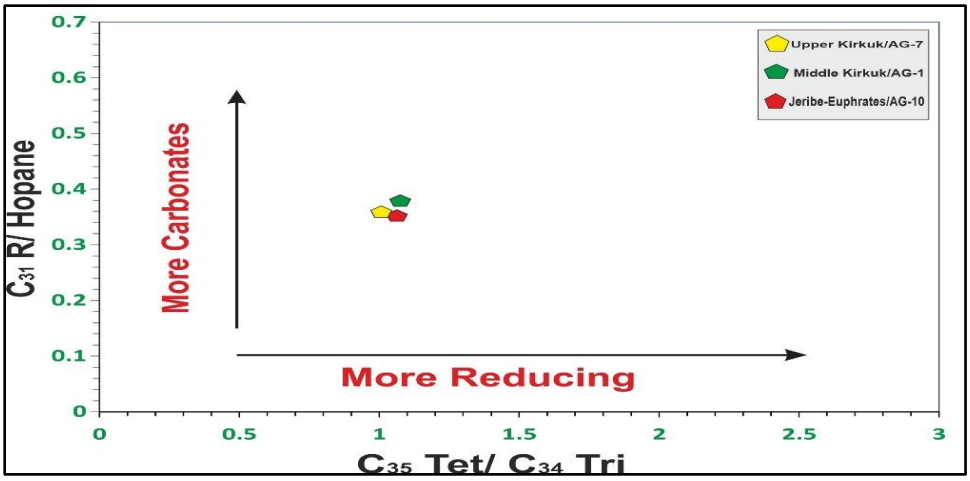

Figure (4-20): Cross plot of C31/Hopane / C35Tei/C34Tri tricyclic terpane of crude oil sample after (Zumberg, 2000).

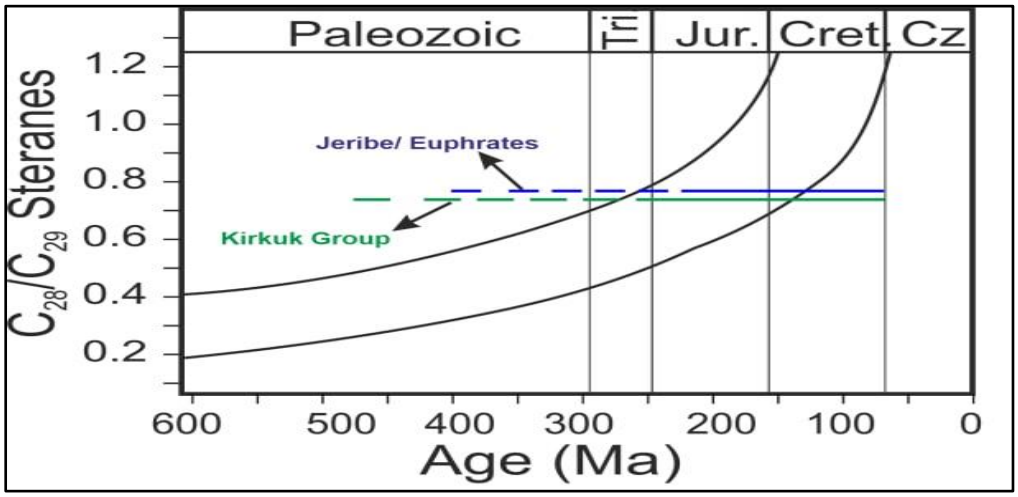

Figure (4-21): Shows the C28/C29 steranes ratios to prospect the age of the source rocks.

Table (4-5): The results of mass chromatograms of hopanes (m/z 191) parameters for Abu Ghirab crude oil sample.

Smp. No.	Well No.	Fm.	Depth (m)	C_{22}/C_{21}	C_{24}/C_{23}	ETR	Tet/C_{23}	C_{26}/C_{25}	C_{28}/H	C_{29}/H	C_{30}X/H	C_{31}R/H	OL/H	GA/31R	$C_{35}S/C_{34}S$	C_{27}Ts/Tm	C_{29}Ts/Tm
1	AG-1	Middle Kirkuk	3030	0.98	0.27	0.99	1.17	0.78	0.01	1.82	0	0.36	0.01	0.21	1.02	0.23	0.09
2	AG-7	Upper Kirkuk	2949	0.99	0.27	0.99	1.21	0.76	0.01	1.81	0	0.37	0.01	0.21	1.05	0.24	0.09
3	AG-10	Jeribe-Euphrates	2941	0.99	0.27	0.99	1.19	0.79	0.01	1.73	0	0.36	0.01	0.21	1.03	0.24	0.09

ETR= Extended tricyclic terpene ratio

4.4.4. biomarker parameters

1- Source–related biomarker parameters

When only one crude oil sample is available for examination, a source related biomarker ratio is very helpful in describing the source rock. Mature basinal source rock samples are typically more difficult to collect than oil samples for a variety of reasons. Nevertheless, indicators found in the oils can be used to determine the depositional environment, organic input, thermal maturity, and even the age of the source rocks (Peters *et al.,* 2005b). These data can be utilized to propose possible source rocks that may be collected later for thorough correlations between oil-source rocks. Different Parameters are used to determine the affinity of crude oils from Abu Ghirab. The Pr / Ph ranges from (0.8-0.94) Less than 1 which denotes anoxic marine depositional conditions and marine carbonate source rocks. The value of phytane/n-c18 of (0.36) is a reference to indicate a source rock made of carbonate, shale, or marine marlcarbonate source rocks or shale. the value of C_{31} / C_{30} rang (0.36-0.37) indicates a source rock made of carbonate, shale, or marine marl. Steranes' ternary diagram used the relationships between C27, C28, and C29 to identify carbonate source rocks. Low Gammacerane values represent indicate with low hypersalinity environments, All of these factors provide compelling evidence that the oils from the Abu Ghirab field were produced in an anoxic marine carbonate environment.

2- Age-Related Biomarker Parameter

(Brock *et al.,* 1999) demonstrates that the majority of microbiological biomarkers have limited capacity to constrain geologic age because they can be found in rocks dating back to the Archean.Oleanane can be found in some Paleozoic rock extracts, although the oldest known angiosperms that produce its precursor date from the early Cretaceous (Peters *et al.*,

2005b). Many of the age-related biomarkers used in this study, such as oleanane, the C28/C29 steranes ratio, and the extended tricyclic terpane ratio (ETR), indicated that the studied samples' oils originated from rocks older than the Early Cretaceous, the Upper Jurassic to Lower Cretaceous.

3- Maturity - Related Biomarker Parameter

The ratio of TS to Tm for the oil samples also shows closed values that indicate the same degree of thermal maturity; all values are less than 1. The ratio of TS to Tm indicates the same level of thermal maturity. The ratio of C29 20 S / R in the ABU GHIRAB oil samples shows that petroleum production has already started to take place in these oils. Oil samples are low mature and have not yet achieved post-mature status, according to the ratio of Sterane to Diasteranes (Peters *et al.*, 2005b). The ratio of C29 20 S / R in Abu Ghirab oil samples indicates that these oils have passed the onset of petroleum generation. According to the ratio of Sterane/diasteranes, oil samples are low mature and have not reached post-mature (Peters *et al.*, 2005b). Odd vs even-predominance of crude oil samples indicates low mature oil as the ratio of pristane and phytane (n-alkanes isoprenoids) decreases with thermal maturity.

Chapter Five

Petroleum System Modeling

Chapter Five

Petroleum System Modeling

5.1. Introduction

Basin models play an important role in reconstructing the history of sedimentary basins. Basin modeling has two main components: thermal modeling and fluid flow simulation. Thermal modeling, as one might expect, deals with maturation, generation, and cracking. The most critical aspects are those linked to the kinetics of generation and the type of organic material in the source rock. Numerous geological factors, such as the time of geological events for the source, carriers, reservoirs, and overburden rock, are also required. This information also covers the extent of deposition, non-deposition, uplift, erosion, and subsidence.

5.2. Petroleum System Concept

The timing of generation is critical because oil accumulation does not exist if reservoirs or traps are not present when source rock begins to generate oil. The timing of petroleum generation is also crucial in terms of the creation of faults, which serve as migratory patterns. This information can be retrieved by simulating the source rock's time-temperature history. The relationship between the timing of petroleum generation and the presence of appropriate traps and migration pathways led to the development of the so-named petroleum system idea, which was first outlined in papers by Magoon and Dow (1994).

The goal of basin and petroleum system modeling is to anticipate the distribution and movement of petroleum within the basin, as well as to determine hydrocarbon generation, migration, and accumulation, as well as temperature histories and pressures.

The two ideas must first be defined independently before being combined to give a complete definition of the petroleum system. When discussing

petroleum, it is important to understand where the word "petroleum" originated. The name "petroleum" is derived from a Latin word, where the first letter "petra" stands for "rock," and the second letter "oleum" stands for "oil." Hydrocarbons that are present in the solid, liquid and gaseous forms are collectively referred to as petroleum.

Let's now outline the mechanism to obtain a description of petroleum. A "system" is a grouping of components that collectively cooperate to achieve a single objective. Therefore, the petroleum system may be thought of as a group of geological elements and processes that contribute to the formation and accumulation of hydrocarbons (Learn, n.d.).

The core components of a TPS are comprised of source rock, reservoir rock, seal rock, overburden rock, and other rocks. Petroleum system's primary processes are generation, migration, accumulation, and trap creation. The Total Petroleum System is a hydrocarbon fluid system that may be found in a specific region of the lithosphere, where it spontaneously originated and has all of the essential components and processes required for the buildup of oil and gas fig (5-1) (L B Magoon & Schmoker, 2000).

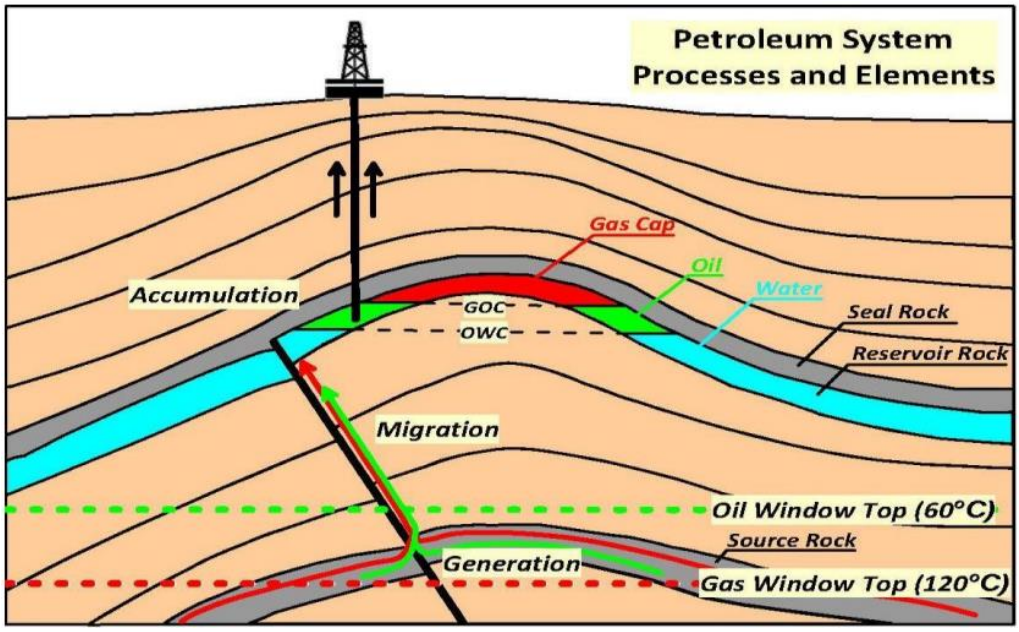

Figure(5-1): Scheme illustrating a typical petroleum system. Modified from (Leslie B Magoon & Dow, 1991)

5.3. Petroleum System Elements

5.3.1. Source rocks

Every oil and/or gas play has a source rock at its base. The source rock determines the efficacy of any petroleum, whether conventional or unconventional, oil or gas. It becomes redundant to show all other components and procedures needed to construct a play if the source rock element for petroleum producing is absent. A source rock is any fine-grained, organically rich rock that may produce petroleum.

Its capacity to produce petroleum is inversely correlated with its volume, organic content, and thermal maturity. The term "organic richness" refers to the quantity and variety of organic substances found inside the rock. How long a source rock has been exposed to heat determines its thermal maturity. When the source rock is buried further down the lithologic column, more heat is created, which leads to the thermal transformation of organic materials in the source rock, which produces petroleum (McCarthy *et al.*, 2011). In this well the hydrocarbon is mixed between Jurassic- Cretaceous sours. The vast majority of the oil that charged reservoir rocks in the Mesopotamian Basin and Zagros fold belt was produced by the Middle Jurassic Sargelu Formation and the Upper Jurassic Najmah Formation and Lower Cretaceous Sulaiy and Yamama Formation. (Pitman *et al.*, 2004; Beydoun *et al.*, 1992; Sadooni, 1997; Al Shididi *et al.*, 1995). Al Habba and Abdullah, 1989; Stoneley, 1990; Al Shididi *et al.*, 1995; Alsharhan and Nairn, 1997; Al-Ameri *et al.*,1999; Al-Khafaji *et al.*, 2019)

5.3.2. Reservoir rocks

The presence of a reservoir is one of the seven prerequisites for a commercial accumulation of hydrocarbons. Theoretically, any rock may serve as a gas or oil reservoir. Although fields can also be discovered in shales and a range of igneous and metamorphic rocks, the main known deposits are located in sandstones and carbonates.

The main oil reservoirs, which contain oil derived from Jurassic source rocks, are Cretaceous and Tertiary rocks. According to Beydoun *et al.* (1992), carbonates are the primary oil reserves in the Cretaceous and Tertiary stratigraphic region.

In Abu Ghirab oil field the major field reservoir Asmari Formation contains the most significant oil accumulations. The Asmari Group's Oligocene-lower Miocene carbonates and its Iraqi, somewhat time-equivalent reservoir, "Main Limestone," the Kirkuk Group's.

5.3.3. Seal and Tarps

Seal rock is an impermeable rock that surrounds or grows on top of a reservoir rock. To stop hydrocarbons from leaving the reservoir, seal rock serves as a barrier. A seal rock might be made of shale, anhydride, and salt. A trap is a rock formation that is ideal for storing hydrocarbons and is sealed with a reasonably impermeable formation to stop the migration of hydrocarbons. The term "traps" refers to both stratigraphic traps, which are generated by changes in the kind of rock, and structural traps, which are formed in geological structures such as faults and folds (Selley, 1998).

The primary Jurassic seal is represented by the Gotnia Formation. In Iraq, it is regarded as a local seal. For nearby hydrocarbons (oil and gas) stored in the Najmah Limestone underneath, it creates a tight seal (Fox & Ahlbrandt, 2002). The evaporites of the Middle Miocene Fatha Formations of the area, which maintained their integrity during the Zagros folding, create a nearly perfect seal (Beydoun *et al.*, 1992).

All traps in Zagros fold NW-trending compressional folds that were created by inversion over extensional faults make up the majority of the traps in the fold belt (Ameen, 1992; Hessami *et al.*, 2001). The thrusted and imbricated zones east of the fold belt are evidence of the first stage, which took place in the Mesozoic (Late Cretaceous). If the fold belt was damaged

by Mesozoic tectonic activity, late Cenozoic folding and faulting then covered the affected area. During the late Paleogene and Neogene Zagros orogenic episode, the fold belt underwent the majority of its structural deformation and trap creation (Pitman *et al.*, 2004).

5.3.4. Overburden rock

In the petroleum system, overburden rock is a series of sedimentary rocks that covers source rock, reservoir rock, and seal rock. The overburden thickness, physical characteristics, and mechanisms that control the temperature of the sedimentary basin all affect the hydrocarbons generated by the thermal decomposition of organic matter in source rocks. The thickness of the overburden is a by-product of the fundamental forces and processes that govern the structural evolution of the sedimentary basin where the overburden is present. The thickness and thermal conductivity of the overburden rock, heat transport, and surface temperature are the key determinants of the temperature of the source rock. Thermal conditions may also be significantly impacted by procedures like ground flow and subsidence (Leslie B Magoon & Dow, 1991).

5.4 Basin Modelling

The petroleum system is a geologic system that includes all of the geological materials and processes necessary for the formation of a hydrocarbon deposit, such as hydrocarbon source rocks and all related oil and gas **(**Magoon and Dow, 1994). A petroleum system model is a digital data model that describes a petroleum system and enables the simulation of interconnected processes and their outcomes to better understand and forecast them.

This model is a dynamic model, which means it gives a comprehensive and unique record of oil and gas generation, migration, accumulation, and loss in the petroleum system across geologic time. Basic

analyses of hydrocarbon creation, ejection, movement, trapping, and preservation are included in petroleum system modeling (Hantschel & Kauerauf, 2009). Petroleum system modeling is becoming more popular as petroleum becomes more difficult to find. It provides an integrated exploration tool that can be used to measure many of the fundamental aspects of a changing basin and the active petroleum systems inside it (Magoon, 1988; Magoon and Dow, 2000). Figure (5-2) shows a list of important risk parameters that the industry had come up with.

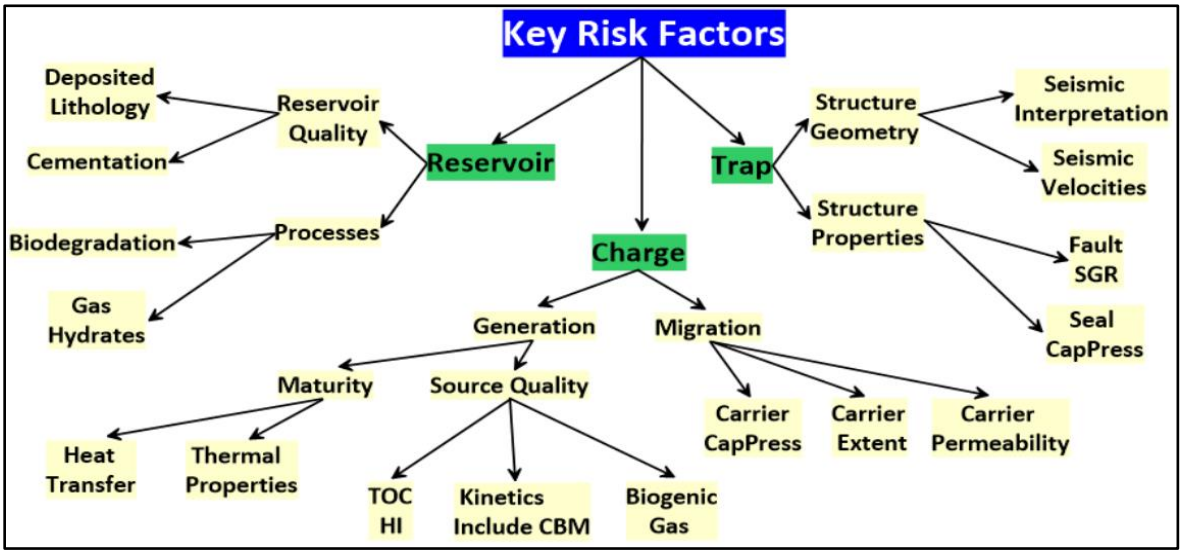

Figure (5-2): Illustrating important risk factors in basin modeling. Modified **after (Wygrala, 2008)**

Structural modeling has recently been the first stage for compaction analysis. The selection and interpretation of seismic data restricted by well logs are frequently used to build structural models. Solving coupled nonlinear partial differential equations with shifting boundaries is part of the basin modeling process. The equations govern fluid flow and deformation in porous media, as well as chemical reactions and energy transmission. The numerical solution of this coupled system on spatial grids and discretized time is required (Al-Hajeri *et al.*, 2009). The workflow and key input parameters are illustrated in Figure (5-3).

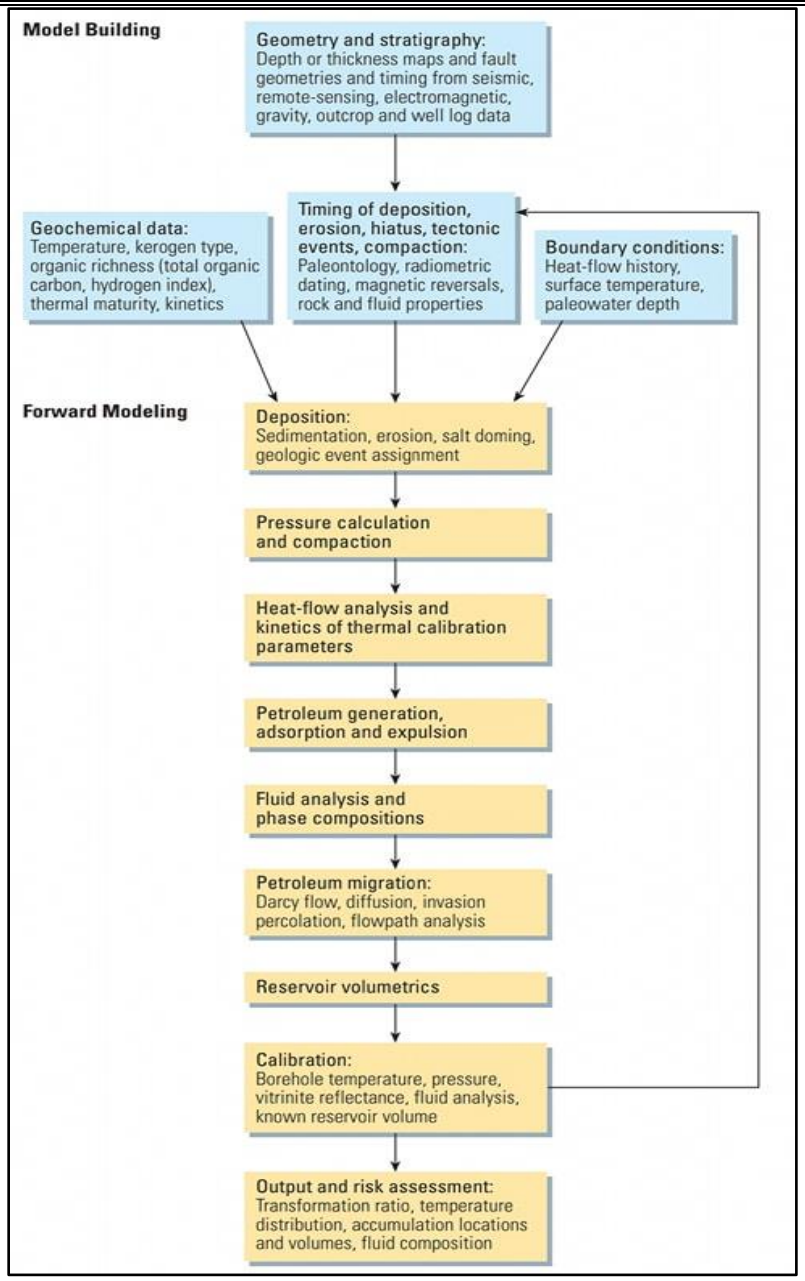

Figure (5-3): The multiple and interrelated steps of basin and petroleum system modeling. Modified from (Al-Hajeri *et al.*, 2009).

5.5. PetroMod Software Basin Modelling

A growing number of input parameters are needed for increasingly complicated basin models, and their values are expected to change across time and space. Table (5-1) provides a list of some of the input variables that are frequently utilized in basin models and their possible impact on model outcomes. For a basin model to be successful, the simulation model must not only choose the best estimate for each input parameter's value but also

comprehend the range of uncertainty surrounding these estimates as well as the uncertainties related to the software's mathematical constraints, approximations, and assumptions.

Basin modeling as characterized by Hantschel and Kauerauf (2009) is "the dynamic modeling of geological processes in a sedimentary basin over geological time spans". Modeling a sedimentary basin entails recreating the basin's complete history, starting with the deposition of the oldest layer and progressing through the sequential deposition of the whole sedimentary sequence until it reaches the current day. Basin modeling is a wide phrase that encompasses a variety of geological disciplines such as formation studies, thermal development of sedimentary basins, and the assessment of probable hydrocarbon reserves (Hantschel and Kauerauf 2009). It is a coordinated exploration system (IES, 2007), for assessing petroleum systems. Basin modeling approaches are used to reduce the risk of petroleum exploration; commercially available basin modeling simulations are used to assess charge risk by incorporating geology and engineering data into models of one or more petroleum systems operating in the exploration region. PetroMod's main goal is to determine the exact time and location of petroleum generation, expulsion, and migration processes (IES,2009). Basin simulations can range from a single well to an entire basin with the use of many wells and pseudo wells (Welte *et al.*, 1997). This technique was developed in the 1980s. The first spatial simulation of petroleum processes was carried out at the end of the 1990s. A quantitative model of petroleum genesis and buildup in basin development was presented in 1984. (Hantschel and Kauerauf,2009).

Table (5-1): The input data for the studied oil fields according to the well final geological report

Formation Name	Formation Top [meter]	Formation Base [meter]	Formation Thickness [meter]	Formation Erosion [meter]	Formation Age		Erosion Age		Formation Lithology	Petroleum System Element	Total Organic Carbon Contents [%]	Source Rock Kinetics	Initial Hydrogen Index [mg/g TOC]
					From [Ma]	To [Ma]	From [Ma]	To [Ma]					
Bakbtiary	0	500	500		1.0	0.0			clay&sand	Overburden Rock			
upper Fars	500	2052	1552		9.0	1.0			sand&anhydrite	Overburden Rock			
lower Fars	2052	2984	932		13.0	10.0	10	8	anhydrite&shale	seal Rock			
jeribie/Euphrates	2984	3046	62		19.0	13.0			dolom&anhydrite	Reservoir Rock			
Upper Kirkuk	3046	3122	76		23.0	20.0	20	19	limestone	Reservoir Rock			
Middle Lower kirkuk	3122	3160	38		33.0	23.0			shale&sandstone	Reservoir Rock			
jaddala	3160	3356	215		49.0	33.0			limestone&shale	Seal Rock			
ailiji	3356	3571	196		63.0	49.0			limestone&shale	Source			
Shiranish	3571	3630	59		70.0	67.0	68	63	limestone&marl	Overburden Rock			
Hartha	3630	3680	50		79.0	70.0			limestone&marl	Reservoir Rock			
Sadi	3680	3800	120		86.0	82.0	81.5	79.5	limestone&marl	Reservoir Rock			
Tanuma	3800	3830	30		88.0	86.0			limestone&marl	Reservoir Rock			
Khasib	3830	3867	37		89.0	88.0			limestone&marl	Reservoir Rock			
Mishrif	3867	4135	268		96.0	92.0	92	89.5	limestone	Reservoir Rock			
Rumaila	4135	4181	46		96.0	98.0			limestone&shale	Overburden Rock			
Ahmadi	4181	4257	77		98.0	101.0	97.5	96	limestone	Overburden Rock			
Mauddud	4257	4428	170		101.0	106.0			limestone	Reservoir Rock			
Nahr Umr	4428	4649	221		106.0	111.0			SAND&shale	Reservoir Rock			
Shuaiba	4649				111.0	116.0	114	110	limestone	Reservoir Rock			

5.6. One-dimensional basin modeling (1D PetroMod)

To determine the burial and temperature history of source rock, as well as the time of hydrocarbon formation, 1D petromod modeling is used. 1-D basin modeling is used to determine the maturity history of one or more source rocks at a single point in a basin, such as a drilled well. Because no lateral parameter information is provided, 1-D basin modeling cannot infer lateral variation in lithology, fluid flow, petro-physical parameters, or charge volume calculation in a basinal sense. (Hantschel and Kauerauf, 2009).

To show burial thermal history, hydrocarbon creation, and expulsion for the Abu Ghirab oil field, one-dimensional petroleum system modeling (also known as 1-D petroMod) was carried out utilizing petroMod basin modeling software **(Table5-2).**

Table (5-2): Formation tops of well Abu Ghirab according to the well final geological report

Formation Name	Formation Top [meter]	Formation Base [meter]	Formation Thickness [meter]	Formation Age		Erosion Age	
				From [Ma]	To [Ma]	From [Ma]	To [Ma]
Mukdadiya	0	500	500	1.0	0.0		
upper Fars (Injana)	500	2052	1552	9.0	1.0		
lower Fars (Fatha)	2052	2984	932	13.0	10.0	10	8
jeribie/Euphrates	2984	3046	62	19.0	13.0		
Upper Kirkuk	3046	3122	76	23.0	20.0	20	19
Middle Lower kirkuk	3122	3160	38	33.0	23.0		
jaddala	3160	3356	215	49.0	33.0		
ailiji	3356	3571	196	63.0	49.0		
Shiranish	3571	3630	59	70.0	67.0	68	63
Hartha	3630	3680	50	79.0	70.0		
Sadi	3680	3800	120	86.0	82.0	81.5	79.5
Tanuma	3800	3830	30	88.0	86.0		
Khasib	3830	3867	37	89.0	88.0		
Mishrif	3867	4135	268	96.0	92.0	92	89.5
Rumaila	4135	4181	46	96.0	98.0		
Ahmadi	4181	4257	77	98.0	101.0	97.5	96
Mauddud	4257	4428	170	101.0	106.0		
Nahr Umr	4428	4649	221	106.0	111.0		
Shuaiba	4649	4841	192.0	111.0	116.0	114	110

5.7. Model development

5.7.1 Chronostratigraphic units

The term "chronostratigraphic units" refers to groups of rocks, whether layered or unlayered, that was created at a specific period of geologic time. In the 1D-model, absolute ages of erosion or absence of deposition are given and defined for chronostratigraphic units (Table 5-3). According to the geologic time scale, depositional and erosional episodes' ages are determined (Sharland *et al.*, 2001). Each unit's facies received a lithology assignment that was represented as end member rock types or as compositional mixtures. The thermal conductivities and heat capacities of the many types and combinations of rocks, as well as their other physical and thermal characteristics, can be either user- or software-defined.

Table (5-3): Units of chronostratigraphy and ages of episodes involving deposition and erosion in the study area.

Formation Name	Formation Age		Erosion Age	
	From [Ma]	To [Ma]	From [Ma]	To [Ma]
Mukdadiya	1.0	0.0		
upper Fars (Injana)	9.0	1.0		
lower Fars (Fatha)	13.0	10.0	10	8
jeribie/Euphrates	19.0	13.0		
Upper Kirkuk	23.0	20.0	20	19
Middle Lower kirkuk	33.0	23.0		
jaddala	49.0	33.0		
ailiji	63.0	49.0		
Shiranish	70.0	67.0	68	63
Hartha	79.0	70.0		
Sadi	86.0	82.0	81.5	79.5
Tanuma	88.0	86.0		
Khasib	89.0	88.0		
Mishrif	96.0	92.0	92	89.5
Rumaila	96.0	98.0		
Ahmadi	98.0	101.0	97.5	96
Mauddud	101.0	106.0		
Nahr Umr	106.0	111.0		
Shuaiba	111.0	116.0	114	110

5.7.2. Temperature and heat flow

Due to the earth's natural geothermal gradient, the temperature is typically a function of depth. A 1.5° F gradient is produced by normal heat flow in the earth's crust for every 100 feet of depth below the surface (Selley, 1984).

In general, temperatures below 20000 feet are too high and only create gas. The temperature needed to produce crude oil occurs between 5000 and 20000 feet in depth. Typically, the substance cannot become crude oil at temperatures higher than 5000 feet (Selley, 1998). Heat flow, the thermal conductivity of the rock matrix, surface temperature, and sediment thickness (both current and historical) are some of the factors that affect when a wave is generated (Pitman, 2004).

The final geological report from the Oil Exploration Company (MOC) for Abu Ghirab well and reservoir and bottom-hole temperature data are utilized to estimate the current heat flow in the researched region as shown in figure (5-3). Using estimated heat flow values equal to (48 mW/m2) in the analyzed area, assuming a mean surface temperature of 27°C throughout the region, a satisfactory match between predicted and observed temperature values is established. The estimated geothermal gradients for the examined well range locally from 18 to 23°C/Km based on the parameters specified in the thermal model, and they are consistent with the documented temperature gradients for this location (Pitman *et al.*, 2004).

According to computed Ro trends for the investigated wells in south Iraq, erosion throughout the late Cenozoic period was typically low (less than 500 m) in this area. Although the quantity of stratigraphic section lost during Mesozoic erosional events has not been documented, sensitivity tests show that, although being locally strong, pre-Tertiary erosion had little of an effect on the Jurassic source rock maturation history (Pitman *et al.*, 2004).

5.8. Model analysis

5.8.1 Burial history

The term "burial history" refers to the subsidence history of a sedimentary basin across geological time. The analysis of subsidence, uplift, and erosion using burial history graphs plays a significant role in determining the current maximum burial depth. The conversion of kerogen to petroleum depends on temperature, and fluid motion requires pressure. The most important factors for creating a burial history are the rate of sedimentation, compaction, uplift, erosion, and depositional environment (Al-Hajeri *et al.*, 2009).

The stratigraphic record of a burial history typically has breaks or gaps because of erosion or lack of deposition. A pause like this in a series of sedimentary rocks is when erosion can partially or completely remove certain layers. For instance, regional erosion processes make it difficult to locate locations where thickness data is maintained, making it difficult to reproduce what has been lost. The histories of heat movement, water depth, and surface temperature add context to the history of burial.

According to the study region, the subsidence rates derived from the aforementioned curves (Figure5-4) are:

- Rapid subsidence during the 23-5 Ma era, corresponds to the formation of the upper Fars (Injana) and Lower Fars (Fatha) Formations.
- During the 62.3–23 Ma epoch, which includes the Aliji, Jaddala, Kirkuk group, and Jeribe–Euphrates formations, there was moderate to rapid subsidence

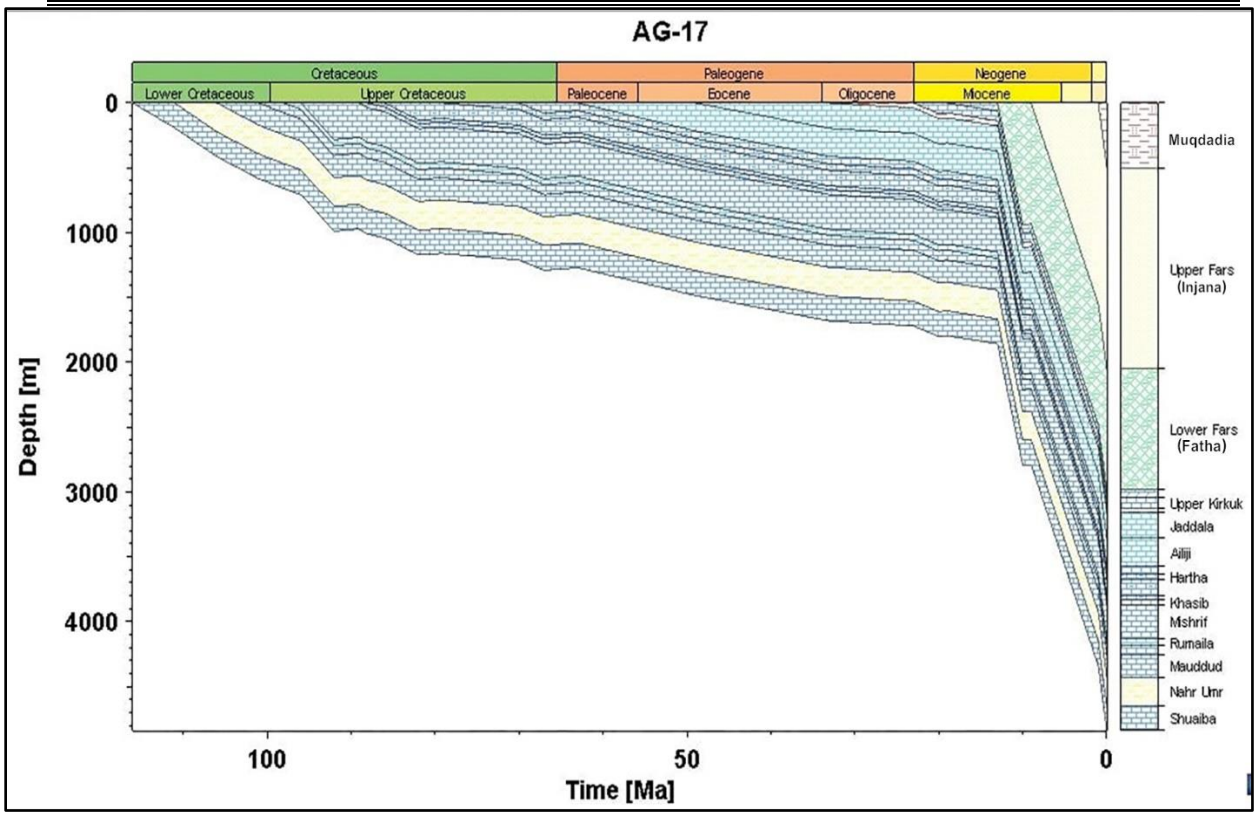

Figure(5-4): Burial history of AG-17

5.8.2. Thermal History

Based on the burial of history and the evolution of heat movement, the thermal history of sedimentary basins may be determined (Allen and Allen, 1990). To identify a basin's potential for oil and gas production and to ascertain the porosities of the reservoir, burial history and thermal history can be used. Paleostructure maps at specific time slices may also be created using burial history curves from various sites (Allen and Allen, 2005). The Paleocene to Miocene must be regarded as the period when the maximum temperature predominated and was coupled with profound burial for the majority of the investigated wells (Fig5-5).

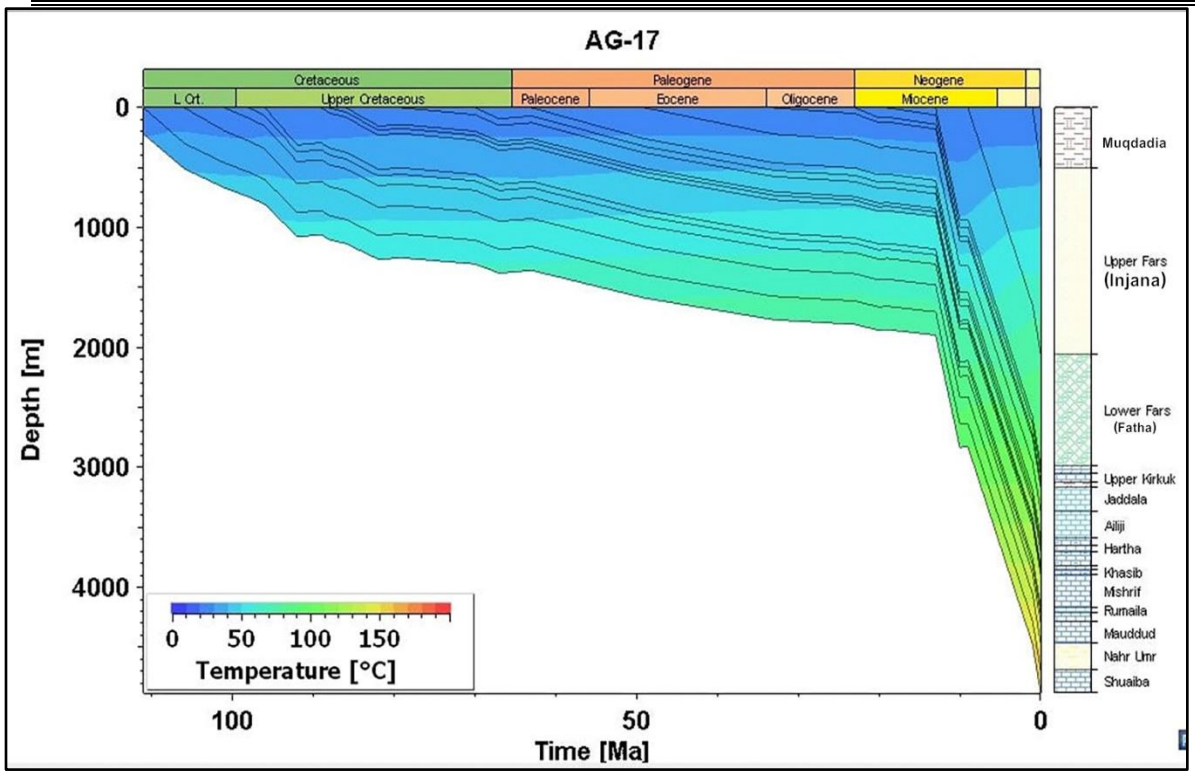

Figure (5-5): Thermal history for AG-17

5.8.3. Petroleum generation

Petroleum generation refers to the process of transforming solid organic materials found in source rocks into liquid or gaseous hydrocarbons. In natural conditions, petroleum formation begins at temperatures of 70-80°C, which frequently corresponds to burial depths of 2.5-3 km, depending on the geothermal gradient.

Organic compounds release gas and oil as temperature and pressure rise during burial. In general, this thermal maturation method results in a series of progressively smaller hydrocarbon molecules, with increasing volatility and hydrogen concentration, culminating in methane gas. Additionally, when the kerogen ages thermally, its chemical makeup gradually modifies, finally transforming it into a carbonaceous residue with a decreased H-content (Hood *et al.*, 1975). In this well the hydrocarbon is mixed between Jurassic-Cretaceous sours(Beydoun *et al*., 1992). Due to the intricate fold geometries in the region, the time and size of generation events in the region are mere

approximations. Nevertheless, information may be gleaned from the transformation ratios and temperatures at important fields. The Late Cretaceous marked the beginning of oil generation (TR 0.01), while the Late Paleogene to Early Neogene was the end (TR 0.95) of oil generation. Temperatures that control generation (70-105°C, with a maximum of 150°C). Late Cretaceous oil production and release is thought to have accumulated in Cretaceous and earlier structural traps, whereas subsequent production charged Tertiary traps (Pitman *et al.*, 2004).

During the Holocene, generation in the Zagros fold belt halted with uplift and exhumation, although by that time, peak oil generation (TR 0.50) had already happened in a significant portion of the area fig(5-6). Even in source rocks that are just a few thousand meters below the surface, generation in the southern half of the fold belt has attained completion (TR 0.95) (Pitman *et al.*, 2004). Oil TRs approach 0.99 in the deepest portions of the Mesopotamian Basin and Zagros fold belt (east flank of foredeep), suggesting that Jurassic source rocks have entered the kerogen-to-gas production zone and gone through the oil window fig(5-7).

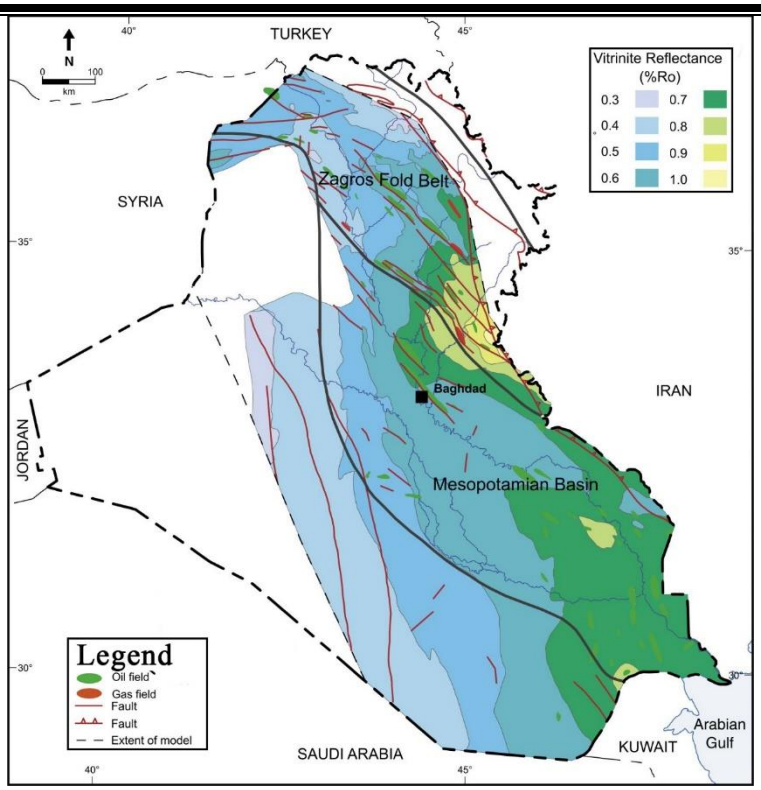

Figure(5-6): Middle-Upper Jurassic source rocks' maturity during the Late Miocene. after (Pitman *et al.*, 2004).

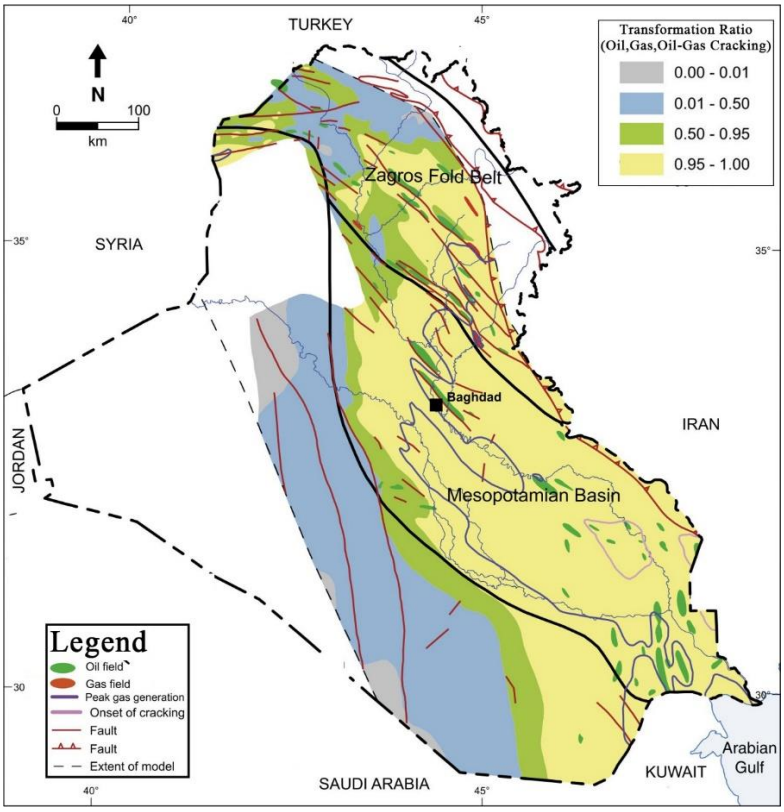

Figure (5-7): Present-day transformation ratio for Middle-Upper Jurassic source rocks. After (Pitman *et al.*, 2004).

5.8.4. Hydrocarbon migration and accumulation

Many factors influence the hydrocarbon migration process, including kerogen expansion, pressure increase, and hydrocarbon expulsion from the source rock. The extraction of oil from the source rock is a dynamic process driven by the production of oil itself. TOC (total organic content) in good source rocks ranges from 3 to 10%. At low TOC, the kerogen may be found within the rock's matrix porosity. Kerogen can be form linked bands within the rock at high TOC. The kerogen then bears a portion of the lithostatic load. This load-bearing kerogen becomes liquid as organic stuff converts into the oil. The fluid pressure of the oil within the black shales can rise to levels high enough to cause microfractures.

Primary migration and secondary migration are the two distinct phases that make up the petroleum migration process. While the secondary migration has been defined as the movement among carrier rocks and reservoir-type rocks, leading to a petroleum accumulation, the primary migration has been defined as the flow of oil and gas inside and out of the nonreservoir source rocks into the permeable reservoir rocks (Hunt, 1996).

According to Beydoun *et al.*, 1992, Pitman, 2004 several wells in the Kirkuk embayment examined oils from Tertiary and Upper, Middle, and Lower Cretaceous reservoirs of the Zagros fold belt fields using sulfur isotope abundance, and identified vertical migration as the origin of Tertiary-reservoir oil in the fold belt of the Zagros foreland basin. They verified that virtually no discernible changes in sulfur isotope composition exist in any particular vertical succession of oils, pointing to a shared origin. Oil first moved into structural traps in the fold belt throughout the Mesozoic and Paleozoic, which are later altered or destroyed during the late Paleogene and Neogene. The oil either migrated back into the earlier (Tertiary) traps or escaped the system as a result of the alteration and destruction of these older traps. The migration models for the late Miocene and present-day record noticeably different

directions and extents of petroleum movement within the area in comparison to the late Oligocene and middle Miocene simulations. As a result, the migration is vertical in this area and it is started before the late Miocene and as early as the Late Cretaceous, when predicted migratory channels began to fill.

Following oil migration, hydrocarbons will gather in porous rocks referred to as traps. Any combination of physical elements that encourages the aggregation and retention of petroleum in one place are known as hydrocarbon traps. Inconsistencies in the subsurface layers caused by geologic processes such as faulting, folding, piercing, deposition, and erosion may lead to the retention of oil and gas in a porous formation, forming petroleum traps (Selley, 1998). When different oil and gas phases coexist in the same traps, the gas often sits on top of the oils because it is less thick. Traps can hold either oil, gas, or both. While hydrodynamic conditions affect the system of hydrocarbon migration in a basin, such as the volumes of hydrocarbons available for entrapment in a certain part of the basin, and trapping energy conditions in the basin, such as the location of potential trapping positions of hydrocarbons and the sealing capacity of rocks and faults, hydrocarbons may accumulate in hydrostatic traps, which include structural, stratigraphic, and combination traps (Verweij, 1993).

In this study, focused on the main reservoir (Asmari Formation) and determined the units of hydrocarbon accumulation (Chapter2,3), and through the seismic section figer (5-8) , the areas of accumulation and migration of hydrocarbon are determined. the late Cretaceous Mishrif and Mauddud reservoir (MOC)

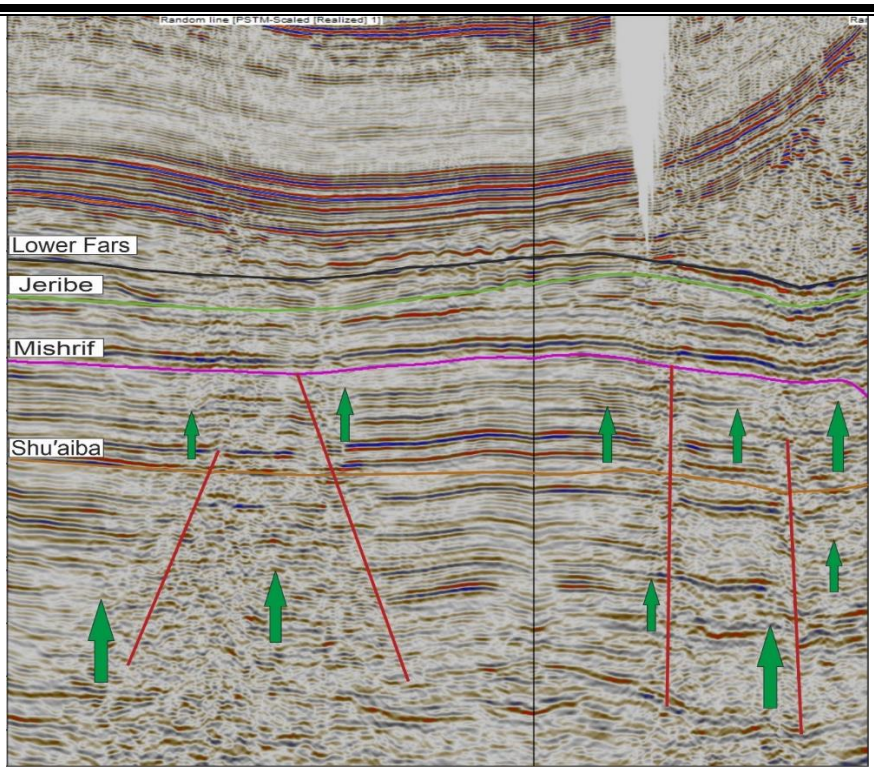

Figure(5-8): Hydrocarbon migration pathways and accumulations are seen in the seismic section of the Abu Girab field's well (AG-17), according to the Iraqi oil ministry.

5.9. Summary

- In this well the hydrocarbon is mixed between Jurassic- Cretaceous sources.
- The Possible source rocks Middle Jurassic Sargelu Formation and the Upper Jurassic Najmah Formation and Upper Jurassic to Lower Cretaceous Sulaiy and Yamama formations, as well as Zubair Nahr Umr formations. The analysis of crude oils suggested Upper Jurassic to Lower Cretaceous Sulaiy and Yamama source rocks orgin.
- The Jurassic seal is represented by the Gotnia Formation. It is regarded as a local seal. Middle Miocene Lower Fars formations of the area.
- The Late Cretaceous beginning of oil generation (TR 0.01), while the Late Paleogene to Early Neogene was the end (TR 0.95) of oil

generation. Temperatures that control generation (70-105°C, with a maximum of 150°C).

- Vertical migration in the area and oil first moved into structural traps in the Basin was throughout of the Mesozoic and Paleozoic, which are later altered or destroyed during the late Paleogene and Neogene.
- The hydrocarbon then accumulated in Tertiary traps such as Asmari Formation.

Chapter Six

Conclusions and Recommendations

6.1.Conclusions

The present study includes the petroleum system of Abu Ghirab oil field in the Zagros basin. The study includs reservoir, source, seal, and overburden rocks as well as generation, migration, and accumulation of petroleum. The main reservoir characterization of the reservoir units in the Asmari Formation. The petrophysical study includes the main and secondary reservoir units and builds three-dimensional models of the reservoir. Three crude oil samples are collected from three wells at different depths in Abu-Gharib oilfield. The samples are subjected to many geochemical analyses, such as GC, GC/Ms, and carbon isotopes, to determine the lithology, age, depositional environments, and maturity of the probable source rocks. The potential source rocks were identified, depending on the biomarker and non-biomarker parameters as well as the results of the carbon isotope analysis. The 1D model of well-17 in the field study is built using the petromode software.To study the petrophysical properties of the Asmari Formation, many well logs are used to make environmental adjustments and interpretations using software such as the Interactive Petrophysics software v3.5 Petrel 2018 .The results indicats that the Asmari Formation is the main reservoir in the field, and the secondary reservoirs are the Mishrif, Mauddud, and Nahr Umr formations .

- The Asmari Formation in Iran is equivalent in Iraq to the Kirkuk group, represented in the study area as Jeribe-Euphrates, Upper Kirkuk, and Middle-Lower Kirkuk .The lithology of the Asmari formation was determined by using a neutron-density cross-plot. The Jeribe-Euphrates Formation consists of dolomite, while the Upper and Middle-Lower Kirkuk formations consist of limestone .The MID and M-N cross plots demonstrated that the Asmari Formation consists of calcite and dolomite .

- The Asmari formation consists of three main units separated by a shale layer, including Jeribe-Euphrates, Upper Kirkuk, and Middle-Lower Kirkuk. The Jeribe-Euphrates unit has low reservoir properties, while the Upper Kirkuk unit has good reservoir properties. According to the results of the reservoir analysis and CPI analysis, it consists of nine eight reservoir units, including A1, A2, A3, B1, B2, B3, B4, and C. Each unit has different petrophysical properties from others in the same well and also from one well to another .
- The Asmari Formation's Middle to Lower Kirkuk reservoir unit is nearly entirely saturated with reservoir water and contains a high amount of shale with only a small amount of oil present.
- The Upper Kirkuk reservoir unit has good petrophysical properties and high hydrocarbon saturation, making it the best reservoir unit for oil.
- Using Petrel software, a 3D geological model is created based on data provided by the Oil Exploration Company. The structural contour map shows that Abu Ghirab oilfield is composed of two asymmetrical anticlinal domes, and its axis extends from northwest to southeast .
- Because the B2 and B3 units of the Asmari Formation, Abu Ghirab oil field, have the highest porosity and lowest water saturation, they are thought to be the main oil yielding unit .
- Many biomarker parameters are obtained from the geochemical analysis of crude oil to define the source rock origin, depositional environment, lithology, age, and maturity. The biomarker parameters indicated that the oil accumulated in the Asmari Formation originated from Middle to Upper Jurassic source rocks that are deposited in a hypersaline carbonate depositional environment. The organic matter is marine algae carbonate and generated oil at a low maturity level.

- To understand the anticipated distribution and movement of petroleum within the basin, as well as to determine hydrocarbon generation, migration, and accumulation, as well as temperature histories and pressures, 1D basin and petroleum system modeling, was built. The Possible source rocks Middle Jurassic Sargelu Formation and the Upper Jurassic Nagma Formation and Lower Cretaceous At Yamama and Sulaiy Formation. Based on the model, analysis results, and data that was obtained, the oil generation in source rocks commenced in the Late Cretaceous in intrashelf basins, peak expulsion took place in the late Miocene and Pliocene when these depocenters had expanded along the Zagros foredeep trend, and generation ended in the Holocene when deposition in the foredeep ceased. The trap is formed in the Early Cretaceous due to the Zagros Orogeny movement. The oil is migrated horizontally and vertically throughout faults and accumulated in the Asmari Formation reservoir units and other Cretaceous reservoirs

6.2. Recommendations

1- Use seismic imaging to learn more about the fault networks in the research region, their role as a migratory route, and their ability to foretell new traps.

2- Several new oil and gas –condensate discoveries could be made in the insufficiently explored of this area of study.

3- To ascertain the structural and stratigraphic subsurface configurations in the Abu Ghirab oilfield area, three-dimensional (3D) seismic studies are crucial.

4- Studying the burial and tectonic history of this interesting area gives a clear picture of other oil reservoirs.

5- To obtain new hydrocarbon sources and to gather information about the source, reservoir, and seal units that can be related to the overlying units to clarify the relationship between their sources and oils as petroleum systems, deep oil well drilling that penetrated at least the Jurassic units in the studied area is required.

Reference

Reference

Akinlua A, Ajayi TR, Adeleke BB (2007) Organic and inorganicgeochemistry of northwestern Niger Delta oils. Geochem J41:271–281

Al Shdidi, S., Thomas, G., & Delfaud, J. (1995). Sedimentology, diagenesis, and oil habitat of Lower Cretaceous Qamchuqa Group, northern Iraq. AAPG Bulletin, 79(5), 763–778.

Al-Ameri, T. K. (1990). Palynofloral evidence for Middle Triassic age, palaeoenvironments and sedimentary provenance of sediments in Borehole 58, western Iraqi desert. *Review of palaeobotany and palynology*, *65*(1-4), 267-274.

Al-Aradi, H. T., Alnajm, F. M., & Al-Khafaji, A. J. (2022). Reservoir Properties of the Upper Sand Member of the Zubair Formation in North Rumaila Oil Field. *The Iraqi Geological Journal*, 97-111.

Al-Baldawi, B. A. (2020). Petrophysical Analysis of Well Logs for Asmari Reservoir in Abu Ghirab Oil Field, South Eastern Iraq. Iraqi Journal of Science, 2990-3001.

Al-Habba, Y. Q., & Abdullah, M. B. (1989). Geochemical study for hydrocarbon source rocks in NE Iraq. Oil Arab Coop 15 (57): 11–51. Arabic.

Al-Hajeri, M. M., Al Saeed, M., Derks, J., Fuchs, T., Hantschel, T., Kauerauf, A., ... & Peters, K. (2009). Basin and petroleum system modeling. *Oilfield Review*, *21*(2), 14-29.

Alhuraishawy, A.K., 2005. Detection of natural fractures in asmari reservoir / Abughirab field by techniques of well logging and well testing, M.Sc. thesis petroleum engineering, university of Baghdad.

Al-Khafaji, A. J. S. (2010). Jurassic-Cretaceous petroleum systems of the Middle Euphrates Region (Kifl, West Kifl, Afaq, Musaiyab, Morjan, and Ekheither oil fields), Middle Iraq (Doctoral dissertation, Ph. D. Thesis,

University of Baghdad, Department of EarthSciences 198).

Al-Khafaji, A. J., Al Najm, F. M., Al Ibrahim, R. N., & Sadooni, F. N. 2019. Geochemical investigation of Yamama crude oils and their Inferred source rocks in the Mesopotamian Basin, Southern Iraq. *Petroleum science and technology*.

Al-K hafaji, Amer Jassim. (2015). The Mishrif, Yamama, and Nahr Umr reservoirs petroleum system analysis, Nasiriya oilfield, Southern Iraq. Arabian Journal of Geosciences, 8(2), 781–798.

Alexander, R., Kagi, R. I., & Woodhouse, G. W. (1981). Geochemical correlation of Windalia oil and extracts of Winning Group (Cretaceous) potential source rocks, Barrow Subbasin, Western Australia. AAPG Bulletin, 65(2), 235-250.

Allen, P. A. and Allen, J.R. (2005): Basin analysis. Blackwell publishing, second edition,549pp.

Allen, P. A., & Allen, J. R. (1990). Basin analysis: principles and applications,

Blackwell Scientific Publications. *Oxford*, *London*.

Al-Musawi, A. D. J., & Nasser, M. E. (2019). The Evaluation of Reservoir Quality of Mishrif Formation in South and North Domes of Buzurgan Oil Field. *Journal of Petroleum Research & Studies*, *25*, 89-106.

Al-Naqib, K. M. (1960). Southern Region Geology Summary for the brigade Kirkuk-Iraq, Iraq Oil Company Limited. In Second Arab Petroleum conference (p. 62).

Al-Sakini, J. A. (1992). Summary of petroleum geology of Iraq and the Middle East: Kirkuk. Northern Oil Company Press, Iraq (in Arabic, p 179).

Alssad, H.F.K., 2010. Study and evaluate the Petrophysical and Geological Properties of the Southern Asmari Reservoir / Southeast Iraq.

Unpublished Msc. Thesis, Basra University.

Ameen, M. S. (1992). Effect of basement tectonics on hydrocarbon generation, migration, and accumulation in northern Iraq. *AAPG bulletin*, *76*(3), 356-370.

Anders, D. (1991). Geochemical Exploration Methods: Chapter 7: GEOCHEMICAL METHODS AND EXPLORATION.

Archie G.E., 1942. The Electrical Resistivity Log as an Aid in Determining Some Reservoir Characteristics: AIME, Vol.146, p.54.

Arps, J.J., 1964. Engineering Concepts Useful in Oil Finding, AAPG Bulletin, Vol.1, No. 48, pp.157-165.

Asif M., Fazeelat T. and Grice K.(2011) Petroleum geochemistry of the Potwar Basin, Pakistan: Oil–oil correlation using biomarkers, d13C and dD. Organic Geochemistry 42.1226–1240

Asquith, G., & Krygowski, D. (2004). AAPG Methods in Exploration, No. 16,

Chapter 2: Spontaneous Potential.

Bacon, C.N., Calver, C.R., Boreham, C.J., Lenman, D.E., Morrison, K.C. Revill, A.T. and Volkman, J.K., 2000. The Petroleum Potential of Onshore

Tasmania: a review, Geological Survey Bulletin, 71, pp. 1-93.

Batten, D.J., 1996, Palynofacies and Petroleum Potential: In Jansonius, J., McGregor, D.C. (eds.), Palynology: Principles and Applications. American Association of Stratigraphic Palynologists Foundation, Vol.3, pp.1065 1084.

Branets, L. V., Ghai, S. S., Lyons, S. L., & Wu, X. H. (2009). Challenges and technologies in reservoir modeling. Communications in Computational Physics, 6(1), 1.

Barwise, A. J. G. (1990) Role of nickel and vanadium in Petroleum Classification. Energy and Fuels, Vol. 4. P. 647-52.

Berberian, M. (1995). Master “blind” thrust faults hidden under the Zagros folds: active basement tectonics and surface morphotectonics. Tectonophysics, 241(3-4), 193-224.

Berberian, M., & King, G. C. P. (1981). Towards a paleogeography and tectonic evolution of Iran. Canadian journal of earth sciences, 18(2), 210-265.

Beydoun, Z R, Clarke, M. W. H., & Stoneley, R. (1992). Petroleum in the Zagros basin: a late tertiary foreland basin overprinted onto the outer edge of a vast hydrocarbon-rich paleozoic-mesozoic passive-margin shelf: chapter 11.

Beydoun, Ziad Rafik. (1991). Arabian plate hydrocarbon geology and potential.

Bellorini , J. P., Casas,J., Gilly,P., Jannes, P., and Matthews, P., 2003. Definition of a 3D Integrated Geological Model in a Complex and Extensive Heavy Oil Field, Oficina Formation, Faja de Orinoco, Venezuela Sincor OPCO, Caracas, Venezuela.

Bowen, D. G., 2003. Formation Evaluation and Petrophysics, 273p. Company, Pub., San Francisco and London, 724P.

Buday, T., & Hak, J. (1980). REPORT ON THE GEOLOGICAL SURVEY OF THE WESTERN PART OF THE WESTERN DESERT, IRAQ.

Catuneana,O.,2006;Principles Sequence Stratigraphy ,First edition .Elsevier,Amsterdam,375P.

CNOOC, 2011. Executive report for reservoir assessment of the M.O.C in eastern Iraq. China National Offshore Oil Corporation Ltd., December, 2011.

Congrès géologique international. Commission de stratigraphie, van Bellen, R. C., Dunnington, H. V., R.. Wetzel, & Morton, D. M. (1959). Lexique Stratigraphique International: Asie. Iraq. Tertiary. Mesozoic and Palaeozoic.

Centre National de la Recherche Scientifique.

Cooper, M. (2007). Structural style and hydrocarbon prospectivity in fold and thrust belts. Deformation of the continental crust: the legacy of mike coward, 272, 447.

Darling, T. (2005) *Well logging and formation evaluation*. Elsevier.

Dembicki, H. (2016). Practical petroleum geochemistry for exploration and production. Elsevier.

Desbrandes,R., 1985. "Encyclopedia of Well Logging".

Dow, W. (2014). Musings on the History of Petroleum Geochemistry–From My Perch.

Dickson, B., Durand, B., Espitalie, J., & Combaz, A. (1974). Influence of nature and diagenesis of organic matter in formation of petroleum. Aapg Bulletin, 58(3), 499–506.

Duan,Y.; Ma, L. (2001). Lipid geochemistry in a sediment core from Ruoergai Marsh deposit (Eastern Qinghai-Tibet Plateau, China), Organic Geochemistry, Vol. 32, 1429-1442.

Dickson, U. J., & Udoessien, E. I. (2012). PHYSICOCHEMICAL STUDIES OF NIGERIA'S CRUDE OIL BLENDS. Petroleum & Coal, 54(3).

Dunnington, H. V. (1959). Iraq. Mesozoic and Palaeozoic. Ekpo O.B., Fubara B.E., Ekpa D.O. and Marynowski L.H. (2012)Determination of Hydrocarbon sources using inN-alkane and PAH distribution indices in sediment from coastle areas of Bonny river in Niger Delta Nigeria. ARPN Journal of Earth Sciences Vol. 1, No. 1: 9-20

Ekweozor CM, Okogun JI, Ekong DEU, Maxwell JR (1981) C24–

El Nady M.M., Harb M.F.and Mohamed S.N. (2014) Biomarker characteristics of crude oils from Ashrafi and GH oilfields in the Gulf of Suez,Egypt: An implication to source input and paleoenvironmental assessments. Egyptian Journal of Petroleum 23, 455–459

Ellis V. D, Singer, M.J., 2008. "Well Logging for Earth Scientists" ,Second Edition, Springer Dordrecht, The Netherlands.

Espitalie, J, Deroo, G., & Marquis, F. (1985). Rock-Eval pyrolysis and its applications (part one). Oil & Gas Science and Technology-Revue d'IFPEN, 40(5), 563–579.

Espitalie, Jean, Madec, M., Tissot, B., Mennig, J. J., & Leplat, P. (1977). Source rock characterization method for petroleum exploration. Offshore Technology Conference.

Fagbote,E.O., Edward,O.2012. Characterization, Distribution, Sources and Origins of Aliphatic Hydrocarbons of the Soils of Agbabu Bitumen Deposit Area, Western Nigeria. African Journal of Scientific Research. 10 (1).pp:263-270.

Fouad, S. F. (2010). Tectonic and structural evolution of the Mesopotamia Foredeep, Iraq. Iraqi Bulletin of Geology and Mining, 6(2), 41-53.

Fouad, S. F. (2012). Tectonic Map of Iraq, scale 1: 1000 000, 3rd edit. GEOSURV, Baghdad, Iraq.

Fouad, S. F. (2012). Western Zagros fold–thrust belt, part I: The low folded zone. Iraqi Bulletin of Geology and Mining, (5), 39-62.

Fouad, S. F., & Sissakian, V. K. (2011). Tectonic and structural evolution of the Mesopotamia Plain. Iraqi Bulletin of geology and mining, (4), 33-46.

Fox, J. E., & Ahlbrandt, T. S. (2002). *Petroleum geology and total petroleum systems of the Widyan Basin and interior platform of Saudi Arabia and Iraq* (Vol. 2202). US Department of the Interior, US Geological Survey.

Gibson, C. R. (1982). Basic well log analysis for geologists. American Association of Petroleum Geologists.

Galarraga, F., Reategui, K., Martïnez, A., Martínez, M., Llamas, J.F., Dickson J.U. and Udoessien I.E. (2012) Physiochemical studies of Nigeria scrude oil blends. Petroleum & Coal 54 (3) 243-251

Halliburton, Energy Service, 2001**.** Basic Petroleum Geology and Log Analysis : Houston, Texas, Halliburton Company. 80p.

Hantschel, T., & Kauerauf, A. I. (2009). *Fundamentals of basin and petroleum systems modeling*. Springer Science & Business Media.

Harris, A. G. (1979). Conodont color alteration, an organo-mineral metamorphic index, and its application to Appalachian basin geology.

Hassanzadeh, J., & Wernicke, B. P. (2016). The Neotethyan Sanandaj-Sirjan zone of Iran as an archetype for passive margin-arc transitions. Tectonics, 35(3), 586-621.

Hessami, K., Koyi, H. A., & Talbot, C. J. (2001). The significance of strike-slip faulting in the basement of the Zagros fold and thrust belt. *Journal of petroleum Geology*, *24*(1), 5-28.

Hessami, K., Nilforoushan, F., & Talbot, C. J. (2006). Active deformation within the Zagros Mountains deduced from GPS measurements. Journal of the Geological Society, 163(1), 143-148.

Hood, A. C. C. M., Gutjahr, C. C. M., & Heacock, R. L. (1975). Organic metamorphism and the generation of petroleum. *AAPG bulletin*, *59*(6), 986-996.

Horsfield B. an Rullkotter J., 1994, Diagenesis Catagenesis and Metagenesis of OM, in, L.B. Magoon and W.G. Dow (eds). The Petroleum System-From Source to Trap, AAPG Memoir 60, pp.189-199.

Hunt, J. M. (1996) Petroleum geochemistry and geology, 2nd edn, Freeman, New York, 743P.indicators: Geochimica et Cosmochimica Acta, v. 43, pp. 739-745.

Hunt, J. M. (1970): The significance of carbon isotope variations in marine sediments, In G.D. Hobson and G.C. Speers, eds., Advances in organic geochemistry, 1966. New York, Pergamon Press, pp. 27 –35.

Hedberg, H.D., 1968. Significance of high-wax oil with respect to genesis of petroleum. Am. Assoc. Petrol. Geol. Bull. 52, 736e750.

Hakimi, M. H., & Najaf, A. A. (2016). Origin of crude oils from oilfields in the Zagros Fold Belt, southern Iraq: Relation to organic matter input and paleoenvironmental conditions. Marine and Petroleum Geology, 78, 547-561.

IES Integrated Exploration Systems (2007) PetroMod, lD/Petrocharge Express, and PetroRisk Software. IES, Bastion strasse 11-19, 52428 Juelich, Germany, (www.ies.de).

IES Integrated Exploration Systems (2009) PetroMod, lD/Petrocharge Express, and PetroRisk Software. IES, Bastion strasse 11-19, 52428 Juelich, Germany, (www.ies.de).

Jarvie, D. M. (1991). Total organic carbon (TOC) analysis: Chapter 11: Geochemical methods and exploration.

Jassim, S. Z., & Goff, J. C. (Eds.). (2006). Geology of Iraq. DOLIN, sro, distributed by Geological Society of London.

Jia, B. (2010). Linking geostatistics with basin and petroleum system modeling: Assessment of spatial uncertainties. STANFORD UNIVERSITY.

Koshnaw, R. I., Stockli, D. F., & Schlunegger, F. (2019). Timing of the Arabia-Eurasia continental collision—Evidence from detrital zircon U-Pb geochronology of the Red Bed Series strata of the northwest Zagros hinterland, Kurdistan region of Iraq. Geology, 47(1), 47-50.

Lafargue, E., Marquis, F., & Pillot, D. (1998). Rock-Eval 6 applications in hydrocarbon exploration, production, and soil contamination studies. Revue de l'institut Français Du Pétrole, 53(4), 421–437.

Larionov v.v. 1969. Borehole Radiometry, Moscow,U.S.S.R.,Nedra.

Le Garzic, E., Vergés, J., Sapin, F., Saura, E., Meresse, F., & Ringenbach, J. C. (2019). Evolution of the NW Zagros Fold-and-Thrust Belt in Kurdistan Region of Iraq from balanced and restored crustal-scale sections and forward modeling. Journal of Structural Geology, 124, 51-69.

Leverson, A. I., 1972. Geology of petroleum 2nd ed., Freeman, W.H. and Company, Pub., San Francisco and London, 724P.Darling, T. (2005) Well logging and formation evaluation. Elsevier.

Learn, W. Y. (n.d.). Energy Resources.

Lehne, E., 2008, Geochemical study on reservoir and source rock asphaltenes and their significance for hydrocarbon generation, Ph.D. unpublished Thesis, Technischen Universit Berlin, 362p.

Leslie, B. (1994). Magoon & Wallace G Dow The petroleum systemfrom source to trap AAPG memoir 60. *The American Association of Petroleum Geologists, Tulsa, Oklahoma, U SA*.

Liu, X., Wen, Z., Wang, Z., Song, C., & He, Z. (2018). Structural characteristics and main controlling factors on petroleum accumulation in Zagros Basin, Middle East. Journal of Natural Gas Geoscience, 3(5), 273-281.

Luo, S., Tan, X., Chen, L., Li, F., Chen, P., & Xiao, D. (2019). Dense brine refluxing: A new genetic interpretation of widespread anhydrite lumps in the Oligocene–Lower Miocene Asmari Formation of the Zagros foreland basin, NE Iraq. Marine and Petroleum Geology, 101, 373-388.

Liu, X., Wen, Z., Wang, Z., Song, C., & He, Z. (2018). Structural characteristics and main controlling factors on petroleum accumulation in Zagros Basin, Middle East. Journal of Natural Gas Geoscience, 3(5), 273-281.

Luo, S., Tan, X., Chen, L., Li, F., Chen, P., & Xiao, D. (2019). Dense brine refluxing: A new genetic interpretation of widespread anhydrite lumps in the Oligocene–Lower Miocene Asmari Formation of the Zagros foreland basin, NE Iraq. Marine and Petroleum Geology, 101, 373-388.

Magoon, L. B. (1988). The petroleum system—a classification scheme for research, exploration, and resource assessment. *Petroleum systems of the*

United States: US Geological Survey Bulletin, *1870*, 2-15.

Magoon, L. B., & Dow, W. G. (1991). The petroleum system-from source to trap. *AAPG Bulletin (American Association of Petroleum Geologists);(United States)*, *75*(CONF-910403-).

Magoon, L. B., & Dow, W. G. (1994). The petroleum system: chapter 1: Part I. Introduction.

Magoon, L. B., & Schmoker, J. W. (2000). The total petroleum system–The natural fluid network that constrains the assessment unit. *US geological survey world petroleum assessment*, 31.

Mahdi, T. A., Aqrawi, A. A., Horbury, A. D., & Sherwani, G. H. (2013). Sedimentological characterization of the mid-Cretaceous Mishrif reservoir in southern Mesopotamian Basin, Iraq. GeoArabia, 18(1), 139-174.

Moldowan, J. M., Seifert, W. K., and Gallegos, E. J. (1985): Relationship between petroleum composition and depositional environment of petroleum source rock. AAPG Bull., V. 69, pp. 1255 –1268.

Masson, F., Chéry, J., Hatzfeld, D., Martinod, J., Vernant, P., Tavakoli, F., & Ghafory-Ashtiani, M. (2005). Seismic versus aseismic deformation in Iran inferred from earthquakes and geodetic data. Geophysical Journal International, 160(1), 217-226.

McCarthy, K., Rojas, K., Niemann, M., Palmowski, D., Peters, K., & Stankiewicz, A. (2011). Basic petroleum geochemistry for source rock evaluation. Oilfield Review, 23(2), 32–43.

McQuarrie, N., & van Hinsbergen, D. J. (2013). Retrodeforming the Arabia-Eurasia collision zone: Age of collision versus magnitude of continental subduction. Geology, 41(3), 315-318.

Merrill, R. K. (1991). Source and migration processes and evaluation techniques.

Moustafa Y and Morsi R (2012). Biomarkers, Chromatography and Its

Applications, Dr. Sasikumar Dhanarasu (Ed.), ISBN: 978-953-51-0357-8, InTech,Availablefrom:http://www.intechopen.com/books/chromatography-and-its applications/biomarkers oils predominantly derived from terrigenous source material.Org Geochem 10:73–84

Nairn, A. E. M., & Alsharhan, A. S. (1997). Sedimentary basins and petroleum geology of the Middle East. Elsevier.

Nairn, A. E. M., & Alsharhan, A. S. (1997). Sedimentary basins and petroleum geology of the Middle East. Elsevier.

Fouad, S. F. (2012). Western Zagros fold–thrust belt, part I: The low folded zone. Iraqi Bulletin of Geology and Mining, (5), 39-62.

Noble, R. A. (1991). Geochemical Techniques in Relation to Organic Matter: Chapter 8: GEOCHEMICAL METHODS AND EXPLORATION.

M_arquez, G., 2008. V/Ni ratio as a parameter in palaeoenvironmental characterisation of nonmature medium-crude oils from several Latin American basins. J. Petrol. Sci. Eng. 61, 9e14.

Makeen Y, Abdullah W, Hakimi M, Hadad Y, Elhassan O and Mustapha K.(2015) Geochemical characteristics of crude oils, their asphaltene and related organic matter source inputs from Fula oilfields in the Muglad Basin, Sudan, Marine and Petroleum Geology 67 (2015) 816e828.

Onojake M, Osuji L. and Abrakasa S (2015) Source, depositional environment and maturity levels of some crude oils in southwest Niger Delta, Nigeria. Chin. J. Geochem. 34(2):224–232

Osuji, L.C. and Antia, B.C., 2005, Geochemical Implication of some Chemical Fossils as Indicators of Petroleum Source Rocks, AAPL Journal, Sci. Environ. Mgt. Vol. 9, No.1, pp. 45-49.

Owen, R. M. S., & Nasr, S. N. (1958). Stratigraphy of the Kuwait-Basra Area: Middle East.

Peters K. E. and Moldowan, J. M. (1993) The biomarker guide, interpreting

molecular fossils in petroleum and ancient sediments. Prentice – Hall, Englewood Cliffs, N.J, pp.863-87.

Peters, E. J. (2006) 'Petrophysics: Department of Petroleum and Geosystems.

Peters, K E. (1986). Guidelines for evaluating petroleum source rock using programmed pyrolysis. AAPG Bulletin, 70(3), 318–329.

Peters, K.E. and Moldowan, J.M., 1991, Effects of Source, Thermal Maturity and Biodegradation on the Distribution and Isomerization of Homohopanes in Petroleum. Organic Geochemistry, Vol. 17, pp. 47-61.

Peters, K.E., Walter, C.C., and Moldowan, J.M. (2005a) The biomarker guide. Vol.1: Biomarkers and isotopes in the environment and human history. The press syndicate of the University of Cambridge, pp. 471.

Peters, K. E., Walters, C. C., & Moldowan, J. M. (2005b). The biomarker guide: Biomarkers and isotopes in petroleum exploration and earth history, Vol. 2. *The Press Syndicate of the University of Cambridge, Cambridge, Mass, USA*.

Peters, Kenneth E, & Cassa, M. R. (1994). Applied source rock geochemistry: Chapter 5: Part II. Essential elements.

Philp, R.P., 2003 a, Formation and Geochemistry of Oil and Gas, in Treatise on Geochemistry, Holland, H.D. and Turekian, K.K. (Executive eds.), Vol. 7 , Sediments, Diagenesis and Sedimentary Rocks, Mackenzie ,F.T. (Volume Editor), Elsevier pergamon, pp.223-256.

Philp, R.P., 2003 b, Petroleum Geochemistry, With a Brief Introduction to Applications to Exploration and Production in Oklahoma, Shale Shaker, pp.69- 79.

Pickett, G. R., 1972. Practical formation evaluation: Golden Colorado, G. R. Pickett, Inc.

Pickett, G.R., 1966. A review of current techniques for determination of water saturation from logs. Journal of petroleum Technology, 18(11), 1425-1433. https://doi.org/10.2118/1446-PA

Pirouz, M., Avouac, J. P., Hassanzadeh, J., Kirschvink, J. L., & Bahroudi, A. (2017). Early Neogene foreland of the Zagros, implications for the initial closure of the Neo-Tethys and kinematics of crustal shortening. Earth and Planetary Science Letters, 477, 168-182.

Pickett, G.R., 1966. Review of Current Techniques for Determination of Water Saturation from Logs. Journal of Petroleum Technology (JPT), pp: 1425-1433.

Pitman, J. K., Steinshouer, D., & Lewan, M. D. (2004). Petroleum generation and migration in the Mesopotamian Basin and Zagros Fold Belt of Iraq: results from a basin-modeling study. GeoArabia, 9(4), 41-72.

Powell, T. G., and McKirdy, D. M. (1973): Relationship between ratio of pristane to phytane, crude oil composition and geological environment in Australia. Nature, Physical Science, V. 243, pp. 37 – 39.

Repsole, 2006; Organic Geochemistry for explorationists. A practical guide to the application of analytical techniques in petroleum exploration projects. Santiago Quesada, Upstream Technology group.

Rullkotter, J., Mukhopadhyay, P. K. and Welte, D. H., 1984, Geochemistry and Petrography of Organic Matter in Sediments from Hole 530A, Angola Basin and Hole 532, Walvis Ridge, Deep Sea Drilling Project. In Hay, W.W., Sibuet, J.C., Init. Repts. DSDP, 75: Washington (U.S. Govt. Printing Office), pp.1069-1087.

Sadooni, F. N. (1997). Stratigraphy and petroleum prospects of Upper Jurassic carbonates in Iraq. *Petroleum Geoscience*, *3*(3), 233-243.

Sadooni, F. N., & Aqrawi, A. A. (2000). Cretaceous sequence stratigraphy and petroleum potential of the Mesopotamian basin, Iraq.

Sadooni, Fadhil N. (1993). Stratigraphie Sequence, Microfacies, and Petroleum Prospects of the Yamama Formation, Lower Cretaceous, Southern Iraq. AAPG Bulletin, 77(11), 1971–1988.Williams, M.E.M,

Davis, R.K., Paillet, F.L., Turpening, R.M.,Soul, S.J.Y., Schneider, G.W., 2009. Review of Borehole Based

Schlumberger, 1970. Well Evaluation Conference, Libya, Services Techniques Schlumberger, France, 2-5, P: 2-6.

Schlumberger, 1972. Log Interpretation charts, Houston, Schumberger well services, Inc., Vol.2.

Schlumberger, 1972. Log Interpretation, Vol. I—Principles: New York, Schlumberger Limited, 112 p.

Schlumberger, 1972. Log Interpretation, Vol. I—Principles: New York, Schlumberger Limited, 112 p.

Schlumberger,2005. Petrel property modeling course .Schlumberger, 10-320p.

Schlumberger, 1984. Log interpretation charts. Schlumberger, 106pp.

Schlumberger, 1987. Log interpretation charts, USA.Toby, 2005. WellL logging and formation evaluation, Gulf Professional Publishing is an imprint of Elsevier Science.

Schlumberger, 2010. Petrel introduction course. Schlumberger, 13-493p.

Schlumberger, 2009. Petrel online help, Petrel Introduction Course.

Adaeze, O. C., & Adiela, U. P. (2016). Facies Modelling and Petrophysical Properties of X-Field, Onshore, Niger Delta, Nigeria. International Journal of Science Inventory Today, IJSIT, 5(2), 136-151.

Schlumberger, 2007. Petrel Structural modeling course. Schlumberger, 105-123p.

Schlumberger, 1974**.** Log Interpretation, vol.II-Applications:New York.

Schlumberger, 1979.Log Interpretation Charts, Schlumberger Well Surveying Corporation, U.S.A., 97p.

Schlumberger, 1982. Natural gamma ray spectrometry-Essentials of N.G.S. interpretation. Schlumberger, 69pp

Seifert WK, Moldowan JM (1980) The effect of thermal stress on sourcerock quality as measured by hopane stereochemistry. Phys Chem Earth 12:229–237

Seifert, W. K. and Moldowan, j. M., 1979. The effect of biodegradation on steranes and terpanes in crude oils. Geochimica et Cosmochimica Acta, 43,pp. 111-126.

Selley, R. C. (1998). Elements of petroleum geology. Gulf Professional Publishing.

Selley, R. C. (2000) *Applied sedimentology*. Elsevier

Senftle, J. T., & Landis, C. R. (1991). Vitrinite Reflectance as a Tool to Assess Thermal Maturity: Chapter 12: Geochemical Methods and Exploration.

Sepehr, M., & Cosgrove, J. W. (2004). Structural framework of the Zagros fold–thrust belt, Iran. Marine and Petroleum geology, 21(7), 829-843.

Sharland, P. R., Archer, R., Casey, D. M., Davies, R. B., Hall, S. H., Heward, A. P., ... & Simmons, M. D. (2001). Arabian plate sequence stratigraphy. GeoArabia, spec Publ 2, gulf PetroLink.

Shubin Wu, G. L., & Lou, R. (2012). Applications of chromatography hyphenated techniques in the field of lignin pyrolysis. Applications of Gas Chromatography, 41.

Sinninghe-Damste, J.; Kenig, F.; Koopmans, M.; Koster, J.; Schouten, S.; Hayes, J. & De-Leeuw, J. (1995). Evidence for gammacerane as an indicator of water column stratification, In: Geochimica et Cosmochimica Acta, Vol. 59, 1895-1900.

Sofer, Z., 1984 ; Stable carbon istope composition of crude oil :Application to source depositional environments and petroleum alteration .Bulltin of the American Association of petroleum Geologists .V.68,PP.31.49.

Staplin, F. L. (1969). Sedimentary organic matter, organic metamorphism, and oil and gas occurrence. Bulletin of Canadian Petroleum Geology,

17(1), 47–66.

Stöcklin, G., & Tornau, W. (1968). Reactions of Nucleogenic Chlorine Atoms with Simple Aromatic Compounds. Radiochimica Acta, 9(2-3), 95-105.

Stoneley, R. (1990). The Middle East basin: a summary overview. Geological Society, London, Special Publications, 50(1), 293–298.

Suarez-Ruiz, I., Flores, D., Mendonca Filho, J. G., & Hackley, P. C. (2012). Review and update of the applications of organic petrology: Part 1, geological applications. International Journal of Coal Geology, 99, 54–112.

Tatar, M., Hatzfeld, D., Martinod, J., Walpersdorf, A., Ghafori-Ashtiany, M., & Chéry, J. (2002). The present-day deformation of the central Zagros from GPS measurements. Geophysical research letters, 29(19), 33-1.

Ten Haven, H.L., de Leeuw, J.W., Rullkotter, J. and Sinninghe Damste, J.S. (1987) Restricted utility of the pristane/ phytane ratios as a paleoenvironmental indicator. Nature, 330. 641-3.

Tiab, D. and Donaldson, C. (2004) 'Petrophysics Second Edition–Theory and Practice of Measuring Reservoir Rock and Fluid Transport Properties'. Golf professional publishing

Timur, A. (1968) 'An investigation of permeability, porosity, and residual -water saturation relationships', in *SPWLA 9th annual logging symposium*. Society of Petrophysicists and Well-Log Analysts.

Tissot, B. D. (1977) The application of results of organic chemical studies in oil and gas exploration. In: Development of petroleum Geology (G. D . Hobson, ed), Vol. 1, pp. 53-82.

Tissot, B. P. and Welte, D.H. (1984) Petroleum Formation and Occurrence. Springer-Verlag, New York.699 P.

Turner A. K. and Gable C. W., 2008. A review of Geological Modelling. Colorado School of Mines, USA, Los Alamos National Laboratory, Los.

Tyracek, J., & Youbert, Y. (1975). Report on the regional geological survey of Western Desert between T1 Oil pumping station and wadi Hauran. Iraq Geological Survey (GEOSURV) Library report, (673).

Tyson, R.V. (1995) Sedimentary Organic Matter. Chapman-Hall, London, pp.615.

Utkucu, M. (2017). Preliminary Seismological Report on the November 12, 2017 Northern Iraq/Western Iran Earthquake. Sakarya University https://doi. org/10.13140/RG, 2(17781.27364).

Vergés, J., Goodarzi, M. G. H., Emami, H., Karpuz, R., Efstathiou, J., & Gillespie, P. (2011). Multiple detachment folding in Pusht-e Kuh arc, Zagros: Role of mechanical stratigraphy.

Vergés, J., Goodarzi, M. G. H., Emami, H., Karpuz, R., Efstathiou, J., & Gillespie, P. (2011). Multiple detachment folding in Pusht-e Kuh arc, Zagros: Role of mechanical stratigraphy.

Verma, M. K., Ahlbrandt, T. S., & Al-Gailani, M. (2004). Petroleum reserves and undiscovered resources in the total petroleum systems of Iraq: reserve growth and production implications. GeoArabia, 9(3), 51-74.

Verweij, J. M. (1993) Hydrocarbon Migration Systems Analysis, Elsevier Science Publishers. B. V. Sara Burgerhartstraat, 272P.

Vu TTA, Zink KG, Mangelsdorf K, Sykes R, Wilkes H, Horsfield B(2009) Changes in bulk properties and molecular compositions within New Zealand Coal Band solvent extracts from early diagenetic to catagenetic maturity levels. Org Geochem 40:963–977

Waples, D. W., and Machihara, T., 1991. Biomarkers for geologists. A practical guide to the application of steranes and triterpanes in petroleum geology. AAPG methods in exploration, AAPG 9, 91p.

Welte. D.H. 1982, Information on Source Rocks of the Arabian Gulf Region.

Unpublished information K. F. AL-Jiilich.

Wang Chunjiang, Fu Jiamo, Sheng Guoying, Xiao Qianhua, Li Jinyou, Zhang Yali, and Piao Mingzhi (2000) Geochemical properties and application of 18α(H)-norneohopanes and17α(H)-diahopanes [J]. Chinese Science Bulletin. 45, 1742–1748.

Wygrala, B. (2008). Petroleum Systems Modeling: Current and Future Applications. In *1 st Annual Meeting, Basin and Petroleum System Modeling, Stanford, USA*.

Wyllie M. R. J., Gregory A. R., and Gardner G. H. F., 1958. An experimental investigation of the factors affecting elastic wave velocities in porous media: Geophysics, v. 23, p. 459–493

Younes,.M.A., and Philp,.R.P., 2005, Source Rock Characterization based on Biological Marker Distribution of Crude Oils in the Southern Gulf of Suez, Egypt, Journal of Petroleum Geology, Vol. 28 No. 3, PP. 301-317.

Zimmer, C. (1993). In the beginning was the tooth. Discover, 14(1), 67–68.

Zumberge, J. E. (1993). Organic geochemistry of Estancia Vieja oils, Río Negro norte block. In Organic Geochemistry (pp. 461-471). Springer, Boston, MA.

Appendix

Appendix (A)

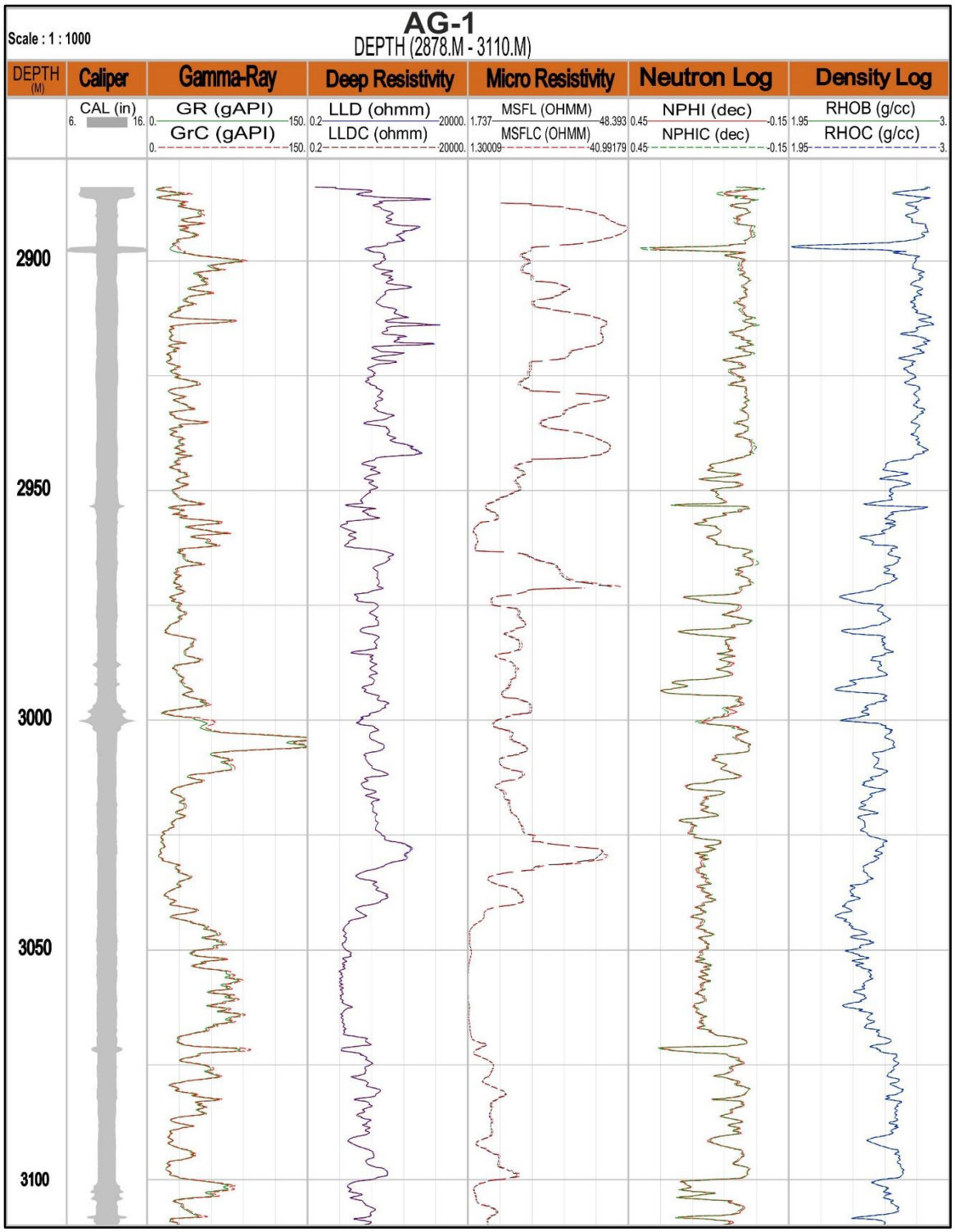

Figure (A-1): Environment correction for well logs measurement inAG-1.

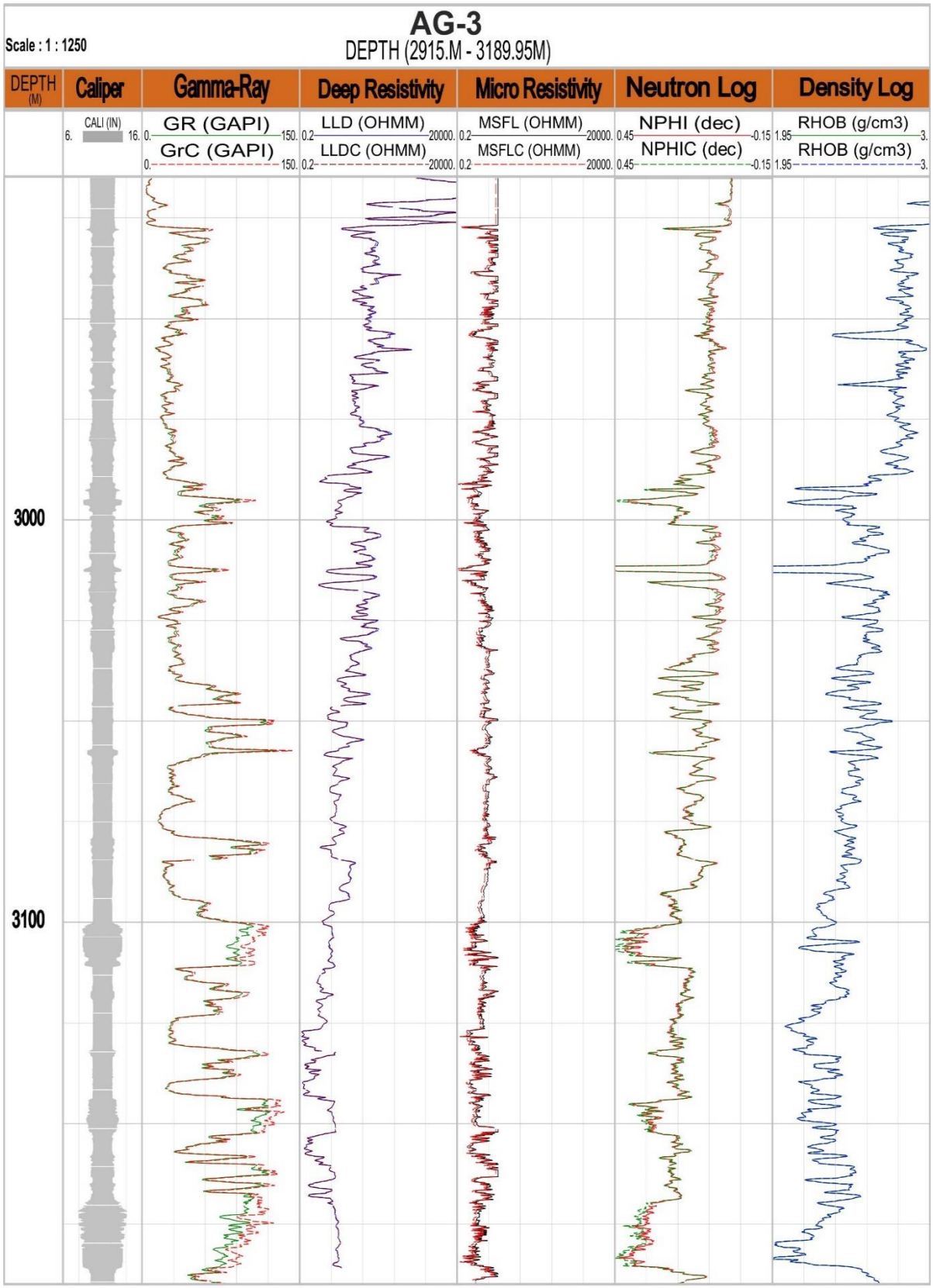

Figure (A-2): Environment correction for well logs measurement inAG-3.

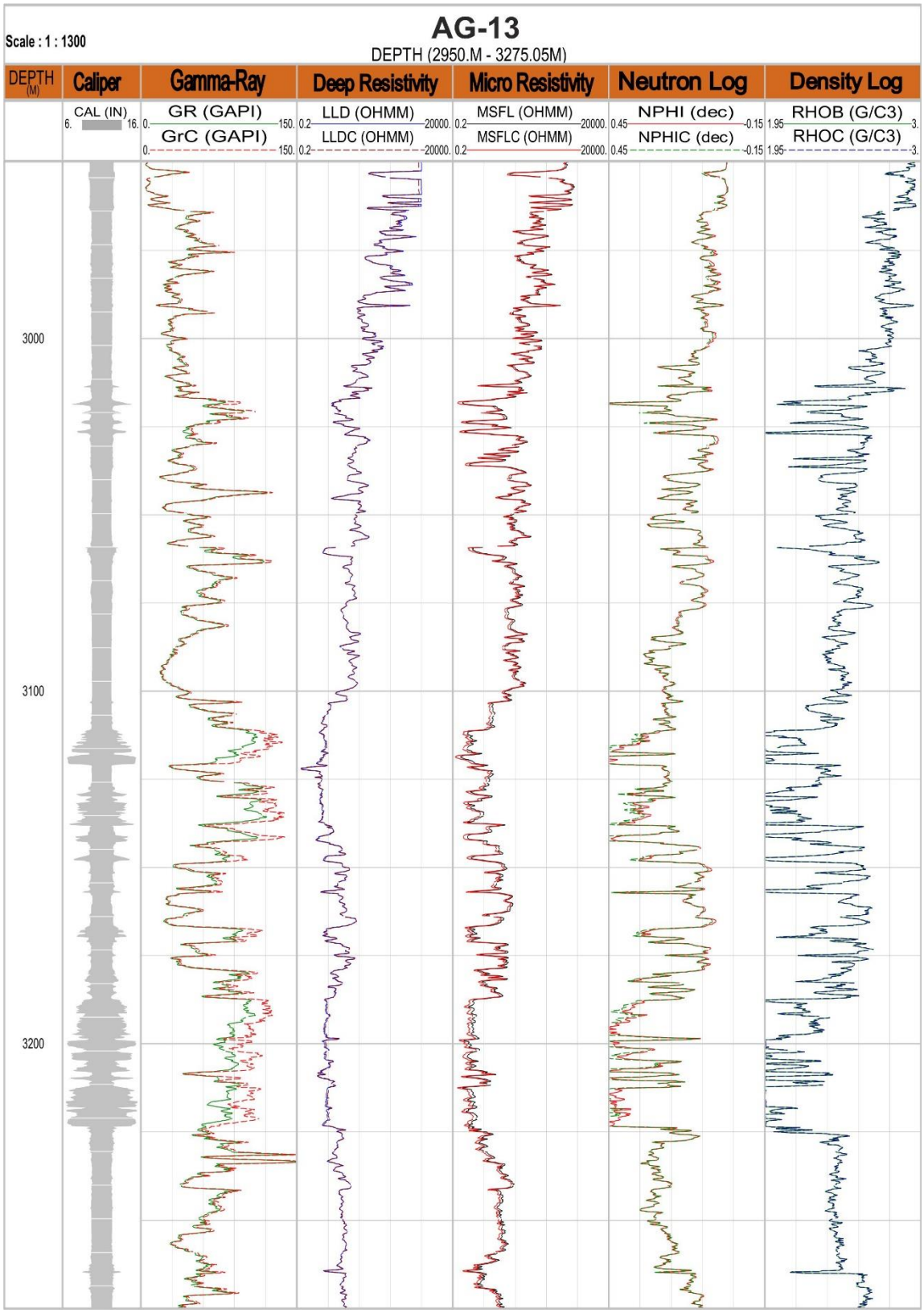

Figure (A-3): Environment correction for well logs measurement inAG-13.

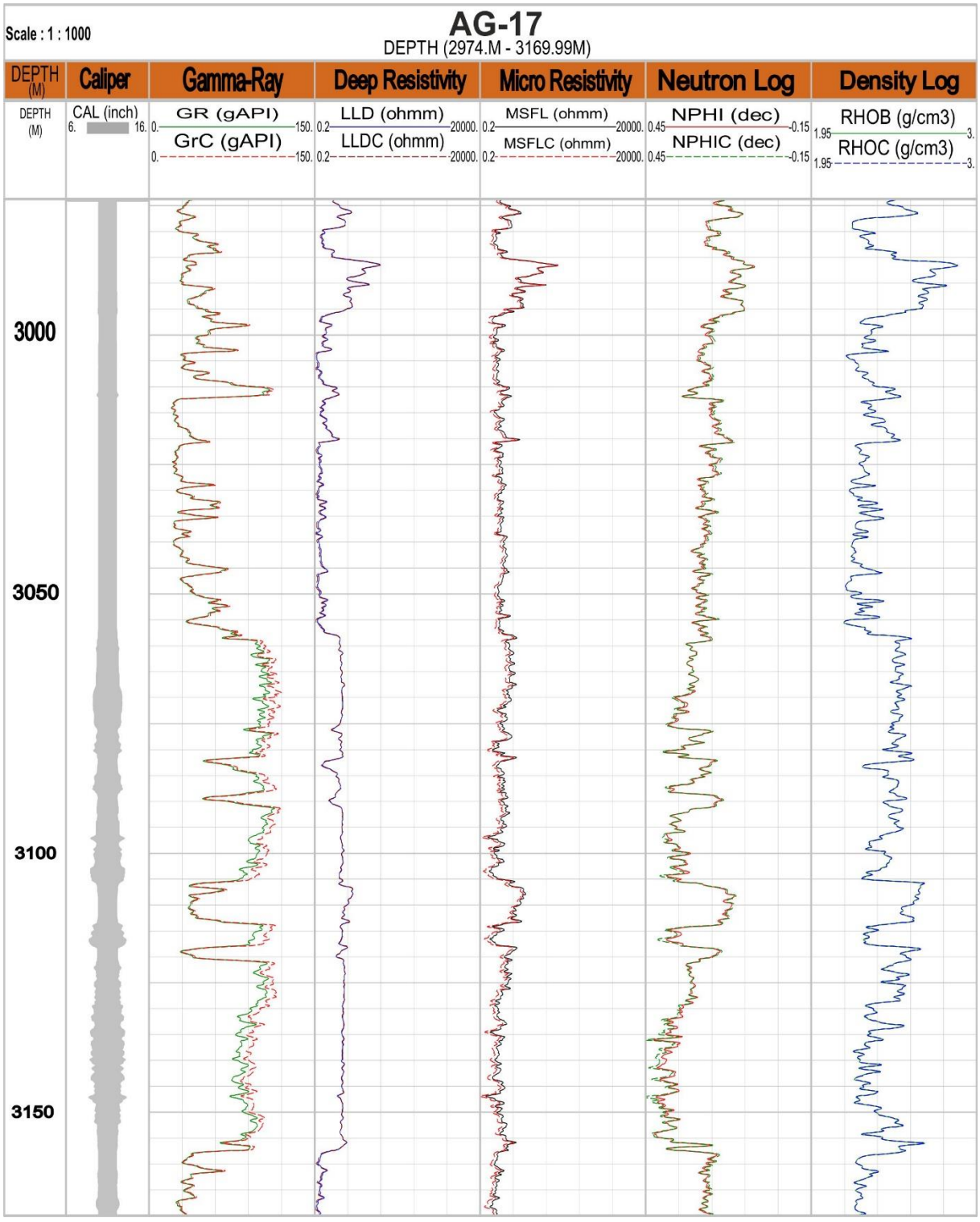

Figure (A-4): Environment correction for well logs measurement inAG-17.

Appendix (B)

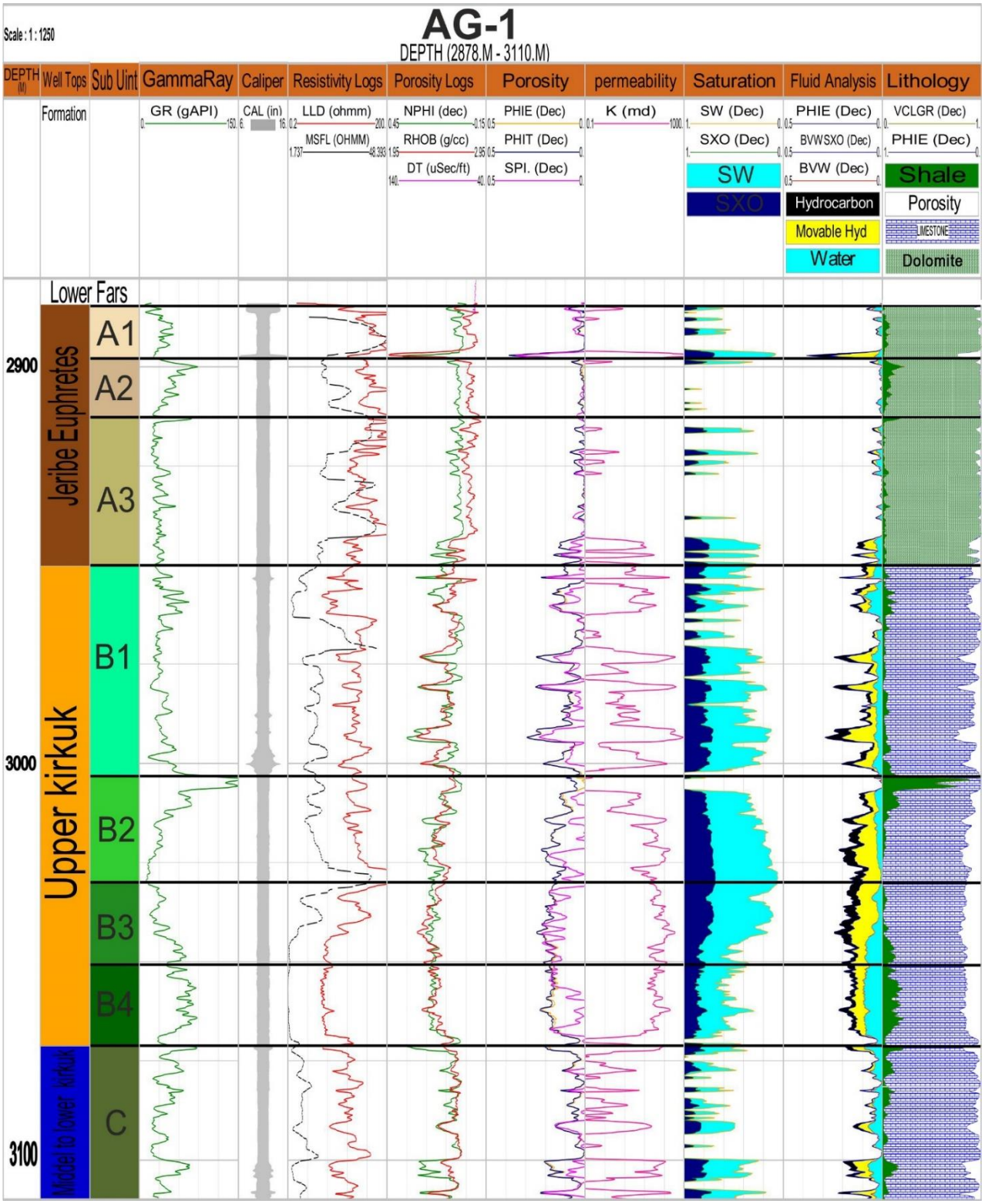

Figure (B-1): Computer Processes Interpretation (CPI) of Asmari reservoir in AG-1.

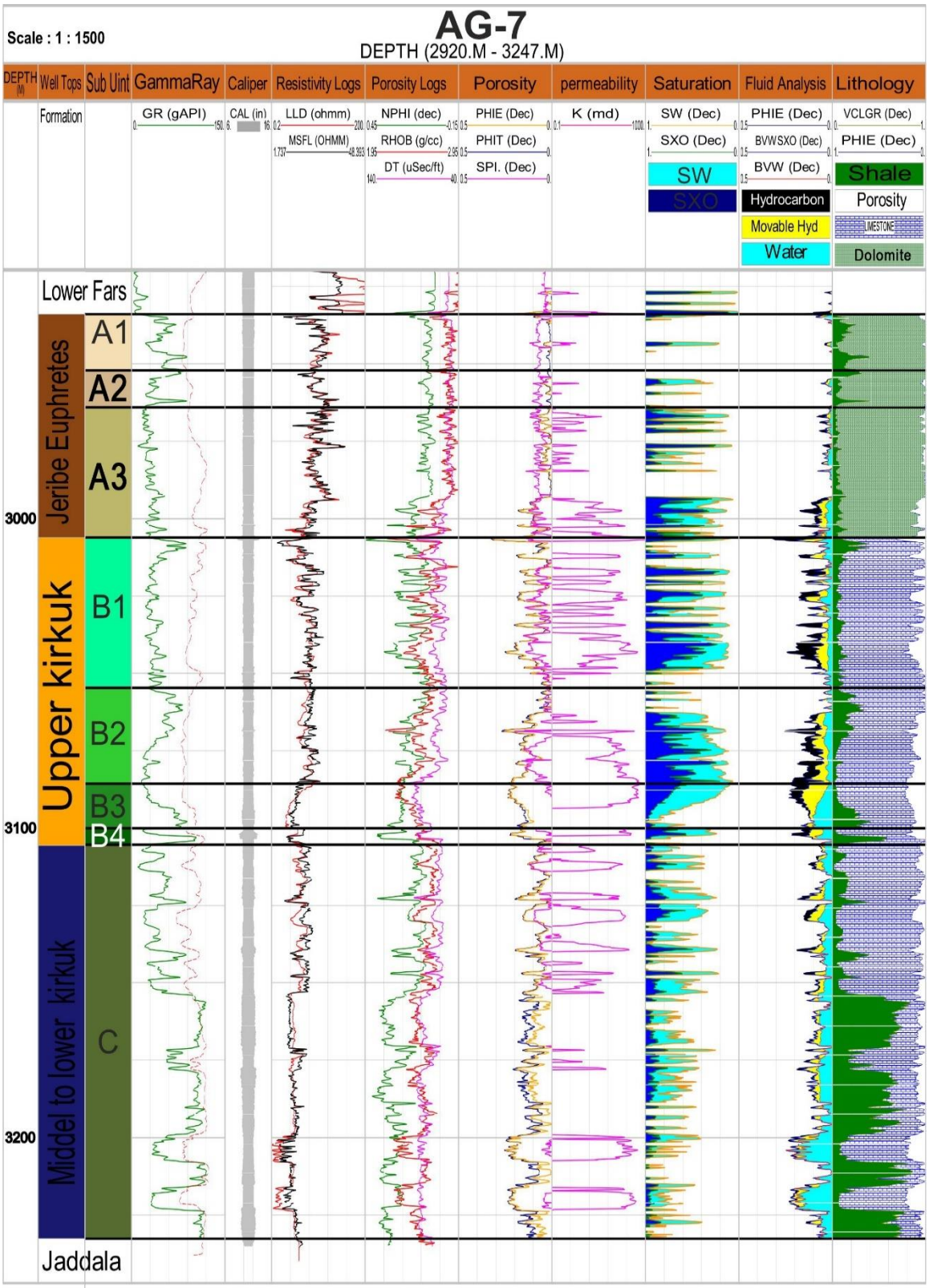

Figure (B-2): Computer Processes Interpretation (CPI) of Asmari reservoir in AG-7.

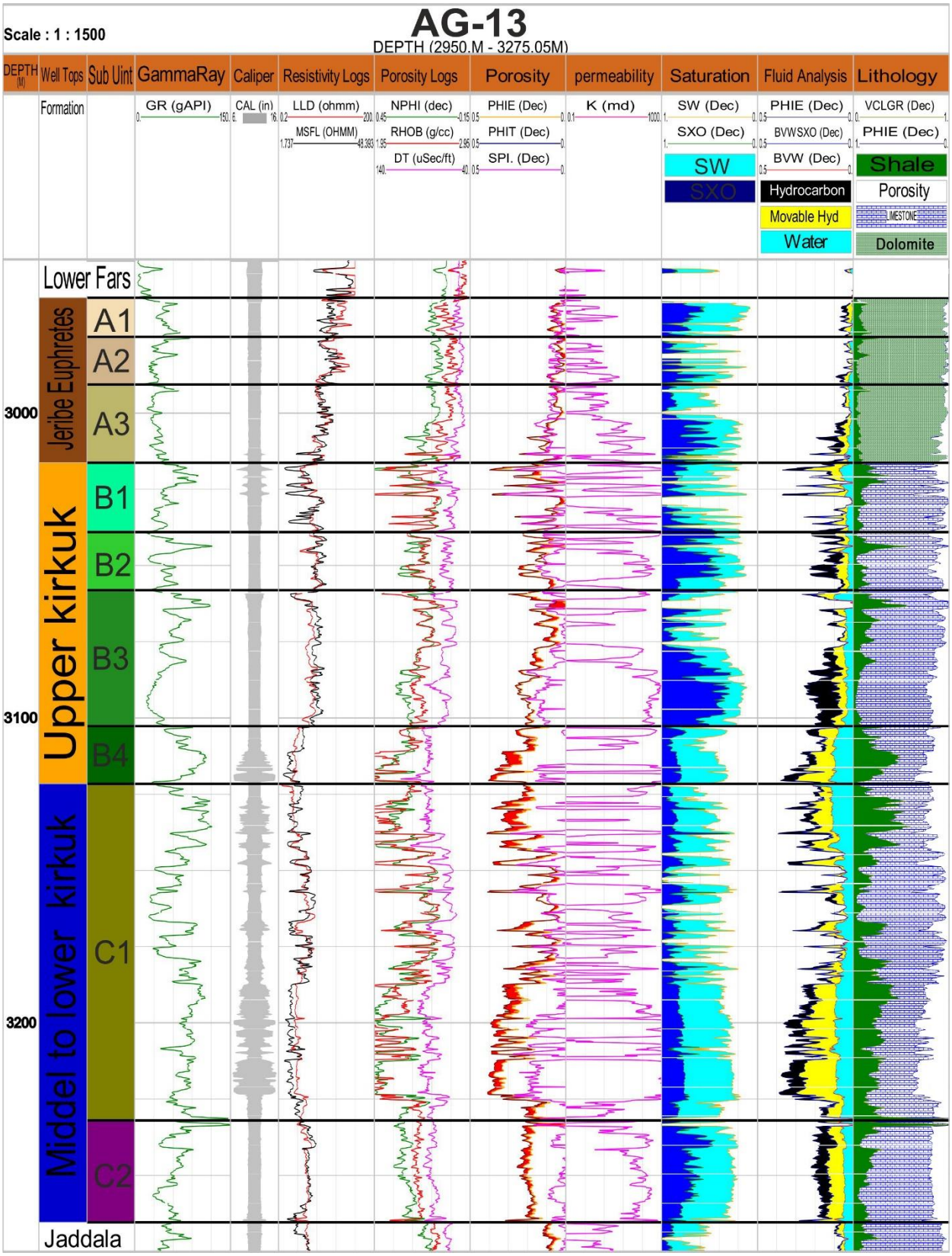

Figure (B-3): Computer Processes Interpretation (CPI) of Asmari reservoir in AG-13.

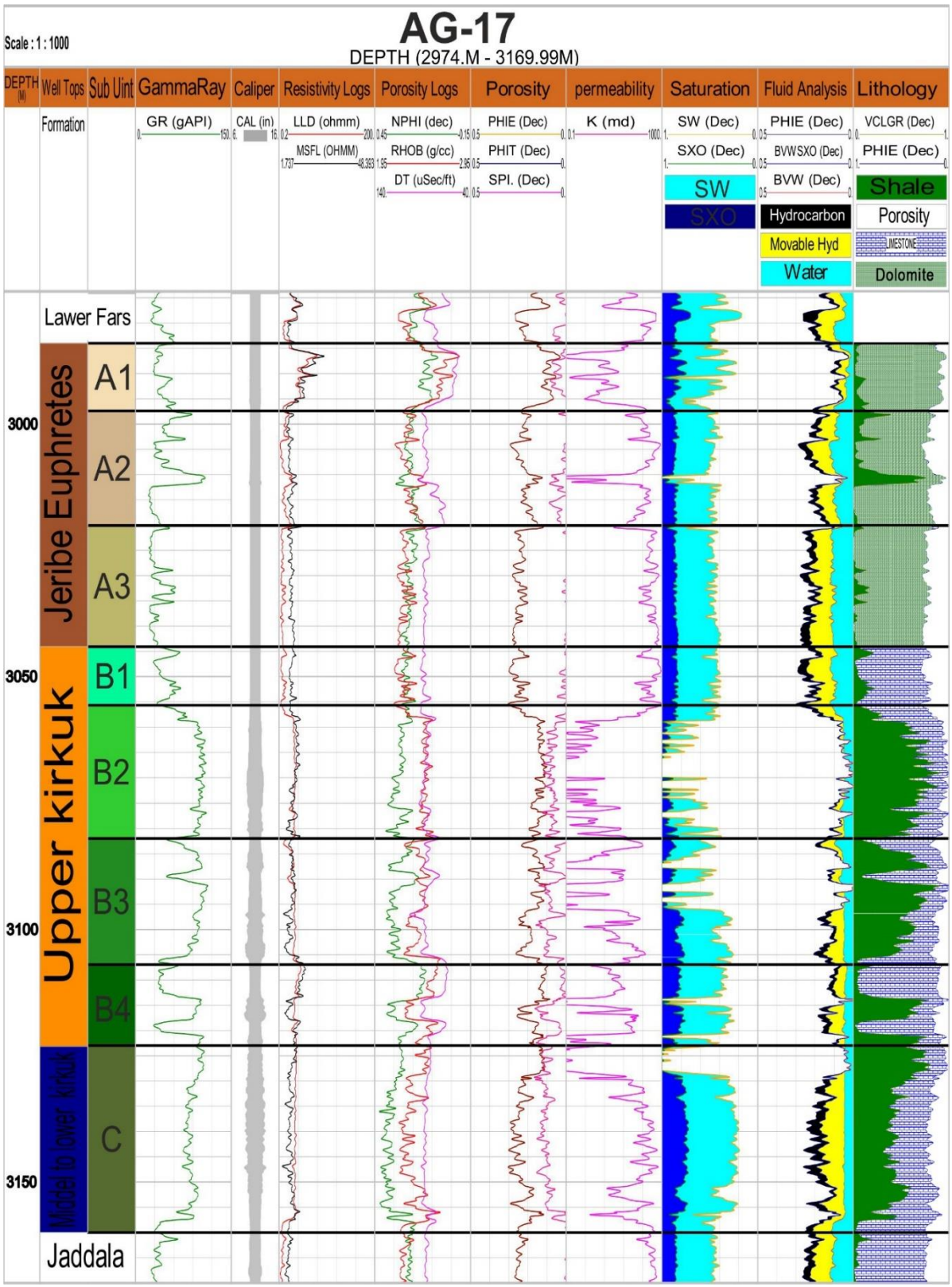

Figure (B-4): Computer Processes Interpretation (CPI) of Asmari reservoir in AG-17

الخلاصة

يمتد حوض طية زاغروس وحوض بلاد ما بين النهرين من شمال العراق إلى جنوبه. تقع معظم حقول النفط الضخمة في هذين الحوضين ، وتحتوي على معظم احتياطيات النفط والغاز في العراق.

تضمنت هذه الدراسة تحديد عناصر وعمليات المنظومة البترولية الكلية لحقل أبو غريب النفطي الواقع في محافظة ميسان جنوب شرق العراق بالقرب من الحدود مع إيران . ويكون مكمن الاسمري هو المكمن الرئيسي للحقل والمكامن الثانويه للحقل المتمثله بتكوين المشرف ونهر عمر ومودود .
ولتحقيق اهداف هذه الدراسة تم جمع البيانات اللازمه لهذه الدراسة من المصادر الرسمية ممثلة بوزارة النفط وشركة نفط ميسان (MOC) ودائرة المكامن وتطوير الحقول وشركة الاستكشافات النفطية.وتم تثبيت واستخدام برامج الضرورية لهذه الدراسه (Didger, IP ,Petrel and PetroMod) والتي تم استخدامها للتعامل مع هذه البيانات,وتم اختيار خمسة ابار عمودية في حقل ابو غرب لهذه وهي (AG1, AG-3, AG-7, AG-13, AG-17) وتم تزويد بثلاث نماذج من النفط الخام من الابار AG-1,AG-7,AG-10 وعمل التحاليل الجيو كيميائية لها باستخدام تقنية (الغاز كروماتوغراف) وتقنية (الغاز كروموتوغراف – الطيف الكتلي) وتحليل نظائر الكربون لدى مختبرات الجيومارك الامريكية.

تمت دراسة الخواص البتروفزيائية للمكمن الرئيسي الاسمري، بناء على تفسيرات سجلات الابار المتاحة باستخدام برنامج V3 Petrophysics Interactive.5 ، كما تم بناء نماذج جيولوجية ثلاثية الابعاد لها لتحديد الخواص البتروفزيائية المتمثله بالنفاذية والمسامية والتشبع المائي. وتم تحديد لثولوجية المكمن على انه يتكون من الحجر الجيري والدلومايت.
يتكون تكوين الاسمري من ثلاث وحدات رئيسية تفصل بينها طبقة من الشيل والتي هي (Jeribe-Euphrates, Upper Kirkuk, Middle-lower Kirkuk). وتم تقسيم هذه الوحدات الريسية الى وحدات ثانوية عدد ثمان وحدات مكمنية حسب قرائات الGR ومحتواها من الشيل والخواص البتروفزيائية والتي هي (A1, A2, A3, B1, B2, B3, B4, C).تتميز الوحدات B2- B3 بخصائص بترو فزيائية ممتازه وتعتبر من افظل وحدات تكوين الاسمري، حيث تحتوي هذه الوحدات على نسب عالية من الهايدروكاربون .وتكون الوحده C تحتوي على نسب عالية من التشبع المائي مع نسب قليلة من النفط عدى بئر AG-13 تحتوي في الاسفل على جزء عالي من النفط.

اجريت التحاليل الجيو كيميائية لثلاث عينات من النفط الخام باستخام تقنية الغاز كروماتوغراف و الغاز كروموتوغراف – الطيف الكتلي من تكوين الجريبي وكركوك الاوسط وكركوك الاعلى واظهرت النتائج ان نفوط غير متاكلة حيويا وغير شمعية وتولدت من ترسبات صخور مصدرية كاربونية ترسبت في بيئة بحرية غير متهوية وقليلة النضوج الحراري.

بسبب عدم تمكن الحفر من الوصول الى الصخور المصدرية في حقل ابو غرب النفطي ، تم استخدام نتائج تحاليل سابقة ودراسات سابقة من قامة بها باحثون للصخور المصدرية.و لفهم التوزيع والحركة المتوقعين للنفط داخل الحوض ، وكذلك لتحديد توليد الهيدروكربونات ، والهجرة ، والتراكم ، وكذلك تواريخ درجات الحرارة والضغوط ، تم بناء نموذج الحوض D1 ونظام البترول وجد ان الصخور المصدرية للمنطقة متمثلة بتكوين ساركلو وتكوين نجمة من العمر الجوراسي وتكاوين يمامه وسلي من العمر الطباشيري. وكذلك حدد وقت تولد النفط من عصر الطباشيري المتاخر وتوقف عند الباليوجين والنيوجين المبكر. حدث ذروة الطرد في أواخر العصر الميوسيني والبليوسيني عندما توسعت هذه المستودعات على طول اتجاه زاغروس الأمامي ، وانتهى التوليد في الهولوسين عندما توقف الترسب في الجرف الأمامي وتجمع هذا النفوط في في مكامن العصر الثلاثي و مكامن العصر الطباشيري وتبينت ان هذه النفوط هي مختلطه من صخور مصدريه الجوراسيه والطباشيرية

وزارة التعليم العالي والبحث العلمي
جامعة بابل / كلية العلـــــوم
قسم علم الارض التطبيقي

النظام النفطي في حقل ابو غرب النفطي في حوض حزام طيات زاكروس ,جنوب شرق العراق

رسالة مقدمة إلى

مجلس كلية العلوم جامعة بابل
كجزء من متطلبات نيل درجة مـــاجستير عـلوم
في عـلم الأرض

من قبل
عبدالله احمد هادي جواد المعموري
بـكـالوريوس علم الارض التطبيقي
2019

الإشراف
أ.د. عامر جاسم الخفاجي
د. علي دعير الموسوي

2022م **1444 هـ**